Distributed Transmission Schemes for Wireless Communication Networks

by

Ousama Salem Alnatouh

A doctoral thesis submitted in partial fulfilment of the requirements for the award of the degree of Doctor of Philosophy (PhD)

April 2014

Advanced Signal Processing Group,
School of Electronic, Electrical and System Engineering,
Loughborough University, Loughborough,
Leicestershire, UK, LE11 3TU

CERTIFICATE OF ORIGINALITY

This is to certify that I am responsible for the work submitted in this thesis, that the original work is my own except as specified in acknowledgements or in footnotes, and that neither the thesis nor the original work contained therein has been submitted to this or any other institution for a degree.

..... (Signed)

..... (candidate)

I dedicate this thesis to

my parents, Salem and Khiria,

my wife, Manal,

my son and daughters, Abdulaziz, Hanin and Arij,

my brothers, Hussam, Abdulhameed,

my sisters, Amani, Enas, Fatma and Fairuz,

and all their family.

Abstract

In this thesis new techniques are presented to achieve performance enhancement in wireless cooperative networks. In particular, techniques to improve transmission rate and maximise end-to-end signal-to-noise ratio are described.

An offset transmission scheme with full interference cancellation for a wireless cooperative network with frequency flat links and four relays is introduced. This method can asymptotically, as the size of the symbol block increases, achieve maximum transmission rate together with full cooperative diversity provided the destination node has multiple antennas. A novel full inter-relay interference cancellation method that also achieves asymptotically maximum rate and full cooperative diversity is then designed for which the destination node only requires a single antenna.

Two- and four-relay selection schemes for wireless cooperative amplify and forward type networks are then studied in order to overcome the degradation of end-to-end bit error rate performance in single-relay selection networks when there are feedback errors in the relay to destination node links. Outage probability analysis for a four-relay selection scheme without interference is undertaken.

Outage probability analysis of a full rate distributed transmission scheme with inter-relay interference is also studied for best single- and two-relay selection networks.

The advantage of multi-relay selection when no interference occurs and when adjacent cell interference is present at the relay nodes is then shown theoretically. Simulation results for outage probability analysis are included which support the theoretical expressions.

Finally, outage probability analysis of a cognitive amplify and forward type relay network with cooperation between certain secondary users, chosen by best single-, two- and four-relay selection is presented. The cognitive amplify and forward relays are assumed to exploit an underlay approach, which requires adherence to an interference constraint on the primary user. The relay selection scheme is performed either with a $max-min$ strategy or one based on maximising exact end-to-end signal-to-noise ratio. The outage probability analyses are again confirmed by numerical evaluations.

Contents

Statement of Originality

The contributions of this thesis are mainly focused on the improvement of transmission rate with the cancellation of interference, and the outage probability analysis in the context of the best single-, two- and four-relay selection schemes. The novelty of the contributions is supported by the following conference papers and international journal outputs:

In Chapter 2, the quasi-orthogonal and Jacket space-time coding schemes for point-to-point and distributed transmissions are compared. This work have been presented in:

1. O. Alnatouh, G. Chen and J. A. Chambers, "Comparison of Quasi-orthogonal and Jacket Space-time Coding Schemes for Point-to-Point and Distributed Transmissions", In Proc. MIC-WCMC, Istanbul, Turkey, Jun, 2011.

In Chapter 3, full interference cancellation and full inter-relay self interference cancellation schemes for synchronous cooperative networks are presented to improve the end-to-end transmission rate and mitigate the interference between the relays. The results have been published in:

2. G. Chen, O. Alnatouh, and J. A. Chambers, "Full inter-relay self interference cancellation for a four relay cooperative network", In Proc. UKIWCWS, New Delhi, India, Dec. 2010.

3. G. Chen, O. Alnatouh, L. Ge and J. A. Chambers, "A Distributed Differential Space-Time Coding With Full Interference Cancellation Scheme for A Cooperative Four Relay Network", In Proc. IET MIC-CSC, Istanbul, Turkey, Oct. 2012.

In Chapter 4, outage probability analysis in the four-relay selection application without interference is presented. The novelty of this work is supported by the following publication:

4. G. Chen, O. Alnatouh, L. Ge and J. A. Chambers, "Performance Analysis of Four Relays Selection Scheme for Cooperative Networks", In Proc. ISSPA, Montreal, Canada, July, 2012.

The contribution of Chapter 5 is an inter-relay self interference cancellation scheme with amplify-and-forward two-path half duplex transmission with relay selection network. This work have been presented in:

5. O. Alnatouh, G. Chen and J. A. Chambers, "Amplify-and-Forward Two-Path Half Duplex Transmission with Relay Selection and Inter-Relay Self Interference Cancellation", In Proc. MIC-CNIT, Dubai, UAE, Dec, 2011.

In Chapter 6, outage probability analysis in the multi-relay selection context with inter-cluster interference is presented. The novelty of this work is reinforced by the following work:

6. G. Chen, O.Alnatouh and J. A. Chambers, "Two- and Four-Relay Selection Schemes for Application in Interference Limited Legacy Networks", EURASIP J. Wire. Communs. and Networking, vol. 2012-351, pp. 1-10, 2012.

In Chapter 7, outage probability analysis for a cognitive amplify-and-forward relay network with single-, two- and four-relay selection is presented. The novelty of this work is supported by the following work:

7. G. Chen, O. Alnatouh and J. A. Chambers, "Outage Probability Analysis for a Cognitive Amplify-and-Forward Relay Network with Single and Multi-relay Selection", IET Commun., Vol. 7, Iss. 17, pp. 1974-1981, 2013.

Acknowledgements

First and foremost, I thank Allah, the most gracious and the most merciful, Almighty for all His countless favours and guidance.

Then, I am deeply indebted to my supervisor Professor Jonathon A. Chambers for his kind interest, generous support and constant advice throughout the past four years. I have benefited tremendously from his rare insight, his ample intuition and his exceptional knowledge. This thesis would never have been written without his tireless and patient mentoring. It is my very great privilege to have been one of his research students. I wish that I will have more opportunities to work with him in the future.

Also, I am extremely thankful to Doctor Gaojie Chen for his support, encouragement and made my research experience very enjoyable.

I am also grateful to all my friends in the Advanced Signal Processing Group for providing a stable and cooperative environment within the Advanced Signal Processing Laboratory.

Last, but most importantly, I really can not find appropriate words or suitable phrases to express my deepest and sincere heartfelt thanks, appreciations and gratefulness to all my family members, especially my parents, my brothers and my sisters and also friends for their constant encouragement, attention, prayers and their support in innumerable ways throughout my PhD and before. I also owe my loving thanks to my beloved wife and my lovely children. Without my wife′s endless love, support, prayers, companionship, friendship and caring words, this would not have been possible. I am deeply grateful for her. And I am really proud of all of them. May Allah save them all.

Ousama Salem Alnatouh

April, 2014

List of Acronyms

3G	Third Generation
3GPP	3rd Generation Partnership Project
4G	Fourth Generation
AF	Amplify-and-Forward
AWGN	Additive White Gaussian Noise
BER	Bit Error Rate
BPSK	Binary Phase Shift Keying
CCI	Co-Channel Interference
CDF	Cumulative Distribution Function
CSI	Channel State Information
DDSTC	Distributed Differential Space-Time Coding
DF	Decode-and-Forward
FCC	Federal Communications Commission
FIC	Full Interference Cancellation
FSA	Fixed Spectrum Access
FSIC	Full inter-relay Self Interference Cancellation

IEEE	Institute of Electrical and Electronic Engineers
i.i.d.	Independent and Identically Distributed
INR	Interference-to-Noise Ratio
IIR	Infinite Impulse Response
IRI	Inter-Relay Interference
ISI	Inter-Symbol Interference
LTE	Long Term Evolution
MAP	Maximum A Posteriori
MGF	Moment Generating Function
MIMO	Multiple-Input Multiple-Output
ML	Maximum Likelihood
MRC	Maximum Ratio Combiner
ODSTC	Orthogonal Distributed Space-Time Code
PDF	Probability Density Function
PEP	Pairwise Error Probability
PU	Primary User
QPSK	Quadrature Phase Shift Keying
RSC	Recursive Systematic Convolutional
SIMO	Single-Input Multiple-Output
SINR	Signal-to-Interference plus Noise Ratio
SISO	Single-Input Single-Output

SNR	Signal-to-Noise Ratio
SU	Secondary User
WiFi	Wireless Fidelity
WiMax	Worldwide Interoperability for Microwave Access

List of Symbols

Scalar variables are denoted by plain lower-case letters, (e.g., x), vectors by bold-face lower-case letters, (e.g., $\mathbf{x}$), and matrices by upper-case bold-face letters, (e.g., $\mathbf{X}$). Some frequently used notations are as follows:

$\mathrm{E}(\cdot)$	Statistical expectation
$\mathrm{Covar}(\cdot)$	Covariance
$(\cdot)^T$	Transpose
$(\cdot)^H$	Hermitian transpose
$(\cdot)^*$	Complex conjugate
$\lvert . \rvert$	Modulus of a complex number
$\lVert . \rVert$	Euclidean norm
$\mathbf{I}$	Identity matrix
$\mathbf{0}_M$	$M \times M$ matrix of zeros
$\mathbf{I}_M$	$M \times M$ unity diagonal matrix
$\mathrm{Tr}(\cdot)$	Trace
$\mathrm{diag}(\cdot)$	Diagonal matrix
$\det(\cdot)$	Matrix determinant
$\bigcap$	OR operation

$\bigcup$	AND operation
$\max(\cdot)$	Maximum value
$\min(\cdot)$	Minimum value
argmax	The argument which maximizes the expression
argmin	The argument which minimizes the expression
$F_{2,1}(\cdot)$	First hypergeometric function
$F_1(\cdot)$	Appell hypergeometric function
$\Gamma(\cdot)$	Gamma function
$\mathrm{Ei}(\cdot)$	Exponential integral

List of Figures

Chapter 1

INTRODUCTION

Cooperative relay communications has recently gained much attention in industrial and academic wireless research centers across the globe due to its potential to enable efficient solutions for challenging problems in wireless communications. Signal propagation through a wireless channel faces more difficulties than through a guided wire, including greater additive noise, fading, multi-path spread, and adjacent channel interference [1]. Fiber and coaxial cables can, on the other hand, be almost free of interference. However, wireless transmission has become the favorable platform to transfer information these days, due to the associated support for user freedom from being physically connected and providing, flexibility and portability [2].

In this chapter conventional MIMO systems will firstly be presented and their main advantages and disadvantages will be underlined. Then, the basic concepts and system features of wireless cooperative networks will be introduced in detail. Moreover, the relay selection schemes in cooperative networks will be introduced in detail. Cooperative relays can also be exploited in cognitive radio, therefore, a brief introduction to cognitive relay networks in particular is included.

1.1 Conventional Multi-Input Multi-Output Systems

In the past few decades, the demands for high data rate wireless communication systems have been increasing dramatically. However, the performance of wireless communication systems at the link level is limited by path loss and multipath propagation effects, which lead to inter-symbol interference (ISI), and interference from other users in the form of co-channel interference (CCI) [3]. These limitations provide a number of technical challenges for reliable wireless communication systems. An important technology to address these challenges is to use multiple antenna wireless communication systems, which have received a great deal of attention recently due to the potential gains in capacity without requiring additional bandwidth or transmit power [4]. By using multiple antennas at both ends of a point-to-point communication link a multi-input multi-output (MIMO) system can be formed, as is shown in Figure 1.1, which can potentially combat multipath fading propagation effects and increase the channel capacity as compared with a conventional single-input single-output (SISO) system. The benefits of using multiple antennas have resulted in MIMO wireless technology being exploited in many wireless communication standards such as IEEE 802.11x wireless fidelity (WiFi) and IEEE 802.16x worldwide interoperability for microwave access (WiMax) and is a major focus for long-term evolution (LTE) and fourth generation (4G) cellular systems [5].

MIMO theoretically offers significant increases in data throughput and link range without additional bandwidth or transmit power. Particularly, some significant advantages will next be presented, such as array gain, spatial multiplexing, and diversity gain.

Firstly, array gain, is an important parameter in MIMO communication systems, which means that a power gain of the transmitted signals can be achieved by using multiple-antennas at the transmitter and/or receiver.

Through exploiting an antenna array, including a correlative combination technique, the average signal-to-noise ratio (SNR) at the receiver can be improved significantly.

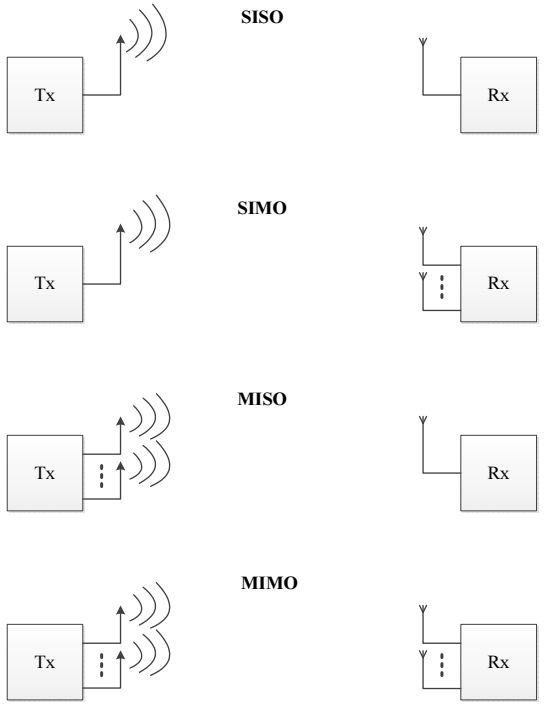

Figure 1.1. *A block diagram illustrating various forms of wireless communication system: single-input single-output (SISO); single-input multiple-output (SIMO); multiple-input single-output (MISO) and multiple-input multiple-output (MIMO).*

Secondly, MIMO can also achieve a linear growth of the capacity of the channel proportional to the maximum spatial multiplexing order $min(N_s, N_d)$ without increasing the power of the transmitter and the bandwidth, where N_s and N_d are the number of antennas at the source and destination node.

Finally, diversity is a significant method to be used in wireless channels to combat fading. Moreover, diversity gain is the increase in signal-to-interference ratio and is commonly expressed in decibels, and sometimes given as a power ratio. The spatial diversity order for frequency flat channels is equivalent to the product of the number of antennas at the source and

destination node ($N_s \times N_d$), if the channel between each transmit-receive antenna pair fades independently from the others.

Modern research on MIMO systems was confirmed that theoretically the channel capacity can significantly increase by using multiple transmit and/or receive antennas assuming independent channels between transmit and receive antennas [6]. The channel capacity is a measure of the maximum quantity of information that can be transmitted over a channel and received with a low probability of error at the receiver. The ergodic capacity of a SISO channel is the ensemble average of the information rate over the distribution of the channel h_{sd} [4], which is given by

$$C_{SISO} = E(log_2(1 + \rho|h_{sd}|^2)) \text{ bit/s} \tag{1.1.1}$$

where h_{sd} is a complex Gaussian random channel coefficient, and ρ is the average SNR ratio at the receiver branch and $E(\cdot)$ denotes the statistical expectation over all channel realizations. Also the ergodic capacity of a MIMO system is given by [6]

$$C_{MIMO} = E(log_2(det(I_{N_d} + \frac{\rho}{N_t} HH^H))) \text{ bit/s} \tag{1.1.2}$$

where I_{N_d} is the $N_d \times N_d$ identity matrix, H is the $N_d \times N_s$ normalized channel response matrix and $det(.)$ denotes the matrix determinant.

Therefore, the requirements of multiple-antenna terminals increases the system complexity and the separation between the antennas increases the terminal size. In addition, MIMO systems suffer from the effect of path loss and shadowing, where path loss refers to the signal attenuation between the source and destination nodes due to propagation distance, while the shadowing is the signal fading due to objects obstructing the propagation path between the source and destination nodes [7]. These different problems limit MIMO systems functionality and applicability which challenge researchers to

look for another innovative technology, and hence wireless cooperative networks have emerged as a new paradigm that can provide effective solutions to deal with the above-mentioned problems.

1.2 Wireless Cooperative Networks

Compared with conventional point-to-point MIMO systems, a cooperative network has different nodes which can share antennas, and thereby generate a virtual multiple antenna array based on cooperation protocols [8] and [9]. Such cooperative relay networks have developed a useful technique that can achieve the same advantage as MIMO systems whilst avoiding some of their disadvantages. Therefore, they have recently been implemented for various new wireless systems such as 3GPP LTE-Advanced [10]. Additionally, they have been considered in different wireless system standards such as IEEE 802.16j and IEEE 802.16m standards (WiMAX) [11] and IEEE 802.11s and IEEE 802.11n standards (WiFi) [12].

Cooperative relay networks can potentially yield several gains, such as, cooperative diversity gain, cooperative multiplexing gain and pathloss gain. Cooperative diversity gain can efficiently combat the detrimental outcomes of severe fading in the wireless channel [8]. Copies of the same information can be sent to the destination node by intermediate relays between the source and destination over independent channels. Therefore, cooperative diversity gain can be achieved in proportion to the number of independent channels in the cooperative relay network, which depends on the number of relay nodes and the environment [16]. For example, in a frequency-flat channel, the maximum cooperative diversity gain $G_d = N_s \times N_r \times N_d$, where N_r is the number of single-antenna relay nodes. Raised cooperative diversity gain leads to improvements in the system performance such as the probability of error P_e or the outage probability P_{out}. The cooperative diversity gain is

related to how fast the probability of error decreases with an increase in the signal strength typically measured by SNR [4]. The cooperative diversity gain or diversity order, G_d, in terms of end-to-end error probability and outage probability is given by [7] and [13]

$$G_d = -\lim_{SNR\to\infty} \frac{log(P_e(SNR))}{log(SNR)} \quad \text{and} \quad G_d = -\lim_{SNR\to\infty} \frac{log(P_{out}(R))}{log(SNR)},$$

where $P_{out}(R)$ denotes the probability that the instantaneous system capacity R is lower than a particular transmission rate threshold R_{th}, such that

$$P_{out} = Pr\{G_m log_2(1 + SNR) \leq R_{th}\},$$

where G_m is the cooperative spatial multiplexing gain which effectively equals the number of independent channels over which different information can be transmitted, which can improve capacity or transmission data rates, R(SNR). The cooperative multiplexing gain as a function of SNR is given by

$$G_m = \lim_{SNR\to\infty} \frac{R(SNR)}{log_2(SNR)}.$$

Finally, using intermediate relay nodes helps in avoiding the pathloss problem because dividing the propagation path between the source and destination nodes into at least two parts yields transmit power gains because the total resultant pathloss of part of the whole path is less than the pathloss of the whole path [13]. This advantage of the cooperative relay network can be stated as pathloss gain. It is known theoretically that SNR is inversely proportional to the signal propagation distance, d, [13].

$$SNR \propto \frac{1}{d^n},$$

where d is the distance between the source node and destination node and n is the pathloss exponent which typically fluctuates between 2 (light-of-sight)

and 6 (highly cluttered environment) based on the type of the propagation environment [13]. According to this relation, a cooperative relay network where the intermediate relay is in the middle between the source and destination node and the power is divided equally between the source and the relay will result in the following gain as compared to the conventional point-to-point system, therefore, pathloss gain can be obtained as

$$G_p = \frac{\frac{1/2}{(d/2)^n} + \frac{1/2}{(d/2)^n}}{1/d^n} = 2^n.$$

which means the cooperative relay network can achieve a transmit power saving of $(10log_{10}2^n)$ dB.

This thesis is focused upon exploiting spatial cooperative diversity gain rather than cooperative multiplexing and pathloss gain. In brief, cooperative relay systems potentially offer several advantages and disadvantages for wireless communications [13] and [14] as follows:

1. Major advantages

a. Performance Gains: large system-wide performance gains can be achieved due to pathloss, diversity and multiplexing gains. These gains can reduce transmission powers and provide higher capacity and transmission rate.

b. Coverage Extension: the coverage of the cell is impacted because of the limit in transmission power. For example, a user at the cell edge may experience insufficient power levels to communicate due to the weak signal of interest from the base station [13]. However, a cooperative relay system can effectively expand the network coverage through the relaying capability, and then the transmitted signal can service more range as compared to point-to-point systems.

2. Major disadvantages

a. Increased interference: the use of relays will certainly generate extra

intra- and inter-cell interference, which potentially causes the system performance to deteriorate [13]. In this thesis, interference cancellation schemes are proposed to mitigate this problem.

b. Strict synchronization: a tight synchronization generally needs to be maintained to facilitate cooperation, which is difficult to achieve, due to the nodes being in different locations and the varying timing delays between nodes. This thesis also considers asynchronous cooperative relay networks, and provides effective solutions to deal with asynchronism.

In the next section, another significant method will be offered to improve performance and reduce system complexity, which is the relay selection scheme.

1.3 Relay Selection in Cooperative Networks

Recently, relay selection has been recommended as an attractive solution to improve the performance of conventional cooperative networks [15]. For instance, in cooperative wireless networks, the relay nodes have different locations so each transmitted signal from the source node to the destination node must pass through different paths causing different attenuations within the signals received at the destination which results in reducing the overall system performance. Therefore, to reduce this effect and benefit from cooperative communication, high quality paths should be chosen by using relay selection techniques. Moreover, several works [15–17] have confirmed that full cooperative diversity order can be achieved with the relay selection scheme.

A transmitter broadcasts its signal toward all the relay nodes at the first stage; the best relay can then be selected, by using local measurements of the instantaneous channel conditions between the source-relay and the relay-destination, and then used to transmit its received signal to the destination node during the second stage. No direct link between the source and desti-

nation is assumed due to path loss and shadowing. A relay selection scheme can be exploited in both decode and forward (DF) and amplify and forward (AF) relaying schemes. In the literature, the DF relay selection scheme has been investigated in [18, 19] over Rayleigh fading channels.

Two selection policies for AF networks can generally be used to choose the best relay node to help the source to transmit its signal to the destination node, which are the max-min and max-harmonic mean schemes as below [15]

$$R_{best} = argmax(min(|h_{sr_i}|^2, |h_{r_id}|^2)) \qquad \text{Policy I}$$
$$R_{best} = argmax\left(\frac{|h_{sr_i}|^2|h_{r_id}|^2}{|h_{sr_i}|^2 + |h_{r_id}|^2}\right) \qquad \text{Policy II.}$$

where h_{sr_i} and h_{r_id} are channel links between the source-relay and relay-destination. On the basis of these two policies, some works in [20–22] have been considered to select the best relay from a cooperative AF network. In this thesis, an exact selection policy will be provided to obtain an accurate outage probability in cooperative AF networks. In the next section, a brief introduction to cognitive relay networks will be presented.

1.4 Cognitive Relay Networks

The radio spectrum and its use are strictly managed by governments in most countries, and spectrum allocation is a legacy command-and-control regulation enforced by regulatory bodies, such as the federal communications commission (FCC) in the United States [23] and Ofcom [24] in the United Kingdom. Most of the existing wireless networks and devices follow fixed spectrum access (FSA) policies to use radio spectrum, which means that radio spectral bands are licensed to dedicated users and services, such as TV, 3G networks, and vehicular ad hoc networks. Licensed users are referred to as the primary users (PUs), and a network consisting of PUs is referred to as a primary network. In this context, only the PUs have the right to

use the assigned spectrum, and others are not allowed to use it, even when the licensed spectral bands are idle. Although interference among different networks and devices can be efficiently coordinated by using FSA, this policy causes significant spectral under-utilization [24].

Therefore, cognitive radio is an emerging paradigm of wireless communication in which an intelligent wireless system utilizes information about the radio environment to adapt its operating characteristics in order to ensure reliable communication and efficient spectrum utilization [25]. Recently, several IEEE 802 standards for wireless systems have considered cognitive radio systems such as IEEE 802.22 standard [26] and IEEE 802.18 standard [27].

Moreover, there are three main spectrum sharing approaches which are overlay, underlay and interweave cognitive approaches [28].

In the overlay approach, the secondary users coexist with primary users and use part of the transmission power to relay the primary users' signals to the primary receiver. This assistance will offset the interference caused by the secondary user transmissions at the primary users' receiver. Hence, there is no loss in primary users' signal-to-noise ratio by secondary users spectrum access.

In the underlay approach, the secondary users access the licensed spectrum without causing harmful interference to primary users' communications. In this method, the secondary users ensure that interference leakage to the primary users is below an acceptable level.

In the interweave approach, identifying spectrum holes in the absence of cooperation between primary and secondary networks is very challenging [29]. For example, a secondary transmitter could be in the shadow region of the primary transmitter which will falsely indicate (to the secondary transmitter) availability of spectrum. The secondary transmission based on this false indication may harm the primary receivers. This hidden terminal problem is deemed to be very challenging and a limiting factor

for the employment of interweave cognitive radio networks. On the other hand, the overlay cognitive radio is very interesting in terms of its theoretical advantages, however, there are even more challenges in terms of practical implementation as this requires the secondary transmitter to have prior knowledge of the primary user transmitted signal. Therefore, the underlay scheme seems more realistic and easy to implement compared to the other schemes. Therefore the underlay cognitive radio is considered in this thesis.

1.5 Challenges and Thesis Contributions

Although cooperative relaying has been considered as an effective method to combat fading by exploiting spatial diversity [30]; compared with traditional systems, relaying can additionally provide high quality of service for users at the cell edge or in shadowed areas; moreover, the relaying capability of this cooperative relay system can cope with the effects of path loss and shadowing, but there are two main challenging problems related to cooperative systems. Firstly, end-to-end transmission rate can be decreased due to the requirement of increasing the number of transmission stages. Therefore, some researchers provide two way transmission schemes to increase the end-to-end transmission rate [31–33]. However, some redundant information has to be transmitted between two destination nodes and relay nodes, which can decrease the efficiency of the system. This thesis addresses the aforementioned challenging problems by exploiting offset transmission with full interference cancellation and full inter-relay self interference cancellation schemes.

The second challenge, due to the random nature of the wireless environment the channel gains between the source, via relay nodes, and destination node are different which results in some relays providing a poor channel quality. This issue can affect the transmission quality to a certain extent.

Therefore, in this thesis, the utilizing of two- and four-relay selection schemes is considered to overcome this problem and decrease the outage probability of cooperative networks. Finally, a cognitive relay network with two- and four-relay selection will be provided to decrease the outage probability and also improve the spectrum efficiency.

In summary, the contributions of this thesis can be summarized into four main parts:

1. Full interference cancellation and full inter-relay self interference cancellation schemes for synchronous cooperative networks are presented to obtain asymptotically unity end-to-end transmission rate and mitigate the interference between the relays.

2. A two- and four-relay selection scheme is proposed based on the local measurements of the instantaneous channel conditions to improve the diversity and decrease the outage probability. And the best two- and four-relay selection scheme is also shown to have robustness against feedback error and to outperform a scheme based on selecting only the best single-relay.

3. An outage probability analysis for two different multi-relay selection policies to select the best two- and four-relay from a group of available relays by using local measurements of the instantaneous channel conditions is examined when inter-cluster interference is present.

4. Three types of outage probability analysis are presented for a cognitive AF network with single-, two- or four-relay selection from the potential cooperative secondary relays based on the underlay approach, while adhering to an interference constraint on the primary user.

1.6 Structure of Thesis

To simplify the understanding of this thesis and its contributions, its structure is summarized as follows:

In Chapter 1, a general introduction to wireless communication systems was presented. Furthermore, a brief introduction to wireless cooperative networks including system features and advantages and disadvantages of the performance were presented. Then, a brief introduction to the relay selection scheme was presented. In addition, because a cognitive relay network has been used as an application for the proposed multi-relay selection scheme, a brief introduction to cognitive radio systems was provided highlighting the main functions of cognitive radio and the features of cooperative cognitive networks.

In Chapter 2, a brief introduction to distributed space-time block coding schemes with orthogonal and quasi-orthogonal codes is presented. A differential distributed space-time code is briefly introduced, which does not need channel state information (CSI) at the receiver for decoding. Two important performance measures, which are the pairwise error probability analysis (PEP) and outage probability analysis, are described. Finally, a simulation study is included to compare the performance of Jacket space-time coding scheme with the orthogonal coding scheme.

In Chapter 3, an offset transmission with full interference cancellation scheme is used to improve end-to-end transmission rate. Using offset transmission, the source can serially transmit signals to the destination node. However, the one group of relays scheme may suffer from inter-relay interference which is caused by the simultaneous transmission of the source and another group of relays. Therefore, the full interference cancellation scheme can be used to remove fully these inter-relay interference terms. Moreover, a full inter-relay self interference cancellation scheme at the relay nodes within a four relay network is provided and the pairwise error probability approach is used to analyze distributed diversity.

In Chapter 4, outage probability analysis of the best single- and four-relay selection schemes in a cooperation AF network without interference is

provided. And the best four-relay selection scheme is shown to have robustness to feedback error and to outperform a scheme based on selecting only the best single-relay.

In Chapter 5, outage probability analysis of the best single- and two-relay selection scheme in a cooperative amplify and forward network with inter-relay interference is provided. Also, BER analysis of the proposed scheme with error in inter-relay interference cancellation is compared.

In Chapter 6, two different selection schemes are proposed to select the best two- and four-relays from a group of available relays in the same cluster by using local measurements of the instantaneous channel conditions in the context of legacy systems, when inter-cluster interference is present only at the relay nodes. Moreover, a new exact closed form expression for outage probability in the high signal-to-noise ratio region is provided.

In Chapter 7, three types of outage probability analysis strategies for a cognitive amplify and forward network with single-, two- or four-relay selection from the potential cooperative secondary relays based on the underlay approach, while adhering to an interference constraint on the primary user, is examined. New analytical expressions for the probability density function, and cumulative distribution function of end-to-end signal-to-noise ratio are derived together with near closed form expressions for outage probability over Rayleigh fading channels. Moreover, the theoretical values for the new exact outage probability are shown to match the simulated results.

Finally, in the last chapter which is Chapter 8, this thesis is concluded by summarizing its contributions and suggestions are given for some future possible research directions.

Chapter 2

RELEVANT LITERATURE REVIEW

2.1 Introduction

Due to the fading effect, transmission over wireless channels can potentially suffer from severe attenuation in signal strength. For a point-to-point wireless communication system, this problem has been theoretically solved by using multiple antennas at the transmitter and/or the receiver, and spatial diversity is exploited by using space-time coding [34], [35]. However, due to physical constraints, when applying multiple antennas at the transmitter and/or the receiver it is hard to obtain independent spatial paths between the transmitter and the receiver. Therefore, recently, with increasing interest in wireless cooperative networks, researchers have been looking for ways to exploit spatial diversity provided by antennas of different users to improve the reliability of transmission [36] [37]. The cooperative diversity is achieved by having different users in the network cooperate in some way.

Recently, cooperative relaying has been considered as an effective method to combat fading by exploiting spatial diversity [8], and as a way for two users with no or weak direct connection to attain a robust link. One or multi relay nodes is generally used in such relaying to forward signals transmitted from the source node to the destination node. In a cooperative communication

system, there are two main cooperative methods: amplify and forward (AF) (transparent relaying protocol) and decode and forward (DF) (regenerative relaying protocol) [13]. In the AF method, the relay nodes only amplify and retransmit their received signals, including noise, to the destination. In the DF method, the relay nodes decode the source information and then re-encode and re-transmit it to the destination. Therefore, comparing between the two methods, AF type schemes have the advantage of simple implementation and low complexity in practical scenarios. In addition to complexity benefits, it has been shown in [38] that an AF scheme asymptotically, in terms of appropriate power control, approaches a DF one with respect to diversity. Therefore, the AF method will be considered in this thesis.

In this chapter, a brief overview of wireless cooperative networks concepts relevant to this thesis are presented. The chapter begins with an introduction to distributed space-time coding schemes and overviews two important codes, orthogonal and quasi-orthogonal codes. Also a coding scheme which avoids the need for channel state information in decoding is represented which is the differential space-time code. This is followed by a description of the performance analysis of wireless AF cooperative networks. Finally, the Jacket space-time coding scheme is compared with the orthogonal coding scheme.

2.2 Distributed Space-Time Coding Schemes

In a general wireless relay network, different relays receive different noisy copies of the same transmitted information symbols. The relays process these received signals and forwards them to the destination node. The distributed processing at the different relay nodes thus forms a virtual antenna array [13]. Therefore, conventional space-time block coding schemes can be applied to

relay networks to achieve cooperative diversity. In this section, the design of distributed space-time block codes based on an AF type relay protocol is the focus. There is some literature on AF type space-time block codes, i.e. [39], [40], [41] and [42]. In this section, the fundamental designs proposed in [42] are considered in detail.

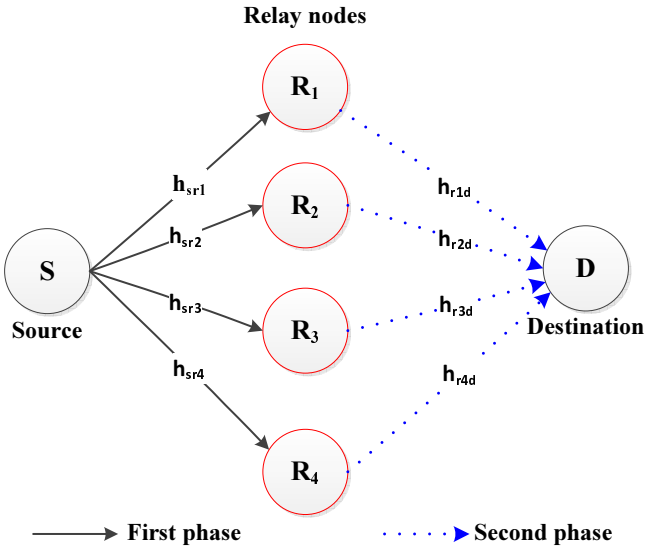

Figure 2.1. *A two-hop wireless cooperative relay network over which distributed linear space time codes can be transmitted. The network consists of a source, four relay and one destination nodes; the frequency flat links are labeled with a scalar coefficient.*

2.2.1 Distributed Transmission Technology

A wireless cooperative relay network is shown in Figure 2.1, it consists of one transmitter node S with one antenna, one destination node D with one antenna and R relay nodes, four in the figure. Each relay node has a half duplex antenna for reception and transmission (not at the same time). It is assumed that the communication channels are quasi-static independent Rayleigh flat fading and the receiver has perfect channel information h_{sri} and h_{rid}, where h_{sri} and h_{rid} denote the channels from the transmitter to the i^{th} relay and from the i^{th} relay to the receiver, respectively. And assuming

there is no direct link between the source and the destination as path loss or shadowing is expected to render it unusable.

It is assumed that the transmitter sends the signal $\mathbf{s} = [s_1, ..., s_M]^T$, which is normalized so that $E[\mathbf{s}^H\mathbf{s}] = 1$ where M is the time slot, $(.)^T$, $(.)^H$ and $E[\cdot]$ denote the transpose, Hermitian transpose and the expectation of a random variable, respectively. The transmission operation has two steps, in step one the transmitter sends signals $\sqrt{P_1 M}\mathbf{s}$ to each relay where P_1 is the average power used at the transmitter for every transmission, whereas in step two, the i^{th} relay sends a signal vector to the receiver. The noise terms at the i^{th} relay within the vectors $\mathbf{v}_i$ and at the receiver $\mathbf{w}_i$ are independent complex Gaussian random variables with zero-mean and unit-variance which is additive white Gaussian noise (AWGN). The received signal vector at the relays is given by

$$\mathbf{r}_i = \sqrt{P_1 M} h_{sri}\mathbf{s} + \mathbf{v}_i. \tag{2.2.1}$$

The i^{th} relay transmits the signal vector $\mathbf{t}_i$ which corresponds to the received signal vector $\mathbf{r}_i$ multiplied by a scaled unitary matrix, as such this approach has more complexity than an amplify-and-forward (AF) scheme and therefore is termed AF-type. The transmitted signal vector from the i^{th} relay node can be generated from

$$\begin{aligned} \mathbf{t}_i &= \sqrt{\frac{P_2}{P_1+1}}(A_i\mathbf{r}_i + B_i\mathbf{r}_i^*) \\ &= \sqrt{\frac{P_1 P_2 T_s}{P_1+1}}(h_{s,ri}A_i\mathbf{s} + h_{s,ri}^* B_i\mathbf{s}^*) + \sqrt{\frac{P_2}{P_1+1}}(A_i\mathbf{v}_i + B_i\mathbf{v}_i^*), \end{aligned} \tag{2.2.2}$$

where A_i and B_i are $M \times M$ complex matrices, which depend on the distributed space time code, the 1 in the denominator scaling terms is the unity noise power, $(.)^*$ denotes the complex conjugate and P_2 is the average transmission power at every relay node. The received signal vector $\mathbf{y}$ at the receiver, assuming perfect synchronization between all the relays and the

destination node, is given by

$$\mathbf{y} = \sum_{i=1}^{R} h_{rid}\mathbf{t}_i + \mathbf{w}. \tag{2.2.3}$$

The special cases that either $A_i = 0_M$, B_i is unitary or $B_i = 0_M$ and A_i is unitary are considered, where 0_M represents the $M \times M$ zero matrix. $A_i = 0_M$ means that the i^{th} relay column of the code matrix only contains the conjugates $s_1^*, ..., s_M^*$ and $B_i = 0_M$ means that the i^{th} relay column contains only the information symbols $s_1, ..., s_M$. Thus the following variables are defined as [43]

$$\hat{A}_i = A_i, \quad \hat{h}_{sri} = h_{sri}, \quad \hat{\mathbf{v}}_i = \mathbf{v}_i, \quad \mathbf{s}^{(i)} = \mathbf{s}, \qquad \text{if } B_i = 0_M$$

$$\hat{A}_i = B_i, \quad \hat{h}_{sri} = h_{sri}^*, \quad \hat{\mathbf{v}}_i = \mathbf{v}_i^*, \quad \mathbf{s}^{(i)} = \mathbf{s}^*, \qquad \text{if } A_i = 0_M.$$

From (2.2.2),

$$\mathbf{t_i} = \sqrt{\frac{P_1 P_2 M}{P_1 + 1}}\hat{h}_{sri}\hat{A}\mathbf{s^{(i)}} + \sqrt{\frac{P_2}{P_1 + 1}}\hat{A}_i\hat{\mathbf{v}}_\mathbf{i}.$$

The signal vector at the receiver can be calculated from equations (2.2.1) and (2.2.3) to be

$$\mathbf{y} = \sqrt{\frac{P_1 P_2 M}{P_1 + 1}} S\mathbf{h} + \mathbf{w}_d^{'}, \tag{2.2.4}$$

where

$$S = [\hat{A}_1\mathbf{s}^{(1)} \ ... \ \hat{A}_R\mathbf{s}^{(R)}], \quad \mathbf{h} = [\hat{h}_{sr1}h_{r1d} \ ... \ \hat{h}_{srn}h_{rnd}]^T \tag{2.2.5}$$

and

$$\mathbf{w}_d^{'} = \sqrt{\frac{P_2}{P_1 + 1}} \sum_{i=1}^{R} h_{sri}\hat{A}_i\hat{\mathbf{v}}_i + \mathbf{w}. \tag{2.2.6}$$

Therefore, without decoding, the relays generate a space-time codeword S distributively at the receiver. The vector $\mathbf{h}$ is the equivalent channel and $\mathbf{w}_d^{'}$

is the equivalent noise. The optimum power allocation is when the transmitter uses half the total power and the relays share the other half [42]. If the total power is P and the number of relays is R, the average powers used at the source and relays are

$$P_1 = \frac{P}{2} \qquad \text{and} \qquad \mathrm{P}_2 = \frac{\mathrm{P}}{2\mathrm{R}}. \tag{2.2.7}$$

If the channel vector $\mathbf{h}$ is known at the receiver, the maximum-likelihood (ML) decoding is

$$\hat{\mathbf{s}} = \arg \min_{\mathbf{s}} ||\mathbf{y} - \sqrt{\frac{P_1 P_2 M}{P_1 + 1}}\ S\ \mathbf{h}||, \tag{2.2.8}$$

where $||.||$ denotes the Euclidean norm, and $arg\ min$ represents finding the smallest Euclidean norm from all possible S formed as in (2.2.5) from the source signal vectors $\mathbf{s}$ defined by the chosen source constellation.

2.2.2 Orthogonal and Quasi-Orthogonal Codes

A) Real Orthogonal Designs

For a real orthogonal distributed space-time code (ODSTC), in which every entry of the code matrix is a linear combination of the information symbols, then $B_i = 0_M$. Actually, from the definition of a real ODSTC, in [35] proves that A_i satisfies

$$\begin{cases} A_i^T A_i = kI_M \\ A_i^T A_j = -A_j^T A_i, \end{cases} \tag{2.2.9}$$

where I_M represents an $M \times M$ unity diagonal matrix. For the case that every symbol appears once only in each column, which is true for most real ODSTCs, A_i has the structure of a permutation matrix whose entries can

be 1, 0, or -1. For example, the application of the 2×2 real ODSTC is

$$S = \begin{bmatrix} s_1 & s_2 \\ -s_2 & s_1 \end{bmatrix}. \tag{2.2.10}$$

It can be applied in two relay schemes, and the matrices used at the relays are

$$A_1 = \begin{bmatrix} 1 & 0 \\ 0 & -1 \end{bmatrix} \quad \text{and} \quad A_2 = \begin{bmatrix} 0 & 1 \\ 1 & 0 \end{bmatrix}. \tag{2.2.11}$$

B) Complex Orthogonal Designs

Similarly, in a complex ODSTC, A_i needs to satisfy

$$\begin{cases} A_i^H A_i = kI_M \\ A_i^H A_j = -A_j^H A_i. \end{cases} \tag{2.2.12}$$

Taking the application of the 2×2 Alamouti ODSTC in [44] as an example, the matrices A_i and B_i which are used at the two relays become

$$A_1 = I_2,\ A_2 = B_1 = 0_2,\ B_2 = \begin{bmatrix} 0 & -1 \\ 1 & 0 \end{bmatrix}.$$

The space-time code word formed at the two relays has the following form:

$$S = \begin{bmatrix} s_1 & -s_2^* \\ s_2 & s_1^* \end{bmatrix}. \tag{2.2.13}$$

It is clear that the space-time code in (2.2.13) is the transpose of the Alamouti structure. By defining $\mathbf{s} = [s_1 \ -s_2^*]^T$, the Alamouti code is obtained which has the structure

$$S = \begin{bmatrix} s_1 & s_2 \\ -s_2^* & s_1^* \end{bmatrix}. \tag{2.2.14}$$

C) Quasi-Orthogonal Designs

For quasi-orthogonal designs in [45] and [46], the matrices A_i and B_i which are used at the four relays become

$$A_1 = I_4,\ A_2 = A_3 = B_1 = B_4 = 0_4,\ A_4 = \begin{bmatrix} 0 & 0 & 0 & 1 \\ 0 & 0 & -1 & 0 \\ 0 & -1 & 0 & 0 \\ 1 & 0 & 0 & 0 \end{bmatrix}$$

$$B_2 = \begin{bmatrix} 0 & -1 & 0 & 0 \\ 1 & 0 & 0 & 0 \\ 0 & 0 & 0 & -1 \\ 0 & 0 & 1 & 0 \end{bmatrix} \quad \text{and} \quad B_3 = \begin{bmatrix} 0 & 0 & -1 & 0 \\ 0 & 0 & 0 & -1 \\ 1 & 0 & 0 & 0 \\ 0 & 1 & 0 & 0 \end{bmatrix}.$$

It is straightforward to see $\hat{A}_i$ for $i = 1, 2, ..., 4$ are unitary, but they do not satisfy the second equation in (2.2.12), therefore the code is quasi-orthogonal. The space-time codeword formed at the four relays has the following form:

$$S = \begin{bmatrix} s_1 & -s_2^* & -s_3^* & s_4 \\ s_2 & s_1^* & -s_4^* & -s_3 \\ s_3 & -s_4^* & s_1^* & -s_2 \\ s_4 & s_3^* & s_2^* & s_1 \end{bmatrix}.$$

Again, it is the transpose of the originally proposed quasi-orthogonal code, and by using $\mathbf{s} = [s_1 \ -s_2^* \ -s_3^* \ s_4]^T$ the original form can be obtained. In the next section, distributed differential space-time coding will be described.

2.3 Differential Distributed Space-Time Coding

In Section 2.2, decoding the DSTC does require full channel information, both the channels from the source node to relay nodes and from the relay nodes to destination node, at the destination node. Therefore, the source

node and the relay nodes have to send training symbols. However, in some situations, because of the cost on time and power and the complexity of channel estimation, using training symbols is not desired [47]. Therefore, the distributed differential space-time coding (DDSTC) in [48] is a useful scheme to solve this problem, because the relay and destination nodes do not require such channel knowledge, however there is a performance loss in bit error rate of 3dB in the decoding process.

The scheme is based on the coherent distributed space-time coding in Section 2.2. The differential scheme uses two blocks that overlap by one block. The first is a reference block for the next. For generality, the $(n-1)^{th}$ and the n^{th} block are considered. According to (2.2.4) and (2.2.6), the received signal vector at the $(n-1)^{th}$ block can be written as

$$\mathbf{y}_d(n-1) = \sqrt{\frac{P_1 P_2 M}{P_1+1}} \left[\hat{A}_1\hat{\mathbf{s}}_1(n-1) \quad \hat{A}_2\hat{\mathbf{s}}_2(n-1)\right] \mathbf{h}(n-1) + \mathbf{w}'(n-1). \tag{2.3.1}$$

The set of possible information is encoded as a set of unitary matrices U, which for the Alamouti code [47], takes the form

$$U = \frac{1}{\sqrt{|s_1|^2 + |s_2|^2}} \begin{bmatrix} s_1 & -s_2^* \\ s_2 & s_1^* \end{bmatrix}, \tag{2.3.2}$$

where $|\cdot|$ denotes the modulus of a complex number. During block n, the signal vector sent by the transmitter is encoded differentially as

$$\mathbf{s}(n) = U(n)\mathbf{s}(n-1). \tag{2.3.3}$$

For the first block, $\mathbf{s}(1) = [1 \;\; 0]^T$ is a reference signal. Therefore, the received

signal vector at the n^{th} block can be written as

$$\mathbf{y}_d(n) = \sqrt{\frac{P_1 P_2 M}{P_1+1}} \left[\hat{A}_1 \hat{U}(n)\hat{\mathbf{s}}_1(n-1) \quad \hat{A}_2 \hat{U}(n)\hat{\mathbf{s}}_2(n-1)\right] \mathbf{h}(n) + \mathbf{w}'(n), \tag{2.3.4}$$

where $\hat{U}(n) = U(n)$ if $B_i = 0_2$ and $\hat{U}(n) = \overline{U(n)}$ if $A_i = 0_2$. If $U(n)\hat{A}_i = \hat{A}_i\hat{U}(n)$, or equivalently,

$$U(n)A_i = A_i U(n) \quad \text{and} \quad U(n)B_i = B_i\overline{U(n)}, \tag{2.3.5}$$

therefore,

$$\mathbf{y}_d(n) = \sqrt{\frac{P_1 P_2 M}{P_1+1}} U(n) \left[\hat{A}_1 \hat{\mathbf{s}}_1(n-1) \quad \hat{A}_2 \hat{\mathbf{s}}_2(n-1)\right] \mathbf{h}(n) + \mathbf{w}'(n).$$

The channel coefficients $h_{s,ri}$ and $h_{ri,d}$ are assumed to be constant over at least two blocks, i.e., $\mathbf{h}(n) = \mathbf{h}(n-1)$, therefore,

$$\mathbf{y}_d(n) = U(n)\mathbf{y}_d(n-1) + \mathbf{w}''(n),$$

where

$$\mathbf{w}''(n) = \mathbf{w}'(n) - U(n)\mathbf{w}'(n-1).$$

The ML decoding can be applied as

$$\hat{U}(n) = \arg\max_{U(n)} \left\|\mathbf{y}_d(n) - U(n)\mathbf{y}_d(n-1)\right\|, \tag{2.3.6}$$

which needs no channel information. In the next section, methods to analyze the performance of cooperative networks are presented.

2.4 Performance Analysis of Wireless Cooperative Networks

In wireless cooperative networks, signal fading arising from multipath propagation is a particularly severe channel impairment that can be mitigated through the application of diversity [49]. Compared with the more conventional forms of single-user space diversity with physical arrays, this section sets up the classical relay channel model and examines the problem of creating and exploiting space diversity using a collection of distributed antennas belonging to multiple terminals. This formula of space diversity is defined as cooperative diversity, because the terminals share their antennas and other resources to create a virtual antenna array through distributed transmission and signal processing [16]. Therefore, pairwise error probability (PEP) analysis is an important method to analyze the cooperative diversity and will be explained in this section. Furthermore, performance characterization in terms of outage events is also an important evaluation of robustness of transmission to fading, typically performed as outage probability analysis. Therefore, the outage probability analysis will be presented in this section.

2.4.1 Pairwise Error Probability Analysis

Chernoff Bound of General Communication System

The analysis of the Chernoff bound for a general communication network is briefly described. A random variable z is assumed together with function $f(z)$, which satisfies

$$f(z) \geq \begin{cases} 1 & z \geq 0 \\ 0 & z < 0. \end{cases} \tag{2.4.1}$$

If the mean of z always exists [50], the Chernoff bound implies that the following inequality always exists:

$$P(z > 0) \leq E(f(z)), \tag{2.4.2}$$

where $E(\cdot)$ represents the statistical expectation operation. Let $f(z) = exp(\lambda z)$, then the Chernoff bound becomes:

$$P(z > 0) \leq E(exp(\lambda z)), \tag{2.4.3}$$

where $\lambda > 0$. Then, a general point-to-point single antenna communication system is considered. The received signal is obtained as $y = hs + n$, where s is the transmission signal, h is the fading coefficient and n is a Gaussian random noise with the spectrum density of N_0 per dimension. And the maximum likelihood (ML) decoding is used as

$$\hat{s} = \arg \max_s P(y|s) = \arg \min_s |y - hs|^2. \tag{2.4.4}$$

For ML decoding, the decoder selects the symbol that has the minimum distance to the received signal. Therefore, the probability that the decoder chooses that an erroneous symbol s_e is transmitted, denoted by $P(s \rightarrow s_e|y, h)$, is given by:

$$P(s \rightarrow s_e|y, h) = P(|y - hs|^2 > |y - hs_e|^2) = P(|y - hs|^2 - |y - hs_e|^2 > 0). \tag{2.4.5}$$

Substituting (2.4.5) into the Chernoff bound of (2.4.3), yields:

$$P(s \rightarrow s_e|y, h) \leq E(exp(\lambda(|y - hs|^2 - |y - hs_e|^2))). \tag{2.4.6}$$

After some algebraic manipulation, (2.4.6) can be obtained as:

$$P(s \to s_e|y,h) \leq exp(-\lambda h^2(1-N_0\lambda)|s-s_e|^2), \tag{2.4.7}$$

where $\lambda = 1/2N_0$, then

$$P(s \to s_e|y,h) \leq exp(-\frac{1}{4N_0}h^2|s-s_e|^2). \tag{2.4.8}$$

Similarly, for a multiple antenna space-time coded system, the transmitted codeword, channel and noise terms become matrices, namely S, H and N, respectively. And the received signal matrix can be represented as:

$$Y = HS + N. \tag{2.4.9}$$

Therefore, the upper bounded PEP of the decoding error can be calculated by using the same method as [42]:

$$P(S \to S_e|Y,H) \leq exp\left(-\frac{1}{4N_0}H^H(S-S_e)^H(S-S_e)H\right). \tag{2.4.10}$$

In the next subsequent sections, the PEP upper bound of distributed space-time coding will be described.

PEP Upper Bound for a Distributed Space-Time Code

This section employs the Chernoff bound to derive the PEP upper bound for an AF type DSTC network. Since in (2.2.6) $\hat{A}_i$ are unitary and ω_j, ν_i the elements of $\mathbf{w}$ and $\hat{\mathbf{v}}_i$ are independent Gaussian random variables, $\mathbf{w}_d^{'}$ is a Gaussian random vector when the $h_{s,ri}$ are known. It is clear that $E(\mathbf{w}_d^{'}) = 0_{M,1}$ and $Covar(\mathbf{w}_d^{'}) = \left(1 + \frac{P_2}{P_1+1}\Sigma_{i=1}^{R}|h_{rid}|^2\right) I_M$. Thus, $\mathbf{w}_d^{'}$ is both spatially and temporally white.

Define $S = [\hat{A}_1\mathbf{s}^{(1)} \ ... \ \hat{A}_R\mathbf{s}^{(R)}]$ as in (2.2.5). Therefore, S is an element matrix in the distributed space-time code set. When both $\hat{h}_{sri}$ and h_{rid} are

known, $\mathbf{x}|\mathbf{s}^{(i)}$ is also a Gaussian random vector with a covariance matrix $\left(1+\frac{P_2}{P_1+1}\Sigma_{i=1}^{R}|h_{rid}|^2\right)I_M$ and mean $\sqrt{\frac{P_1P_2M}{P_1+1}}S\mathbf{h}$. Then,

$$P(\mathbf{x}|\mathbf{s}^{(i)}) = \frac{e^{-\frac{\left(x-\sqrt{\frac{P_1P_2M}{P_1+1}}S\mathbf{h}\right)^H\left(x-\sqrt{\frac{P_1P_2M}{P_1+1}}S\mathbf{h}\right)}{1+\frac{P_2}{P_1+1}\Sigma_{i=1}^{R}|h_{rid}|^2}}}{\pi^M\left(1+\frac{P_2}{P_1+1}\Sigma_{i=1}^{R}|h_{rid}|^2\right)^M}. \tag{2.4.11}$$

The ML decoding of the system can be seen to be

$$\hat{\mathbf{s}} = \arg\ \max_{\mathbf{s}} P(\mathbf{x}|\mathbf{s}^{(i)}) = \arg\ \min_{\mathbf{s}} ||\mathbf{y} - \sqrt{\frac{P_1P_2M}{P_1+1}}\ S\ \mathbf{h}||. \tag{2.4.12}$$

Since S is linear in $\mathbf{s}^{(i)}$, by splitting the real and imaginary parts, the decoding is equivalent to the decoding of a real linear system. Therefore, sphere decoding can be used [51] and [52].

According to the Chernoff bound, with the ML decoding in (2.4.12), the PEP, averaged over the channel coefficients, of mistaking $\mathbf{s}^{(i)}$ by $\mathbf{s}^{(e)}$ has the bound [42]:

$$P(S\rightarrow S_e|Y,\mathbf{h}) \leq exp\left(-\frac{P_1P_2M}{4(1+P_1+P_2\Sigma_{i=1}^{R}|h_{rid}|^2)}\mathbf{h}^H(S-S_e)^H(S-S_e)\mathbf{h}\right). \tag{2.4.13}$$

Integrating over $\hat{h}_{sri}$, yields

$$P(S\rightarrow S_e|Y,h_{rid},i=1,..,N) \leq det^{-1}\left[I_R+\frac{P_1P_2M}{4(1+P_1+P_2g)}CG\right], \tag{2.4.14}$$

where $C=(S-S_e)^H(S-S_e)$, $G=diag\{|h_{r1,d}|^2,...,|h_{rn,d}|^2\}$ and $g=\Sigma_{i=1}^{R}|h_{rid}|^2$, and $det(.)$ and $diag(.)$ denote the matrix determinant and diagonal matrix, respectively. In order to derive the final PEP upper bound, average (2.4.14) over $h_{rid}, i=1,...,N$. Unfortunately, the expectations over all h_{rid} are difficult to calculate in a closed form, therefore, some approximation

has to be considered. Note that $g = \Sigma_{i=1}^{R} |h_{rid}|^2$ is Gamma distributed [53]:

$$f(g) = \frac{g^{N-1} e^{-g}}{(N-1)!}, \tag{2.4.15}$$

whose mean and variance are both N. For large N, g can be approximated by its mean, that is $g \approx N$ [42]. Therefore, (2.4.14) becomes

$$P(S \to S_e | Y, h_{rid}, i = 1, .., N) \leq det^{-1} \left[I_R + \frac{P_1 P_2 M}{4(1 + P_1 + P_2 N)} CG \right], \tag{2.4.16}$$

which is minimized when $\frac{P_1 P_2 M}{4(1+P_1+P_2 N)}$ is maximized. Assume $P = P_1 + N P_2$ is the total power in the whole network. Therefore,

$$\frac{P_1 P_2 M}{4(1 + P_1 + P_2 N)} = \frac{P_1 (P - P_1) M}{4R(1 + P)} \leq \frac{P^2 M}{16R(1 + P)},$$

with equality when

$$P_1 = \frac{P}{2} \quad \text{and} \quad P_2 = \frac{P}{2N}. \tag{2.4.17}$$

Thus, the optimal power allocation strategy allocates half of the total power to the source and the relays share the other half. Finally, substituting (2.4.17) into (2.4.16), gives

$$P(S \to S_e | Y, h_{rid}, i = 1, .., N) \leq det^{-1} \left[I_R + \frac{PM}{16N} CG \right]. \tag{2.4.18}$$

Then, integrating the above equation with respect to $|h_{rid}|^2$ and assuming that C is a full rank matrix and $M \geq N$, the average PEP of the distributed space-time coding can be approximated as: [42]

$$P(S \to S_e | Y) \leq det^{-1}[C] \left(\frac{8N}{M} \right)^N P^{-N(1 - \frac{loglogP}{logP})}. \tag{2.4.19}$$

Therefore, the diversity order of DSTC is $N(1 - \frac{loglogP}{logP})$ when C is a full rank matrix and $M \geq N$. When P is very large, $\frac{loglogP}{logP} \to 0$, and the asymptotic

diversity order is N. However, when $M \geq N$ is assumed, for the general case, the rank of C will be $min(M, N)$ instead of N, therefore, the diversity order achieved by the DSTC is $min(M, N)(1 - \frac{loglogP}{logP})$. Next, the outage probability analysis for certain cooperative networks is considered.

2.4.2 Outage Probability Analysis

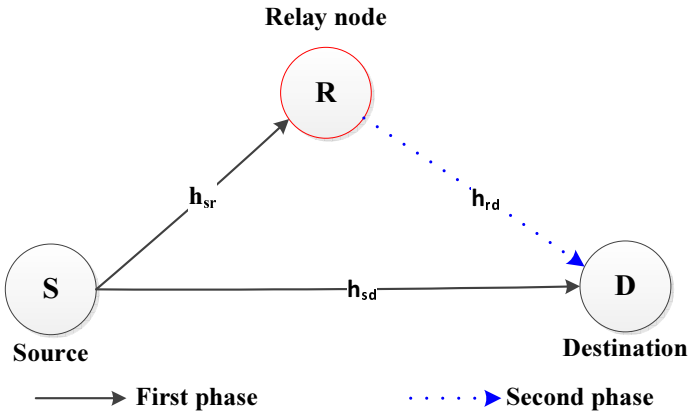

Figure 2.2. *A basic wireless cooperative network with a direct link and single relay node.*

In this section, outage events and outage probabilities are shown to characterize performance of the system in Figure 2.2, which denotes the basic cooperative network including a direct link. According to different types of processing by the relay node and different types of combining at the destination node, the outage probability analysis of the direct link, fixed, selection and incremental relaying will be discussed, respectively; I denotes the mutual information, and for a target rate R, $I < R$ and $P(I < R)$ denote the outage event and outage probability, respectively.

A. Direct transmission

For the direct transmission case, the source transmits directly the signal to the destination node, the relay node is not working at the same time, therefore, the maximum average mutual information between input and output

is given by

$$I_D = log_2(1 + SNR|h_{sd}|^2). \tag{2.4.20}$$

The outage event for spectral efficiency R is given by $I_D < R$ and is equivalent to the event

$$|h_{sd}|^2 < \frac{2^R - 1}{SNR}. \tag{2.4.21}$$

For Rayleigh fading, i.e., $|h_{sd}|^2$ is exponentially distributed with parameter σ_{sd}^{-2}, the outage probability satisfies

$$\begin{aligned} P_D^{out}(SNR, R) &= P(I_D < R) = P(|h_{sd}|^2 < \frac{2^R - 1}{SNR}) \\ &= 1 - exp(-\frac{2^R - 1}{SNR\sigma_{sd}^2}) \approx \frac{1}{\sigma_{sd}^2} \cdot \frac{2^R - 1}{SNR}, \end{aligned} \tag{2.4.22}$$

where σ_{sd}^2 is the channel variance from the source to the destination. Obviously, the outage probability is inversely proportional both to SNR and to channel variance σ_{sd}^2.

B. Fixed relaying

For fixed relaying, the relay can either amplify its received signals subject to its power constraint, or to decode, re-encode, and retransmit the messages.

1) Amplify and forward: the AF scheme with a direct link and transmission over two time slots produces an equivalent one-input, two-output complex Gaussian noise channel with different noise levels in the outputs, and the maximum average mutual information between input and output is given by

$$I_{AF} = \frac{1}{2} log_2(1 + SNR|h_{sd}|^2 + f(SNR|h_{sr}|^2, SNR|h_{rd}|^2)), \tag{2.4.23}$$

where $f(x, y) = \frac{xy}{x+y+1}$. The outage event for spectral efficiency R is given by $I_D < R$ and is equivalent to the event

$$|h_{sd}|^2 + \frac{1}{SNR} f(SNR|h_{sr}|^2, SNR|h_{rd}|^2)) < \frac{2^{2R} - 1}{SNR}. \tag{2.4.24}$$

For Rayleigh fading, i.e., $|h_{ij}|^2$ is exponentially distributed with parameter σ_{ij}^{-2}, the outage probability satisfies [16]

$$P_{AF}^{out}(SNR, R) = P(I_{AF} < R) \approx (\frac{\sigma_{sr}^2 + \sigma_{rd}^2}{2\sigma_{sd}^2\sigma_{sr}^2\sigma_{rd}^2})(\frac{2^{2R}-1}{SNR})^2, \tag{2.4.25}$$

where σ_{ij}^2, $i \in (s, r)$ and $j \in (r, d)$, are the channel variances.

2) Decode and forward: A particular decoding structure is applied at the relay in order to analyze DF transmission. In [16], the maximum average mutual information for repetition-coded DF can be shown to be

$$I_{DF} = \frac{1}{2} min\{log_2(1 + SNR|h_{sr}|^2), log_2(1 + SNR|h_{sd}|^2 + SNR|h_{rd}|^2)\}, \tag{2.4.26}$$

where the first term of (2.4.26) denotes the maximum rate at which the relay can reliably decode the source message, and the second term of (2.4.26) represents the maximum rate at which the destination can reliably decode the source message given repeated transmissions from the source and relay. The outage event for spectral efficiency R is given by $I_{DF} < R$ and is equivalent to the event

$$min\{|h_{sr}|^2, |h_{sd}|^2 + |h_{rd}|^2\} < \frac{2^{2R}-1}{SNR}. \tag{2.4.27}$$

For Rayleigh fading, the outage probability for repetition-coded DF can be computed as [16]

$$\begin{aligned} P_{DF}^{out}(SNR, R) &= P(I_{DF} < R) = P(|h_{sr}|^2 < \frac{2^{2R}-1}{SNR}) \\ &+ P(|h_{sr}|^2 \geq \frac{2^{2R}-1}{SNR}) P(|h_{sd}|^2 + |h_{rd}|^2 < \frac{2^{2R}-1}{SNR}), \end{aligned} \tag{2.4.28}$$

when $SNR \to \infty$, this becomes

$$P_{DF}^{out}(SNR, R) \approx \frac{2^{2R}-1}{\sigma_{sr}^2 SNR}, \tag{2.4.29}$$

where σ_{sr}^2 is channel variance from the source to the relay. Clearly, the

outage probability is inversely proportional both to SNR and to channel variance σ_{sr}^2.

C. Selection relaying

Selection relaying builds upon fixed relaying by allowing transmitting nodes to choose a suitable cooperative or noncooperative action according to the measured SNR. Selection relaying can be applied to overcome the weakness of the DF transmission in [16], i.e. when the relay cannot decode, direct transmission is implemented. As an example analysis, considering the performance of selection DF, its mutual information is somewhat involved to write down in general; however, in the case of repetition coding at the relay, using (2.4.20) and (2.4.26), it can be shown [16] to be

$$I_{SDF} = \begin{cases} \frac{1}{2} log_2(1 + 2SNR|h_{sd}|^2), & |h_{sr}|^2 < \frac{2^{2R}-1}{SNR} \\ \frac{1}{2} log_2(1 + SNR|h_{sd}|^2 + SNR|h_{rd}|^2), & |h_{sr}|^2 \geq \frac{2^{2R}-1}{SNR}. \end{cases} \tag{2.4.30}$$

In the first case in (2.4.30), the relay can not decode and the source must repeat its transmission. Therefore, the mutual information is that of repetition coding from the source to the destination, hence the extra factor of two in the SNR. Similarly, for the second case in (2.4.30), the mutual information is that of repetition coding from the source and relay to the destination. The outage event for spectral efficiency R is given by $I_{SDF} < R$ and is equivalent to the event

$$\begin{aligned} &(\{|h_{sr}|^2 < \frac{2^{2R}-1}{SNR}\} \bigcap \{(2|h_{sd}|^2 < \frac{2^{2R}-1}{SNR}\}) \bigcup \\ &(\{|h_{sr}|^2 \geq \frac{2^{2R}-1}{SNR}\} \bigcap \{|h_{sd}|^2 + |h_{rd}|^2 < \frac{2^{2R}-1}{SNR}\}), \end{aligned} \tag{2.4.31}$$

where $\bigcap$ and $\bigcup$ denote "OR" and "AND" operations. Because the events in the union of (2.4.31) are mutually exclusive, the outage probability becomes

a sum

$$P_{SDF}^{out}(SNR,R) = P(I_{SDF} < R) = P(|h_{sr}|^2 < \frac{2^{2R}-1}{SNR})P(2|h_{sd}|^2 < \frac{2^{2R}-1}{SNR}) + P(|h_{sr}|^2 \geq \frac{2^{2R}-1}{SNR})P(|h_{sd}|^2 + |h_{rd}|^2 < \frac{2^{2R}-1}{SNR}), \quad (2.4.32)$$

when $SNR \to \infty$, it becomes approximately

$$P_{SDF}^{out}(SNR,R) \approx (\frac{\sigma_{sr}^2 + \sigma_{rd}^2}{2\sigma_{sd}^2\sigma_{sr}^2\sigma_{rd}^2})(\frac{2^{2R}-1}{SNR})^2. \quad (2.4.33)$$

where σ_{ij}^2, $i \in (s,r)$ and $j \in (r,d)$, are the channel variances. Clearly, for large SNR, the performance of selection DF is identical to that of fixed AF. In the next subsection uncoded and coded transmission schemes will be introduced.

2.4.3 Coding Gain

Coding gain is the measure in the difference between the SNR levels between the uncoded system and coded system required to reach the same BER levels. It also can reduce error rate to improve system performance, however, compared with diversity gain, the nature of coding gain is different. Diversity gain attests itself by increasing the magnitude of the slope of the BER curve, whereas coding gain generally just shifts the error rate curve to the left [4], see Figure 2.3. In space-time coding the number of uncorrelated paths over which the code is transmitted determines the diversity gain; for example for a two transmitter one receive scenario with the Alamouti code the diversity gain is two, but there is no coding gain, whereas for the QO-STBC code with a four transmitter and one receiver situation the diversity gain is four. In the following section, convolution coding will be briefly introduced.

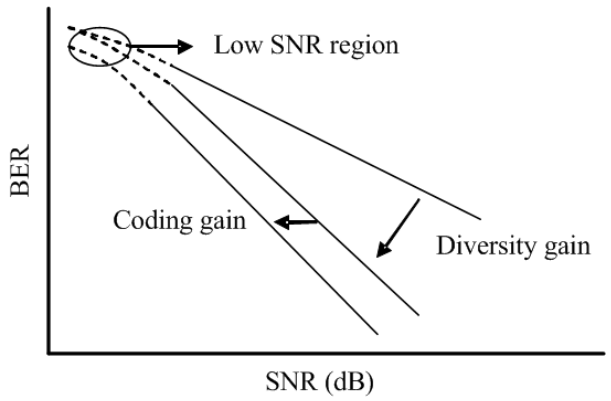

Figure 2.3. *The difference in the effects of coding gain and diversity gain on bit error rate.*

2.4.4 Convolution Coding

Convolutional codes are used extensively in practical applications in order to achieve reliable data transfer, i.e. third generation (3G) cellular communication system. A convolution code generates coded symbols by passing the information bits through a linear finite-state shift register as shown in Figure 2.4. The shift register consists of K stages with k bits per stage. There are n binary addition operations with input taken from all K stages: these operators produce a codeword of length n for each k bit input sequence. Moreover, the rate of the code is k/n, because the binary input data are shifted into each stage of the shift register k bits at a time, and each of these shifts produces a coded sequence of length n. The number of shift register stages K is called the constraint length. A half rate $(n = 2, k = 1, K = 3)$ convolution coding will be used to improve the BER performance. A well known scheme can be employed to decode the convolution coding, which is the Viterbi algorithm, full details of which can be found in [54]. To obtain increased coding gain iterative decoding can be employed, a review of which is given in the next section.

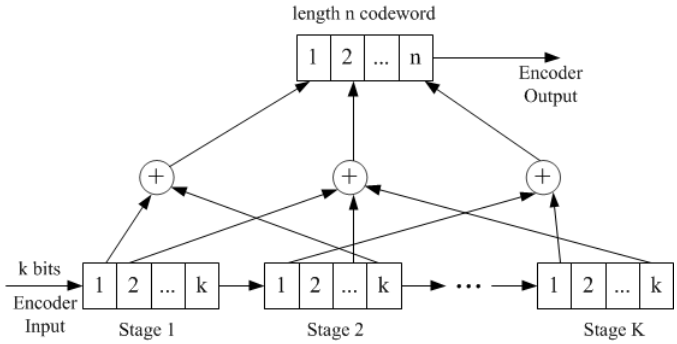

Figure 2.4. *Convolution encoder structure.*

2.4.5 Constituent Encoders

Due to the operation of the decoder, convolutional codes are most advantageous due to the existence of maximum a posteriori (MAP) soft decoding algorithms. While all block codes can be described with a trellis, the number of states in this trellis could be large. For convolutional codes, the trellis descriptions are known and the number of states is fixed by the memory order of the encoder. Throughout the literature, recursive systematic convolutional (RSC) encoders have been primarily used in the turbo schemes. Moreover, the infinite impulse response (IIR) nature of these encoders allows for interleaver designs which obtain large global Hamming distances for the turbo code [55]. For example, consider the four-state RSC with generator (5,7) shown in Figure 2.5. This encoder has a feedback polynomial and parity polynomial which are $g_b = 1 + D^2$ and $g_a = 1 + D + D^2$, where D represents time delay.

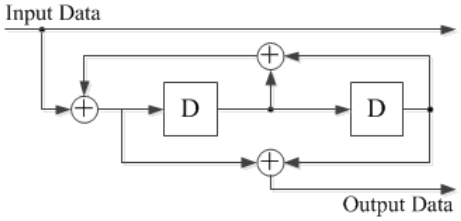

Figure 2.5. *A 4-state, half rate RSC structure with generator polynomial (5,7).*

In the next section, Jacket space-time coding scheme will be compared with the orthogonal coding scheme.

2.5 Jacket Space-Time Coding Scheme

In this section, the performance of space-time coding schemes based on the recently proposal jacket transform and quasi-orthogonal (QO) designs over multiple-input single-output(MISO) point-to-point and equivalent distributed, two-hop, systems are compared. In the comparison over both frequency flat and frequency selective channels the total transmit power is fixed and uncoded quadrature phase shift keying (QPSK) transmission is used. Simulation studies in terms of bit error rate confirm that the closed-loop QO designs yields the best performance and that the jacket transform has worse performance than all open-loop QO designs, and therefore its suitability for space-time code design for four transmit antennas is limited.
Signal transmission through a wireless channel faces more difficulties than through a guided wire, which can be approximately free of interference. These obstructions may include additive noise, fading, adjacent channel interference and multi-path spread. Nowadays, due to the desire to support user freedom from being physically connected, a wireless channel has become the favourable platform to transfer information.

In wireless communications, multiple-input multiple-output (MIMO) type systems have been shown to provide robustness to fading as compared to a single-antenna communication system by exploiting spatial diversity [46] at the expense of increased transmit and receive hardware. In order to utilize this diversity space-time block coding (STBC) has received significant attention [44]. Typically, STBC has been designed for point-to-point MIMO systems. However, due to physical space limitations, the paths between antennas are generally correlated, and therefore diversity gain is degraded.

Over the last ten years various schemes have been proposed for STBC, the Alamouti scheme being the simplest approach for two transmit antennas. Schemes for four transmit antennas were proposed by Jafarkhani and others [43] to obtain larger diversity gain. Very recently, in [56], the jacket transform has been proposed for point-to-point and distributed STBC [57]. However, a fair comparison of these schemes has not been undertaken. For fair comparison, the total power of all transmit antennas should be equal. In this section, the jacket transform and QO designs using the same total average power allocation and the uncoded QPSK constellation are compared.

2.5.1 Space-time block codes

Alamouti Design

The Alamouti scheme provides full diversity $2M_r$, where M_r is the number of receive antennas, one in this work, full data rate and improves the quality of the received signal by transmitting signals across two transmit antennas and M_r receiver antennas with two different time symbol periods. Perfect channel knowledge is assumed at the receiver and no knowledge of channel state information (CSI) at the transmitter is assumed. The open-loop Alamouti space time encoder uses the simple orthogonal code given as

$$C_A = Q_{12} = \begin{bmatrix} x_1 & x_2 \\ -x_2^* & x_1^* \end{bmatrix} \tag{2.5.1}$$

where the columns of the matrix represent the number of transmitter antennas and the rows represent the number of time symbol periods. The orthogonality of the columns can be verified by calculating the inner product of the columns as

$$(x_1, -x_2^*).(x_2, x_1^*) = x_1 x_2^* - x_2^* x_1 = 0 \tag{2.5.2}$$

which is the basis for the orthogonality of the code [44]. Moreover, $Q_{12}^H Q_{12} = \alpha I$, where $\alpha = |x_1|^2 + |x_2|^2$ and therefore symbolwise decoding is possible. This code is only suitable for two transmit antennas so we consider extensions for four antennas in order to increase diversity gain.

Quasi Orthogonal Designs

An introduction of the class of STBC based on QO designs for four transmit antennas can be generated by [45] as:

$$C_{QO} = \begin{pmatrix} Q_{12} & Q_{34} \\ -Q_{34}^* & Q_{12}^* \end{pmatrix} \tag{2.5.3}$$

so that the QO transmit matrix is

$$C_{QO} = \begin{pmatrix} x_1 & x_2 & x_3 & x_4 \\ -x_2^* & x_1^* & -x_4^* & x_3^* \\ -x_3^* & -x_4^* & x_1^* & x_2^* \\ x_4 & -x_3 & -x_2 & x_1 \end{pmatrix}. \tag{2.5.4}$$

This matrix is not orthogonal and therefore symbolwise decoding is not possible, however it is full rate. Schemes to perform pairwise decoding have been proposed [45] but these are more computationally complex; constellation rotation can be used at the transmitter to improve performance.

Jacket Transform Designs

Recently, a new transmit code matrix for the four transmit antennas case has been designed on the basis of the matrix product [56]

$$C_J = M_4 S_J, \tag{2.5.5}$$

where

$$S_J = \begin{pmatrix} Q_{12} & 0 \\ 0 & Q_{34} \end{pmatrix} \tag{2.5.6}$$

and $S_J^H S_J = diag(Q_{12}^H Q_{12}, Q_{34}^H Q_{34})$. In [56], it is shown if Q_{ij} is an orthogonal design, S_J is an orthogonal STBC, whereas, if Q_{ij} is a quasi-orthogonal matrix, S_J is a quasi-orthogonal STBC. So the properties of the matrix S_J depends on Q_{ij}, but, in this section the orthogonal STBC is adopted.

In the proposed approach, the code matrix C_J may be written as

$$C_J = M_4 \begin{bmatrix} Q_{12} & 0 \\ 0 & Q_{34} \end{bmatrix} \tag{2.5.7}$$

where

$$M_4 = \begin{pmatrix} 1 & 1 & 1 & 1 \\ 1 & -1 & 1 & -1 \\ 1 & 1 & -1 & -1 \\ 1 & -1 & -1 & 1 \end{pmatrix} \tag{2.5.8}$$

which is the 4×4 Hadamard matrix [56], and the transmit matrix

$$C_J = \begin{pmatrix} x_1 - x_2^* & x_2 + x_1^* & x_3 - x_4^* & x_4 + x_3^* \\ x_1 + x_2^* & x_2 - x_1^* & x_3 + x_4^* & x_4 - x_3^* \\ x_1 - x_2^* & x_2 + x_1^* & -x_3 + x_4^* & -x_4 - x_3^* \\ x_1 + x_2^* & x_2 - x_1^* & -x_3 - x_4^* & -x_4 + x_3^* \end{pmatrix} \tag{2.5.9}$$

which is an orthogonal code matrix as

$$C_J^H C_J = \begin{pmatrix} b_0 & 0 & 0 & 0 \\ 0 & b_0 & 0 & 0 \\ 0 & 0 & b_1 & 0 \\ 0 & 0 & 0 & b_1 \end{pmatrix}, \tag{2.5.10}$$

where $b_0 = 4\sum_{i=1}^{2}|x_i|^2$, $b_1 = 4\sum_{i=3}^{4}|x_i|^2$, but the elements of C_J are no longer from the QPSK constellation. Next, the transmission models which will use to compare the QO and jacket designs are presented.

2.5.2 Transmission schemes

Point-to-Point: Frequency Flat and Frequency Selective Channels.

A multi-input single-output (MISO) communication system with four transmit and one receive antennas is considered. The channels between the transmitters and receiver are denoted by $f_i, i = 1, 2, ..., 4$ as shown in Figure 2.6, which are assumed to be quasi static Rayleigh fading, and frequency flat or frequency selective with L paths [58]. The noise n at the receiver is complex zero mean Gaussian distributed with variance $\frac{N_0}{2}$ per dimension.

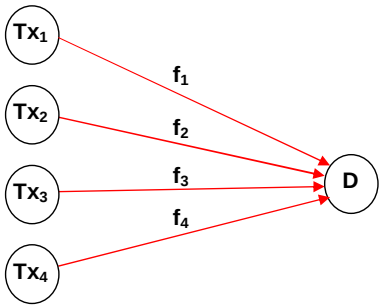

Figure 2.6. *Basic MISO structure of point-to-point transmission for four transmit and one receive antennas.*

Distributed relay network: Frequency Flat and Frequency Selective Links.

A wireless relay network as represented in Figure 2.7 with relay nodes R_i, $i = 1, 2$ and source and destination nodes are considered in this section. Each relay node has one receive antenna and two transmit antennas which operate in a half-duplex mode. For simplicity, the channel coefficients are unchanged during the transmission of a signal code block (quasi-static Rayleigh distributed). Denote the fading channel between S and the i-th relay as g_i,

$i = 1, 2$. And the fading channels between relays and D as f_j, $j = 1, 2, 3, 4$. Assume that g_i, and f_j are independent and identically distributed zero-mean complex Gaussian random variables with unity variance (i.e., $\sigma^2 = 1$). And the distance from the source node S to the destination node D is so far that S can not reliably communicate with D directly. At S, the information sequences are first broadcasted to the relay nodes R. Then, during the second stage, at the relay nodes, the received signals are decoded and space-time coded as in the point-to-point case before being forwarded to D. In the case of frequency selective links the coding is performed across fre-

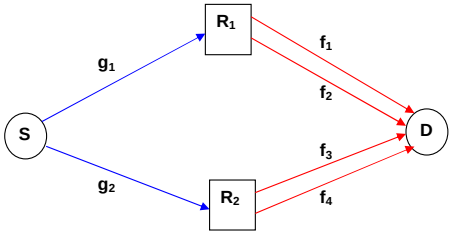

Figure 2.7. *Basic structure of two-hop relay network for two relays each using one receive and two transmit antennas.*

quencies, i.e. space-frequency coding is used, so that the spatial diversity is exploited, we do not exploit the temporal diversity in this context [4].

2.5.3 Simulation Results

In this section, the performance of the MATLAB based simulations of the proposed jacket transform and QO designs over the point-to-point and distributed systems for frequency flat and frequency selective channels are provided. The total transmit power is fixed over all designs, and the performance is shown by the end-to-end bit error rate (BER) using uncoded QPSK symbols.

In Figure 2.8 the point-to-point BER performance of STBC with open-loop and closed-loop designs is shown. The QO schemes clearly outperform the jacket transform. For example to attain a BER 10^{-4} approximately

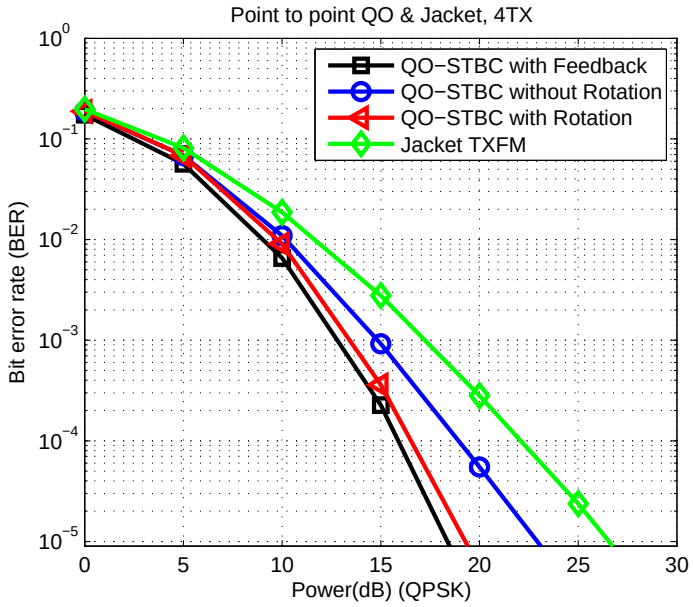

Figure 2.8. *Point-to-Point BER performance comparison of QO and jacket STBC schemes.*

$22dB$ total power is required in the case of the jacket transform, however, in the case of QO-STBC with feedback approximately $16dB$ is required, about $6dB$ less than the jacket transform design. The open-loop QO designs with and without symbol rotation also require $5dB$ and $3dB$ less than the jacket approach. Similarly, the end-to-end bit error rates of the distributed

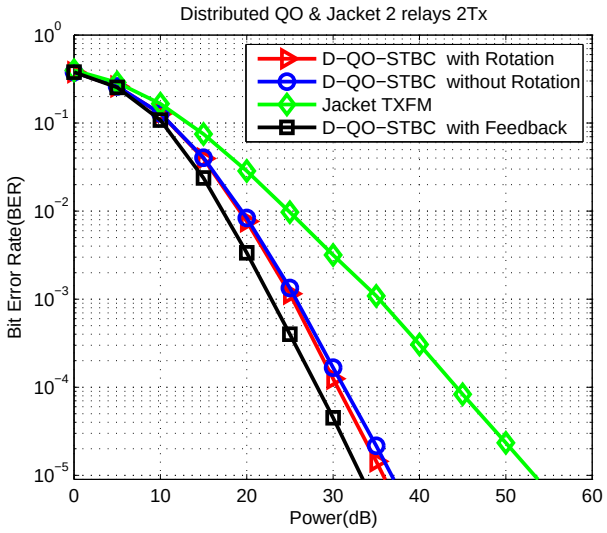

Figure 2.9. *End-to-end BER performance comparison of QO and jacket distributed STBC schemes.*

schemes are shown in Figure 2.9. The jacket transform again has the worst performance requiring $44dB$ total power at 10^{-4} BER, however, in the case of QO-STBC with feedback approximately $28dB$ is required, about $16dB$ less than the jacket transform design. The open-loop QO designs with and without symbol rotation also require $13dB$ less than the jacket approach.

In Figure 2.10 the point-to-point BER performance of SFBC over frequency selective links with channel length $L = 4$ is shown. The QO schemes clearly again outperform the jacket transform. For example to attain a BER 10^{-2} approximately $16dB$ total power is required in the case of the jacket transform, however, in the case of QO-SFBC with feedback approximately $11dB$ is required, about $5dB$ less than the jacket transform design. The open-loop QO designs with and without symbol rotation also require $4dB$

less than the jacket approach. Similarly, the end-to-end bit error rates of the distributed schemes are shown in Figure 2.11. The jacket transform again has the worst performance requiring $21dB$ total power at 10^{-2} BER, however, in the case of QO-SFBC with feedback approximately $18dB$ is required, about $3dB$ less than the jacket transform design. The open-loop QO designs with and without symbol rotation also require $2dB$ less than the jacket approach.

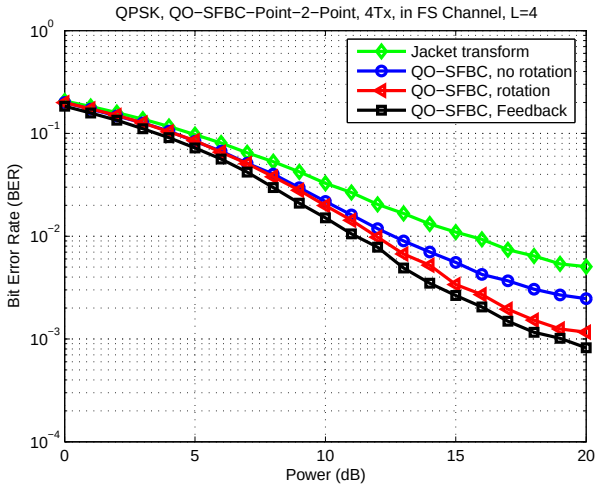

Figure 2.10. *Point-to-Point BER performance comparison of QO and jacket SFBC schemes.*

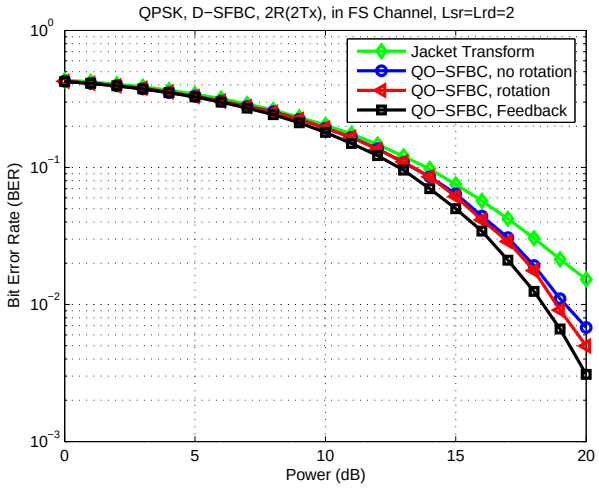

Figure 2.11. *End-to-end BER performance comparison of QO and jacket distributed SFBC schemes.*

The comparison of the performance of space-time and space-frequency coding schemes based on the recently proposed jacket transform and QO designs over point-to-point and distributed systems is provided. In the comparison the total transmit power is fixed and uncoded quadrature phase shift keying (QPSK) transmission is used. Simulation studies in terms of bit error rate confirm that the closed-loop QO designs yields the best performance and that the jacket transform has the weakest performance of designs. Its suitability for space-time code design for four transmit antennas appears therefore to be limited.

2.6 Summary

This chapter presented an overview of the various methodologies in cooperative networks that are of interest in the thesis. A brief introduction to distributed space-time coding schemes with orthogonal and quasi-orthogonal codes was given. An important method for distributed space-time coding, which does not need channel state information (CSI) at the receiver for decoding, which is differential space-time code, was discussed. This was followed by the performance analysis of cooperative networks. One approach was the pairwise error probability analysis, and the other was outage probability analysis. Finally, methods to achieve coding gain in transmission were considered. A simulation study was included to confirm the comparing the Jacket transform coding with other coding schemes. In the next chapter, in order to improve transmission rate in distributed space-time coding techniques, full interference cancellation and full self-interference cancellation schemes for synchronous systems will be described.

Chapter 3

A FULL RATE DISTRIBUTED TRANSMISSION SCHEME WITH INTERFERENCE

In this chapter, firstly, a simple full inter-relay self interference cancellation (FSIC) scheme is used at the relay nodes within a two-hop cooperative four relay network with asynchronism in the second stage. The four single antenna relay nodes are arranged as two spatially well separated groups of two relays with offset transmission scheduling. This approach can achieve the full available diversity order and its end-to-end transmission rate can asymptotically approach full rate when the number of samples is large. Pairwise error probability analysis is used to confirm the available diversity and simulation studies are employed to verify the end-to-end bit error rate as a function of the level of inter-relay interference. Secondly, a distributed differential space-time code is used with partial channel information at the destination, which can achieve full cooperation diversity and improve the transmission rate. Finally, uncoded and coded bit error rate simulations confirm the utility of the scheme.

3.1 Introduction

A cooperative network is one of the most popular approaches to exploit spatial diversity in wireless systems, in particular, through distributed space-time block coding [35], [43] and [44]. Relay nodes can not only provide independent channels between the source and the destination, to leverage spatial diversity [4], but they also can help two users with no or weak direct connection to attain a robust link. Although these schemes achieve the maximal cooperative diversity, i.e. in [44], the full diversity is two with two relays; the full diversity is four with closed feedback in [43], its end-to-end transmission rate is only a half. Therefore, offset transmission is an efficient method to improve the end-to-end transmission rate from a half to asymptotically unity.

3.2 FSIC for A Cooperative Four Relay Network

Jing and Hassibi in [42] proposed a new cooperative strategy, distributed space-time coding, which has two steps. However, this model lacks a direct link between the source node and the destination node. In [59] and [38] a direct link is consider, but the end-to-end transmission rate is only a half. In order to improve the transmission rate, an offset transmission scheme and full inter-relay interference cancellation has been applied in [60]. However, the interference cancellation is performed at the destination node, and so multiple antennas have to be used which maybe infeasible to achieve in practice. This problem is solved in [61] by using full inter-relay self interference cancellation at the relay nodes. However, in [61], the diversity order is only two without using an additional precoder scheme. In this work, therefore, an FSIC scheme is employed at the relay nodes so that the inter-relay interference (IRI) terms can be removed totally and diversity order 3.5 can be achieved without a precoder together with asymptotically full rate.

3.2.1 System Model

The relay model for the four-path relay scheme is illustrated in Figure 3.1, where $h_{sri} \sim CN(0, \gamma_{sri}^2)$ $(i = 1, ..., 4)$ denote the channels from the transmitter to the four relays and $h_{rid} \sim CN(0, \gamma_{rid}^2)$ $(i = 1, ..., 4)$ denote the channels from the four relays to the destination. It is assumed that only the inter-relay channels $h_{r1} \sim CN(0, \gamma_{r1}^2)$ and $h_{r2} \sim CN(0, \gamma_{r2}^2)$ are considered between R1 and R2 and between R3 and R4, respectively. This can be achieved in practice by constraining the locality of the relay pairs. And the inter-relay channels are assumed reciprocal. There is a direct link $h_{sd} \sim CN(0, \gamma_{sd}^2)$ between the source and the destination. The channels are quasi-static flat-fading: hence h_{sri}, h_{rid} and h_{sd} are independent and identically distributed (i.i.d.) zero-mean and unit-variance complex Gaussian random variables. The destination node is assumed to know perfectly all the channel coefficients. The relaying protocol is next defined.

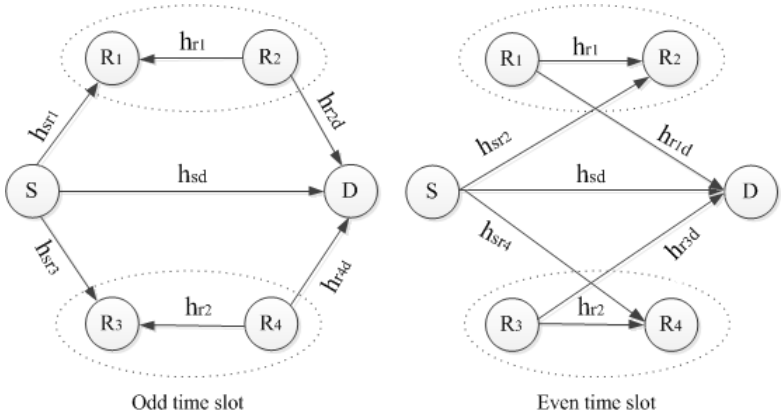

Figure 3.1. *AF four-path relaying scheme.*

3.2.2 Four-Path Relaying with Inter-Relay Interference Cancellation at the Relay

A) Transmission Protocol

At the source node, the source transmission is divided into frames, each containing L data vectors of the form

$$\mathbf{x}(l) = \begin{bmatrix} x_{1,R}(l) + jx_{1,I}(l) \\ x_{2,R}(l) + jx_{2,I}(l) \end{bmatrix} \text{ where } \ l = 1, 2, ..., L.$$

At the time slot 1, $\mathbf{x}(1)$ is sent from S to R1, R3 and D so that

$$\begin{aligned} \mathbf{y}_{r1}(1) &= \sqrt{\rho}\mathbf{x}(1)h_{sr1} + \mathbf{n}_{r1}(1) \\ \mathbf{y}_{r3}(1) &= \sqrt{\rho}\mathbf{x}(1)h_{sr3} + \mathbf{n}_{r3}(1) \\ \mathbf{y}_{d}(1) &= \sqrt{\rho}\mathbf{x}(1)h_{sd} + \mathbf{n}_{d}(1), \end{aligned}$$

where $\mathbf{n}_{ri}(1) \sim CN(\mathbf{0}, \sigma^2 I)$ and $\mathbf{n}_d(1) \sim CN(\mathbf{0}, \sigma^2 I)$ are the additive white Gaussian noise (AWGN) vectors at the i^{th} relay and D respectively for the 1^{st} time slot, and these noise terms take the same form for the later time slots. Notice that $\mathbf{y}_d(1)$ contains only $\mathbf{x}(1)$ because R2 and R4 do not transmit in the first time slot.

Then for time slot 2, $\mathbf{x}(2)$ is transmitted from S to D, R2 and R4; at the same time, the transmitted signal at R1 is sent to R2, the transmitted signal at R3 is sent to R4, which are respectively the inter-relay interferences.

$$\begin{aligned} \mathbf{y}_{r2}(2) &= \sqrt{\rho}\mathbf{x}(2)h_{sr2} + h_{r1}\mathbf{x}_{r1}(2) + \mathbf{n}_{r2}(2) \\ \mathbf{y}_{r4}(2) &= \sqrt{\rho}\mathbf{x}(2)h_{sr4} + h_{r2}\mathbf{x}_{r3}(2) + \mathbf{n}_{r4}(2) \\ \mathbf{y}_{d}(2) &= \sqrt{\rho}\mathbf{x}(2)h_{sd} + h_{r1d}\mathbf{x}_{r1}(2) + h_{r3d}\mathbf{x}_{r3}(2) + \mathbf{n}_{d}(2), \end{aligned}$$

where $\mathbf{x}_{r1}(2) = Ag_{r1}(2)\mathbf{y}_{r1}(1)$ and $\mathbf{x}_{r3}(2) = Bg_{r3}(2)\overline{\mathbf{y}_{r3}(1)}$. And matrices A

and B are used to encode the signals at the relay nodes, which are

$$A = \begin{bmatrix} 1 & 0 \\ 0 & 1 \end{bmatrix} \quad B = \begin{bmatrix} 0 & -1 \\ 1 & 0 \end{bmatrix}$$

and $g_{ri}(l)$ is the power scaling factor at the i^{th} relay, which will be defined later.

At time slot 3, $\mathbf{x}(3)$ is sent from S to D, R1 and R3, while $\mathbf{x}_{r2}(3)$ and $\mathbf{x}_{r4}(3)$ are sent from R2 to R1 and from R4 to R3, respectively, so that

$$\begin{aligned}\mathbf{y}_{r1}(3) =& \sqrt{\rho}\mathbf{x}(3)h_{sr1} + h_{r1}\mathbf{x}_{r2}(3) + \mathbf{n}_{r1}(3) = \sqrt{\rho}\mathbf{x}(3)h_{sr1} + Ah_{r1}g_{r2}(3) \\ & [\sqrt{\rho}\mathbf{x}(2)h_{sr2} + h_{r1}\mathbf{x}_{r1}(2) + \mathbf{n}_{r2}(2)] + \mathbf{n}_{r1}(3),\end{aligned}$$

$$\begin{aligned}\mathbf{y}_{r3}(3) =& \sqrt{\rho}\mathbf{x}(3)h_{sr3} + h_{r2}\mathbf{x}_{r4}(3) + \mathbf{n}_{r3}(3) = \sqrt{\rho}\mathbf{x}(3)h_{sr3} + Bh_{r2}g_{r4}(3) \\ & [\overline{\sqrt{\rho}\mathbf{x}(2)h_{sr4} + h_{r2}\mathbf{x}_{r3}(2) + \mathbf{n}_{r4}(2)}] + \mathbf{n}_{r3}(3) \\ & \mathbf{y}_d(3) = \sqrt{\rho}\mathbf{x}(3)h_{sd} + h_{r2d}\mathbf{x}_{r2}(3) + h_{r4d}\mathbf{x}_{r4}(3) + \mathbf{n}_d(3),\end{aligned}$$

where $\mathbf{x}_{r2}(3) = Ag_{r2}(3)\mathbf{y}_{r2}(2)$ and $\mathbf{x}_{r4}(3) = Bg_{r4}(3)\overline{\mathbf{y}_{r4}(2)}$. Notice that $\mathbf{y}_{r1}(3)$ and $\mathbf{y}_{r3}(3)$ contain the inter-relay self interference terms, $Ah_{r1}g_{r2}(3)h_{r1}\mathbf{x}_{r1}(2)$ and $Bh_{r2}g_{r4}(3)\overline{h_{r2}\mathbf{x}_{r3}(2)}$, respectively, which are known perfectly at R1 and R3, and thus can be removed. Therefore, the transmit signals at slot 4 from R1 and R3 will be

$$\begin{aligned}\mathbf{x}_{r1}(4) =& Ag_{r1}(4)[\mathbf{y}_{r1}(3) - Ah_{r1}g_{r2}(3)h_{r1}\mathbf{x}_{r1}(2)] = Ag_{r1}(4)\{\sqrt{\rho}\mathbf{x}(3)h_{sr1} \\ & + Ah_{r1}g_{r2}(3)[\sqrt{\rho}\mathbf{x}(2)h_{sr2} + \mathbf{n}_{r2}(2)] + \mathbf{n}_{r1}(3)\},\end{aligned} \tag{3.2.1}$$

and

$$\begin{aligned}\mathbf{x}_{r3}(4) =& Bg_{r3}(4)[\overline{\mathbf{y}_{r3}(3) - Bh_{r2}g_{r4}(3)\overline{h_{r2}\mathbf{x}_{r3}(2)}}] = Bg_{r3}(4)\{\overline{\sqrt{\rho}\mathbf{x}(3)h_{sr3}} \\ &+ \overline{Bh_{r2}g_{r4}(3)}[\sqrt{\rho}\mathbf{x}(2)h_{sr4} + \mathbf{n}_{r4}(2)] + \overline{\mathbf{n}_{r3}(3)}\}.\end{aligned} \tag{3.2.2}$$

At time slot 4, $\mathbf{x}(4)$ is sent from S to D, R2 and R4, while $\mathbf{x}_{r1}(4)$ and $\mathbf{x}_{r3}(4)$ are sent from R1 and R3. Therefore, at R2, R4 and D,

$$\begin{aligned}\mathbf{y}_{r2}(4) &= \sqrt{\rho}\mathbf{x}(4)h_{sr2} + h_{r1}\mathbf{x}_{r1}(4) + \mathbf{n}_{r2}(4) \\ \mathbf{y}_{r4}(4) &= \sqrt{\rho}\mathbf{x}(4)h_{sr4} + h_{r2}\mathbf{x}_{r3}(4) + \mathbf{n}_{r4}(4) \\ \mathbf{y}_{d}(4) &= \sqrt{\rho}\mathbf{x}(4)h_{sd} + h_{r1d}\mathbf{x}_{r1}(4) + h_{r3d}\mathbf{x}_{r3}(4) + \mathbf{n}_{d}(4).\end{aligned}$$

The transmit signals at time slot 5 from R2 and R4 are $\mathbf{x}_{r2}(5) = Ag_{r2}(5)\mathbf{y}_{r2}(4)$ and $\mathbf{x}_{r4}(5) = Bg_{r4}(5)\overline{\mathbf{y}_{r4}(4)}$, respectively. There is no inter-relay interference at R2 and R4 because $\mathbf{x}_{r2}(3)$ and $\mathbf{x}_{r4}(3)$ do not exist in the received signals due to the cancellation in R1 and R3 as shown in (3.2.1) and (3.2.2). Using the same method, L symbols will have been transmitted from the source to the destination.

From the equations above, the transmitted signals at R1, R2, R3 and R4 in the l^{th} time slot can be generalized as

$$\mathbf{x}_{r1}(l)\begin{cases} Ag_{r1}(l)\mathbf{y}_{r1}(l-1) & \text{for } l = 2 \\ Ag_{r1}(l)[\mathbf{y}_{r1}(l-1) - Ah_{r1}g_{r2}(l-1)h_{r1}\mathbf{x}_{r1}(l-2)], & \\ & \text{for } l = 4, 6, 8, ..., L, \end{cases}$$

$$\mathbf{x}_{r3}(l)\begin{cases} Bg_{r3}(l)\overline{\mathbf{y}_{r3}(l-1)} & \text{for } l = 2 \\ Bg_{r3}(l)[\overline{\mathbf{y}_{r3}(l-1) - Bh_{r2}g_{r4}(l-1)\overline{h_{r2}\mathbf{x}_{r3}(l-2)}}, & \\ & \text{for } l = 4, 6, 8, ..., L. \end{cases}$$

$\mathbf{x}_{r2}(l) = Ag_{r2}(l)\mathbf{y}_{r2}(l-1)$, $\mathbf{x}_{r4}(l) = Bg_{r4}(l)\overline{\mathbf{y}_{r4}(l-1)}$ for $l = 3, 5, 7, ..., L-1$,

respectively, where $g_{ri}(l)$ are defined as

$$g_{rm}(l)\begin{cases}\sqrt{\frac{\rho}{\gamma_{s,rm}^2\rho+\sigma^2}} & \text{for } l=2\\ \sqrt{\frac{\rho}{\gamma_{s,rm}^2\rho+\gamma_{rw}^2 g_{rn}^2(l-1)(\gamma_{s,rn}^2\rho+\sigma^2)+\sigma^2}} & \\ & \text{for } l=4,6,8,...,L,\end{cases}$$

$$g_{rn}(l)=\sqrt{\frac{\rho}{\gamma_{s,rn}^2\rho+\gamma_{rw}^2\rho+\sigma^2}},\quad \text{for}\quad l=3,5,7,...,L-1,$$

where $m=1$ or 3, $n=2$ or 4 and $w=1$ or 2. And ρ is the average transmitted power at the source and the four relays. The gains $g_{r2}(l)$ and $g_{r4}(l)$ are constant for $l=3,5,7,...,L-1$. Thus, $g_{r1}(l)$ and $g_{r3}(l)$ which depend on $g_{r2}(l-1)$ and $g_{r4}(l-1)$ are also constant for $l=4,6,...,L$, respectively. Therefore, the time index l can be removed hereafter.

B) Equivalent MIMO Channel

According to all the equations in Section 3.2.2-A, the received signal at the destination can be rewritten as

$$\mathbf{y}_d=\sqrt{\rho}\mathbf{H}\tilde{\mathbf{x}}+\mathbf{n}_d+\mathbf{C}\mathbf{n}_r \tag{3.2.3}$$

where $\mathbf{y}_d=[y_{d1}(1)\ y_{d2}(1)\ y_{d1}(2)\ y_{d2}(2)\ ...\ y_{d1}(L)\ y_{d2}(L)]^T$, and in order to analyze the pairwise error probability (PEP) and diversity order, rewrite the real and imaginary parts of the signals and the noise to be vectors, which are

$\tilde{\mathbf{x}}=[x_{1,R}(1)\ x_{2,R}(1)\ x_{1,R}(2)\ x_{2,R}(2)\ ...\ x_{1,R}(L)\ x_{2,R}(L)\ jx_{1,I}(1)\ jx_{2,I}(1)\ jx_{1,I}(2)\ jx_{2,I}(2)\ ...\ jx_{1,I}(L)\ jx_{2,I}(L)]^T$, $\mathbf{n}_d=[n_{d1,R}(1)\ n_{d2,R}(1)\ n_{d1,R}(2)\ n_{d2,R}(2)...\ n_{d1,R}(L)\ n_{d2,R}(L) jn_{d1,I}(1)\ jn_{d2,I}(1)\ jn_{d1,I}(2)\ jn_{d2,I}(2)\ ...\ jn_{d1,I}(L)\ jn_{d2,I}(L)]^T$ and $\mathbf{n}_r=[n_{r11,R}(1)\ n_{r12,R}(1)\ n_{r21,R}(2)\ n_{r22,R}(2)\ ...\ n_{r21,R}(L)\ n_{r22,R}(L)\ jn_{r11,I}(1)\ jn_{r12,I}(1)\ jn_{r21,I}(2)\ jn_{r22,I}(2)\ ...\ jn_{r21,I}(L)\ jn_{r22,I}(L)\ n_{r31,R}(1)\ n_{r32,R}(1)\ n_{r41,R}(2)\ n_{r42,R}(2)\ ...\ n_{r41,R}(L)\ n_{r42,R}(L)\ jn_{r31,I}(1)\ jn_{r32,I}(1)\ jn_{r41,I}$

(2) $jn_{r42,I}(2)$ ... $jn_{r41,I}(L)$ $jn_{r42,I}(L)]^T$. Let $H(p,q)$ and $C(p,q)$ denote the elements at the p^{th} row and q^{th} column of $\mathbf{H}$ and $\mathbf{C}$ respectively. Then, the non-zero elements of $\mathbf{H}$ and $\mathbf{C}$ are given as

$$H(m,m) = H(m,m+12) = h_{sd}, \quad m = 1,2,...,2L,$$

$$H(m,m-2) = H(m+1,m-1) = H(m+1,m+11) = H(m,m+10) = \begin{cases} h_{r1d}h_{sr1}g_{r1} & \text{for } m = 3,7,...,2L-1 \\ h_{r2d}h_{sr2}g_{r2} & \text{for } m = 5,9,...,2L-1, \end{cases}$$

$$H(m,m-1) = -H(m+1,m-2) = -H(m,m+11) = H(m+1,m+10) = \begin{cases} -h_{r3d}h^*_{sr3}g_{r3} & \text{for } m = 3,7,...,2L-1 \\ h_{r4d}h^*_{sr4}g_{r4} & \text{for } m = 5,9,...,2L-1, \end{cases}$$

$$H(m,m-4) = H(m+1,m-3) = H(m,m+8) = H(m+1,m+9) = \begin{cases} h_{r2d}h_{sr1}g_{r2}h_{r1}g_{r1} - h_{r4d}h_{sr3}g_{r4}h^*_{r2}g^*_{r3} & \text{for } m = 5,9,...,2L-1 \\ h_{r1d}h_{sr2}g_{r1}h_{r1}g_{r2} - h_{r3d}h_{sr4}g_{r3}h^*_{r2}g^*_{r4} & \text{for } m = 7,11,...,2L-1, \end{cases}$$

$$H(m,m-6) = H(m+1,m-5) = H(m,m+6) = H(m+1,m+7) = g_{r2}h_{r2d}h_{r1}g_{r1}h_{r1}g_{r2}h_{sr2} \quad \text{for} \quad m = 9,13,...,2L-1,$$

$$H(m,m-5) = -H(m+1,m-6) = -H(m,m+7) = H(m+1,m+6) = g_{r4}h_{r4,d}h^*_{r2}g_{r3}h_{r2}g_{r4}h^*_{s,r4} \quad \text{for} \quad m = 9,13,...,2L-1.$$

Furthermore,

$$C(m,m-2) = C(m+1,m-1) = C(m+1,m+11) = C(m,m+10) = \begin{cases} h_{r1d}g_{r1} & \text{for } m = 3,7,...,2L-1 \\ h_{r2d}g_{r2} & \text{for } m = 5,9,...,2L-1, \end{cases}$$

$$C(m,m+23) = -C(m+1,m+22) = C(m+1,m+34) = -C(m,m+35) = \begin{cases} -h_{r3d}g_{r3} & \text{for } m = 3,7,...,2L-1 \\ -h_{r4d}g_{r4} & \text{for } m = 5,9,...,2L-1, \end{cases}$$

$$C(m,m-4) = C(m+1,m-3) = C(m+1,m+9) = C(m,m+8) = \begin{cases} h_{r2d}g_{r2}h_{r1}g_{r1} & \text{for } m = 5,9,...,2L-1 \\ h_{r1d}g_{r1}h_{r1}g_{r2} & \text{for } m = 7,11,...,2L-1, \end{cases}$$

$$C(m,m+20) = C(m+1,m+21) = C(m+1,m+33) = C(m,m+32) = \begin{cases} -h_{r4d}g_{r4}h_{r2}^{*}g_{r3}^{*} & \text{for } m = 5,9,...,2L-1 \\ -h_{r3d}g_{r3}h_{r2}^{*}g_{r4}^{*} & \text{for } m = 7,11,...,2L-1, \end{cases}$$

$$C(m,m-6) = C(m,m+6) = C(m+1,m-5) = C(m+1,m+7) = g_{r2}h_{r2d}h_{r1}g_{r1}h_{r1}g_{r2} \quad \text{for} \quad m = 9,13,...,2L-1,$$

$$C(m,m+19) = -C(m,m+31) = -C(m+1,m+18) = C(m+1,m+30) = g_{r4}h_{r4d}h_{r2}^{*}g_{r3}h_{r2}g_{r4} \quad \text{for} \quad m = 9,13,...,2L-1.$$

Notice that $\mathbf{Cn}_r$ is the residual noise from the relays and it is in general not white. Rewriting (3.2.3) as

$$\mathbf{y}_d = \sqrt{\rho}\mathbf{H}\tilde{\mathbf{x}} + \mathbf{C}'\mathbf{n}, \tag{3.2.4}$$

where $\mathbf{C}' = [\mathbf{C}\ \mathbf{I}_{12}\ \mathbf{I}_{12}]$, and $\mathbf{n} = [\mathbf{n}_r\ \mathbf{n}_d]$.

Then, the mutual information of the four-path relaying is given as (3.2.5) from the mutual information of the equivalent MIMO system in (3.2.4). Following the derivation in [62],

$$I(\mathbf{x};\mathbf{y}_d) = \frac{L}{L+2} log_2 det(\mathbf{I} + \mathbf{H}\mathbf{R}_x\mathbf{H}^H(\mathbf{C}'\mathbf{R}\mathbf{C}'^H)^{-1}), \tag{3.2.5}$$

where $\mathbf{R}_x = E[\tilde{\mathbf{x}}\tilde{\mathbf{x}}^H] = \rho\mathbf{I}$ and $\mathbf{R} = E[\mathbf{n}\mathbf{n}^H] = \sigma^2\mathbf{I}$. Since two additional time

slots are required at the end as the terminating sequence, the mutual information is decreased by $\frac{L}{L+2}$, however, the slight loss is asymptotical zero for large values of L. Moreover, because $\mathbf{C'RC'}^H = \sigma^2[\mathbf{C}\ \mathbf{I}_{12}\ \mathbf{I}_{12}][\mathbf{C}\ \mathbf{I}_{12}\ \mathbf{I}_{12}]^H = \sigma^2(\mathbf{CC}^H + 2\mathbf{I})$, the mutual information can be simplified to

$$I(\mathbf{x};\mathbf{y}_d) = \frac{L}{L+2} log_2 det(\mathbf{I} + \frac{\rho}{\sigma^2}\mathbf{HH}^H(\mathbf{CC}^H + 2\mathbf{I})^{-1}). \tag{3.2.6}$$

3.2.3 Pairwise Error Probability and Diversity Analysis

In this section, the PEP of the four-path relaying is derived. First, express the received signal in (3.2.3) as

$$\mathbf{y}_d = \sqrt{\rho}\mathbf{Xh} + \mathbf{w}, \tag{3.2.7}$$

where $\mathbf{X} = [\mathbf{X_{Re}}\ j\mathbf{X_{Im}}]$, and $\mathbf{h} = [\mathbf{h}_R\ \mathbf{h}_I]^T$

$\mathbf{X_{Re}} =$

$$\begin{bmatrix}
x_{1,R}(1) & 0 & 0 & 0 & 0 & 0 & 0 & 0 & 0 & 0 & 0 & 0 \\
x_{2,R}(1) & 0 & 0 & 0 & 0 & 0 & 0 & 0 & 0 & 0 & 0 & 0 \\
x_{1,R}(2) & x_{2,R}(1) & x_{1,R}(1) & 0 & 0 & 0 & 0 & 0 & 0 & 0 & 0 & 0 \\
x_{2,R}(2) & 0 & x_{2,R}(1) & x_{1,R}(1) & 0 & 0 & 0 & 0 & 0 & 0 & 0 & 0 \\
x_{1,R}(3) & 0 & 0 & 0 & x_{2,R}(2) & x_{1,R}(2) & x_{1,R}(1) & 0 & 0 & 0 & 0 & 0 \\
x_{2,R}(3) & 0 & 0 & 0 & 0 & x_{2,R}(2) & x_{2,R}(1) & x_{1,R}(2) & 0 & 0 & 0 & 0 \\
x_{1,R}(4) & x_{2,R}(3) & x_{1,R}(3) & 0 & 0 & 0 & 0 & 0 & x_{1,R}(2) & 0 & 0 & 0 \\
x_{2,R}(4) & 0 & x_{2,R}(3) & x_{1,R}(3) & 0 & 0 & 0 & 0 & x_{2,R}(2) & 0 & 0 & 0 \\
x_{1,R}(5) & 0 & 0 & 0 & x_{2,R}(4) & x_{2,R}(3) & x_{1,R}(4) & 0 & 0 & x_{2,R}(2) & x_{1,R}(2) & 0 \\
x_{2,R}(5) & 0 & 0 & 0 & 0 & x_{2,R}(4) & x_{2,R}(3) & x_{1,R}(4) & 0 & 0 & x_{2,R}(2) & x_{1,R}(2) \\
x_{1,R}(6) & x_{2,R}(5) & x_{1,R}(5) & 0 & 0 & 0 & 0 & 0 & x_{1,R}(4) & 0 & 0 & 0 \\
x_{2,R}(6) & 0 & x_{2,R}(5) & x_{1,R}(5) & 0 & 0 & 0 & 0 & x_{2,R}(4) & 0 & 0 & 0
\end{bmatrix}$$

$$\mathbf{X_{Im}} =$$

$$\begin{bmatrix}
x_{1,I}(1) & 0 & 0 & 0 & 0 & 0 & 0 & 0 & 0 & 0 & 0 & 0 \\
x_{2,I}(1) & 0 & 0 & 0 & 0 & 0 & 0 & 0 & 0 & 0 & 0 & 0 \\
x_{1,I}(2) & x_{2,I}(1) & x_{1,I}(1) & 0 & 0 & 0 & 0 & 0 & 0 & 0 & 0 & 0 \\
x_{2,I}(2) & 0 & x_{2,I}(1) & x_{1,I}(1) & 0 & 0 & 0 & 0 & 0 & 0 & 0 & 0 \\
x_{1,I}(3) & 0 & 0 & 0 & x_{2,I}(2) & x_{1,I}(2) & x_{1,I}(1) & 0 & 0 & 0 & 0 & 0 \\
x_{2,I}(3) & 0 & 0 & 0 & 0 & x_{2,I}(2) & x_{2,I}(1) & x_{1,I}(2) & 0 & 0 & 0 & 0 \\
x_{1,I}(4) & x_{2,I}(3) & x_{1,I}(3) & 0 & 0 & 0 & 0 & 0 & x_{1,I}(2) & 0 & 0 & 0 \\
x_{2,I}(4) & 0 & x_{2,I}(3) & x_{1,I}(3) & 0 & 0 & 0 & 0 & x_{2,I}(2) & 0 & 0 & 0 \\
x_{1,I}(5) & 0 & 0 & 0 & x_{2,I}(4) & x_{1,I}(4) & x_{1,I}(3) & 0 & 0 & x_{2,I}(2) & x_{1,I}(2) & 0 \\
x_{2,I}(5) & 0 & 0 & 0 & 0 & x_{2,I}(4) & x_{2,I}(3) & x_{1,I}(4) & 0 & 0 & x_{2,I}(2) & x_{1,I}(2) \\
x_{1,I}(6) & x_{2,I}(5) & x_{1,I}(5) & 0 & 0 & 0 & 0 & 0 & x_{1,I}(4) & 0 & 0 & 0 \\
x_{2,I}(6) & 0 & x_{2,I}(5) & x_{1,I}(5) & 0 & 0 & 0 & 0 & x_{2,I}(4) & 0 & 0 & 0
\end{bmatrix}$$

$$\mathbf{h}_R = \begin{bmatrix}
h_{sd} \\
-g_{r3}h_{r3d}h^*_{sr3} \\
g_{r1}h_{r1d}h_{sr1} \\
g_{r3}h_{r3d}h^*_{sr3} \\
-g_{r4}h_{r4d}h^*_{sr4} \\
g_{r2}h_{r2d}h_{sr2} \\
g_{r2}h_{r2d}h_{r1}g_{r1}h_{sr1} - g_{r4}h_{r4d}h^*_{r2}g^*_{r3}h_{sr3} \\
g_{r4}h_{r4d}h^*_{sr4} \\
g_{r1}h_{r1d}h_{r1}g_{r2}h_{sr2} - g_{r3}h_{r3d}h^*_{r2}g^*_{r4}h_{sr4} \\
g_{r4}h_{r4d}h^*_{r2}g_{r3}h_{r2}g_{r4}h^*_{sr4} \\
g_{r2}h_{r2d}h^2_{r1}g_{r1}g_{r2}h_{sr2} \\
-g_{r4}h_{r4d}h^*_{r2}g_{r3}h_{r2}g_{r4}h^*_{sr4}
\end{bmatrix},$$

$$\mathbf{h}_I = \begin{bmatrix} h_{sd} \\ g_{r3}h_{r3d}h^*_{sr3} \\ g_{r1}h_{r1d}h_{sr1} \\ -g_{r3}h_{r3d}h^*_{sr3} \\ g_{r4}h_{r4d}h^*_{sr4} \\ g_{r2}h_{r2d}h_{sr2} \\ g_{r2}h_{r2d}h_{r1}g_{r1}h_{sr1} - g_{r4}h_{r4d}h^*_{r2}g^*_{r3}h_{sr3} \\ -g_{r4}h_{r4d}h^*_{sr4} \\ g_{r1}h_{r1d}h_{r1}g_{r2}h_{sr2} - g_{r3}h_{r3d}h^*_{r2}g^*_{r4}h_{sr4} \\ -g_{r4}h_{r4d}h^*_{r2}g_{r3}h_{r2}g_{r4}h^*_{sr4} \\ g_{r2}h_{r2d}h^2_{r1}g_{r1}g_{r2}h_{sr2} \\ g_{r4}h_{r4d}h^*_{r2}g_{r3}h_{r2}g_{r4}h^*_{sr4} \end{bmatrix}.$$

Here, it is assumed that $L = 6$, $\mathbf{X}$ is a $2L \times 24$ matrix consisting of the transmitted symbols, $\mathbf{h}$ is the equivalent channel vector, and $\mathbf{w} = \mathbf{C}\mathbf{n}_r + \mathbf{n}_d$ conditioned on $\mathbf{h}$ is the correlated Gaussian noise with covariance matrix $\sum_W = \sigma^2(\mathbf{C}\mathbf{C}^H + 2\mathbf{I})$. Then, use ML decoding at the receiver. If $\mathbf{X}$ is transmitted, then from [63], the PEP of mistaking $\mathbf{X}$ with $\mathbf{X}_e$ has the following Chernoff upper bound

$$P(\mathbf{X} \to \mathbf{X}_e) \leq \mathbf{E}_h\{e^{-\frac{1}{4}\rho\mathbf{h}^H(\mathbf{X}-\mathbf{X}_e)^H\sum_W^{-1}(\mathbf{X}-\mathbf{X}_e)\mathbf{h}}\}. \tag{3.2.8}$$

Since the covariance matrix $\sum_W$ is not a diagonal matrix, (3.2.5) cannot be easily analyzed. However, the covariance matrix $\sum_W$ is a positive semi-definite matrix, therefore, the PEP can be upperbounded by $\sum_W \leq tr(\sum_W)\mathbf{I}$, where $tr(\sum_W)$ is the trace of $\sum_W$. With this, it follows that

$$P(\mathbf{X} \to \mathbf{X}_e) \leq \mathbf{E}_h\{e^{-\frac{\rho}{4tr(\sum_W)}\mathbf{h}^H(\mathbf{X}-\mathbf{X}_e)^H(\mathbf{X}-\mathbf{X}_e)\mathbf{h}}\}. \tag{3.2.9}$$

In order to calculate the expectation in (3.2.9), express $\mathbf{h} = (\mathbf{T_1}\mathbf{U}_1 + \mathbf{T_2}\mathbf{U}_2)\mathbf{v}$, where $\mathbf{v} = [h_{sd,R}\ h_{sr1,R}, ..., h_{sr4,R}\ h_{sd,I}\ h_{sr1,I}, ..., h_{sr4,I}]^T$, and $\mathbf{T}_1$, $\mathbf{T}_2$, $\mathbf{U}_1 = [\mathbf{U}_{11}; \mathbf{U}_{11}]$ and $\mathbf{U}_2 = [\mathbf{U}_{21}; \mathbf{U}_{21}]$ are shown as

$$\mathbf{T}_1 = diag\left(\begin{bmatrix} 0.5 \\ -0.5g_{r3}h_{r3d} \\ 0.5g_{r1}h_{r1d} \\ 0.5g_{r3}h_{r3d} \\ -0.5g_{r4}h_{r4d} \\ 0.5g_{r2}h_{r2d} \\ 0.5g_{r2}h_{r2d}h_{r1}g_{r1} \\ 0.5g_{r4}h_{r4d} \\ 0.5g_{r1}h_{r1d}h_{r1}g_{r2} \\ 0.5g_{r4}h_{r4d}h^*_{r2}g_{r3}h_{r2}g_{r4} \\ 0.5g_{r2}h_{r2d}h^2_{r1}g_{r1}g_{r2} \\ -0.5g_{r4}h_{r4d}h^*_{r2}g_{r3}h_{r2}g_{r4} \\ 0.5 \\ 0.5g_{r3}h_{r3d} \\ 0.5g_{r1}h_{r1d} \\ -0.5g_{r3}h_{r3d} \\ 0.5g_{r4}h_{r4d} \\ 0.5g_{r2}h_{r2d} \\ 0.5g_{r2}h_{r2d}h_{r1}g_{r1} \\ -0.5g_{r4}h_{r4d} \\ 0.5g_{r1}h_{r1d}h_{r1}g_{r2} \\ -0.5g_{r4}h_{r4d}h^*_{r2}g_{r3}h_{r2}g_{r4} \\ 0.5g_{r2}h_{r2d}h^2_{r1}g_{r1}g_{r2} \\ 0.5g_{r4}h_{r4d}h^*_{r2}g_{r3}h_{r2}g_{r4} \end{bmatrix}\right)$$

$$\mathbf{T}_2 = diag\left(\begin{bmatrix} 0.5 \\ -0.5g_{r3}h_{r3d} \\ 0.5g_{r1}h_{r1d} \\ 0.5g_{r3}h_{r3d} \\ -0.5g_{r4}h_{r4d} \\ 0.5g_{r2}h_{r2d} \\ -0.5g_{r4}h_{r4d}h^*_{r2}g^*_{r3} \\ 0.5g_{r4}h_{r4d} \\ -0.5g_{r3}h_{r3d}h^*_{r2}g^*_{r4} \\ 0.5g_{r4}h_{r4d}h^*_{r2}g_{r3}h_{r2}g_{r4} \\ 0.5g_{r2}h_{r2d}h^2_{r1}g_{r1}g_{r2} \\ -0.5g_{r4}h_{r4d}h^*_{r2}g_{r3}h_{r2}g_{r4} \\ 0.5 \\ 0.5g_{r3}h_{r3d} \\ 0.5g_{r1}h_{r1d} \\ -0.5g_{r3}h_{r3d} \\ 0.5g_{r4}h_{r4d} \\ 0.5g_{r2}h_{r2d} \\ -0.5g_{r4}h_{r4d}h^*_{r2}g^*_{r3} \\ -0.5g_{r4}h_{r4d} \\ -0.5g_{r3}h_{r3d}h^*_{r2}g^*_{r4} \\ -0.5g_{r4}h_{r4d}h^*_{r2}g_{r3}h_{r2}g_{r4} \\ 0.5g_{r2}h_{r2d}h^2_{r1}g_{r1}g_{r2} \\ 0.5g_{r4}h_{r4d}h^*_{r2}g_{r3}h_{r2}g_{r4} \end{bmatrix}\right)$$

$$\mathbf{U}_{11} = \begin{bmatrix} 1 & 0 & 0 & 0 & 0 & 1 & 0 & 0 & 0 & 0 \\ 0 & 0 & 0 & 1 & 0 & 0 & 0 & 0 & -1 & 0 \\ 0 & 1 & 0 & 0 & 0 & 0 & 1 & 0 & 0 & 0 \\ 0 & 0 & 0 & 1 & 0 & 0 & 0 & 0 & -1 & 0 \\ 0 & 0 & 0 & 0 & 1 & 0 & 0 & 0 & 0 & -1 \\ 0 & 0 & 1 & 0 & 0 & 0 & 0 & 1 & 0 & 0 \\ 0 & 1 & 0 & 0 & 0 & 0 & 1 & 0 & 0 & 0 \\ 0 & 0 & 0 & 0 & 1 & 0 & 0 & 0 & 0 & -1 \\ 0 & 0 & 1 & 0 & 0 & 0 & 0 & 1 & 0 & 0 \\ 0 & 0 & 0 & 0 & 1 & 0 & 0 & 0 & 0 & -1 \\ 0 & 0 & 1 & 0 & 0 & 0 & 0 & 1 & 0 & 0 \\ 0 & 0 & 0 & 0 & 1 & 0 & 0 & 0 & 0 & -1 \end{bmatrix} \quad \mathbf{U}_{21} = \begin{bmatrix} 1 & 0 & 0 & 0 & 0 & 1 & 0 & 0 & 0 & 0 \\ 0 & 0 & 0 & 1 & 0 & 0 & 0 & 0 & -1 & 0 \\ 0 & 1 & 0 & 0 & 0 & 0 & 1 & 0 & 0 & 0 \\ 0 & 0 & 0 & 1 & 0 & 0 & 0 & 0 & -1 & 0 \\ 0 & 0 & 0 & 0 & 1 & 0 & 0 & 0 & 0 & -1 \\ 0 & 0 & 1 & 0 & 0 & 0 & 0 & 1 & 0 & 0 \\ 0 & 0 & 0 & 1 & 0 & 0 & 0 & 0 & 1 & 0 \\ 0 & 0 & 0 & 0 & 1 & 0 & 0 & 0 & 0 & -1 \\ 0 & 0 & 0 & 0 & 1 & 0 & 0 & 0 & 0 & 1 \\ 0 & 0 & 0 & 0 & 1 & 0 & 0 & 0 & 0 & -1 \\ 0 & 0 & 1 & 0 & 0 & 0 & 0 & 1 & 0 & 0 \\ 0 & 0 & 0 & 0 & 1 & 0 & 0 & 0 & 0 & -1 \end{bmatrix}$$

Thus, by taking expectation over $\mathbf{v}$ first yields

$$\begin{aligned} & P(\mathbf{X} - \mathbf{X}_e) \\ & \leq \mathbf{E}_T\{\int \frac{1}{\pi^3} e^{-\frac{\rho}{4tr(\sum_W)}\mathbf{v}^H(\mathbf{T}_1^H\mathbf{U}_1^H + \mathbf{T}_2^H\mathbf{U}_2^H)(\mathbf{X}-\mathbf{X}_e)^H(\mathbf{X}-\mathbf{X}_e)(\mathbf{T_1}\mathbf{U}_1+\mathbf{T_2}\mathbf{U}_2)\mathbf{v}} e^{-\mathbf{v}^H\mathbf{v}} d\mathbf{v}\} \\ & = \mathbf{E}_T\{det^{-1}(\mathbf{I} + \frac{\rho}{4tr(\sum_W)})\}, \end{aligned}$$

where $\mathbf{A} = (\mathbf{X} - \mathbf{X}_e)(\mathbf{T_1}\mathbf{U}_1 + \mathbf{T_2}\mathbf{U}_2)$, $tr(\cdot)$ represents trace of a matrix. Using the diversity criterion in [34] the diversity order can be analyzed, which is determined by the rank of $\mathbf{A}$. It can be observed that $\mathbf{T}_1$ and $\mathbf{T}_2$ are full rank. The rank of $\mathbf{U}_1$ and $\mathbf{U}_2$ are 5. The rank of $\mathbf{A}$ is determined by the rank of the product $(\mathbf{X} - \mathbf{X}_e)$ and $(\mathbf{U}_1 + \mathbf{U}_2)$.

Because the real and imaginary parts of $x_j(i)$ have the same effect for the rank of the product $(\mathbf{X} - \mathbf{X}_e)$, consider only the real part $x_{j,R}(i)$, where

$i = 1, 2, ..., L$ and $j = 1$ or 2. There are three scenarios.

Initially, only the first symbol at the odd time slots is different between $\mathbf{X}$ and $\mathbf{X}_e$. If only $x_{1,R}(1)$ is different, there are four independent columns in $(\mathbf{X} - \mathbf{X}_e)$ (1, 3, 4, 7). However, both $\mathbf{U}_1$ and $\mathbf{U}_2$ have three and four independent rows in (1, 3, 4, 7), respectively. Using the same method, only the second symbol at the odd time slots is different, such as $x_{2,R}(1)$. There are four independent columns in $(\mathbf{X} - \mathbf{X}_e)$ (1, 2, 3, 7). However, both $\mathbf{U}_1$ and $\mathbf{U}_2$ only have three and four independent rows in (1, 2, 3, 7). Therefore, the product terms in $\mathbf{A}$, i.e. $(\mathbf{X} - \mathbf{X}_e)\mathbf{U}_1$ and $(\mathbf{X} - \mathbf{X}_e)\mathbf{U}_2$, have limited rank of three and four, respectively.

Secondly, only the first symbol at the even time slot is different, in this case there are six independent columns in $(\mathbf{X} - \mathbf{X}_e)$ (1, 6, 8, 9, 11, 12). However, the limited rank of the product terms are three and four, because there are only three and four independent corresponding rows in $\mathbf{U}_1$ and $\mathbf{U}_2$, respectively. If the second symbol at the even time slot is different, there are six independent columns in $(\mathbf{X} - \mathbf{X}_e)$ (1, 5, 6, 9, 10, 11), but both $\mathbf{U}_1$ and $\mathbf{U}_2$ only have three and four independent rows in $(\mathbf{X} - \mathbf{X}_e)$ (1, 5, 6, 9, 10, 11). Therefore, the product terms in $\mathbf{A}$ have limited rank of three and four, respectively.

Thirdly, if all of the symbols are different, the matrix $(\mathbf{X} - \mathbf{X}_e)$ is full rank, the rank of the product is equal to five as $\mathbf{U}_1$ and $\mathbf{U}_2$ are both rank five matrices. Based on the above three cases, the minimum rank of the product terms are three and four, respectively. Therefore, the overall diversity order is between three and four.

Furthermore, some special situations are discussed in the following:

Firstly, if there is no direct path from the source to destination ($h_{sd} = 0$), then minimum diversity order of two can be achieved, because the first row of $\mathbf{U}_1$ and $\mathbf{U}_2$ are removed.

Secondly, if h_{r1} and h_{r2} do not exist ($h_{r1} = h_{r2} = 0$), then the (7, 9,

10, 11, 12) diagonal elements of $\mathbf{T}_1$ and $\mathbf{T}_2$ will be 0. Thus, if one symbol is different between $\mathbf{X}$ and $\mathbf{X}_e$, there are three independent rows in $\mathbf{U}_1$ and $\mathbf{U}_2$. Therefore, the diversity order of three can still be obtained without the h_{r1} and h_{r2} in the equivalent channel matrix.

Thirdly, if γ_{r1}^2 and γ_{r2}^2 increase, both g_{r2} and g_{r4} will approach 0 and both g_{r1} and g_{r3} will approach to a constant value. And the 5^{th} to 12^{th} diagonal elements of $\mathbf{T}_1$ and $\mathbf{T}_2$ will be 0. Therefore, when γ_{r1}^2 and γ_{r2}^2 increase, the diversity order will be decreased.

3.2.4 Simulation Studies

In this section, the simulated performance of the proposed scheme is shown i.e. four-path relaying with inter-relay self interference cancellation. The performance is shown by the end-to-end BER using QPSK symbols. The length of symbol L is assumed to be six, and all average channel gains are normalized to 0 dB. And the asymptotic achievable rate can be obtained where L is sufficiently large and hence $\frac{L}{L+2} \to 1$.

Figure 3.2 compares the average rate as a function of the signal-to-noise ratio. Equation (3.2.6) is used to calculate the average rate. The average rate decreases when γ_{sd}^2 is lower than other channels, i.e. γ_{sd}^2 is -20 dB. However, when γ_{ri}^2 $i \in (1, 2)$ increases to 10 dB, the average rate is sightly decreased, i.e. the average rate decreases from 70 (bit/s/Hz) to 66 (bit/s/Hz) when the SNR is equal to 30 dB.

Figure 3.3 contrasts the BER performance with different inter-relay channel gains. Obviously, the diversity order decreases with the increase of γ_{ri}^2, from 3.5 to essentially two. However, when $\gamma_{ri}^2 = 0$, the diversity order is three.

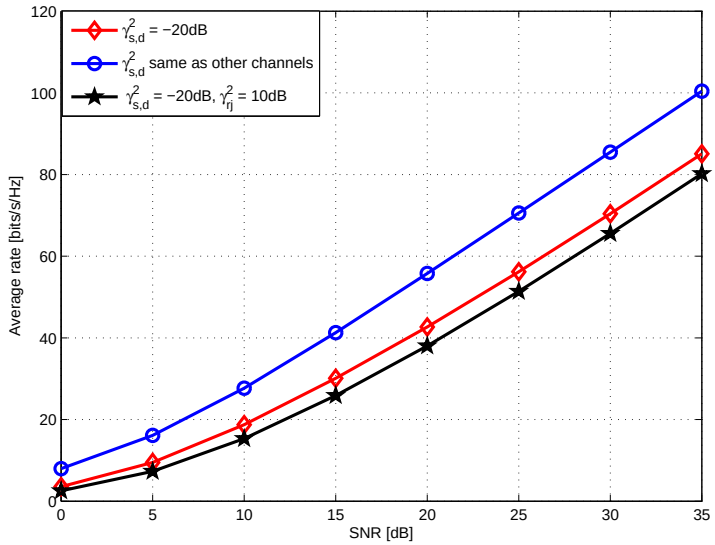

Figure 3.2. *Comparison of average rate between the different channel coefficients as a function of SNR.*

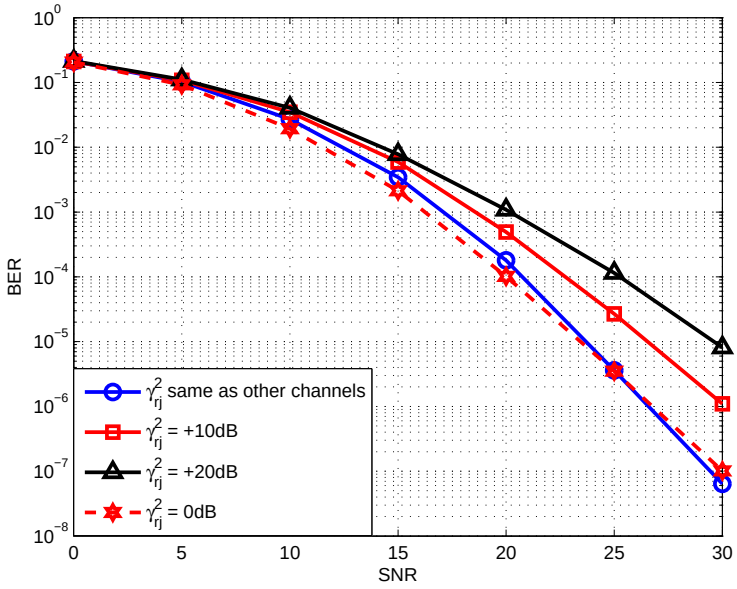

Figure 3.3. *Comparison of BER performance for different levels of IRI as a function of SNR.*

3.3 DDSTCing with FIC Scheme for A Cooperative Four Relay Network

In the last subsection, using the DSTC scheme does require full channel information at the destination node, both the channels from the transmitter to

relays and the channels from relays to the destination. Therefore, the source and relay nodes have to exchange training symbols. However, in some situations, regular training is not possible, because of the cost on time and power and the complexity of the channel estimation. Therefore, the differential transmission scheme for wireless relay networks with no channel information at either relays or the destination was proposed in [47]. In order to use the FIC scheme, the previous assumption of no channel knowledge at the destination must be relaxed and the relay to destination channels are assumed to be known which are easier to estimate than the other channel values. Moreover, the destination node needs to know the inter-relay channels between the relay nodes.

3.3.1 Distributed Differential Space Time Block Coding Model

In this section, the use of DSTC and DDSTC within a two-hop cooperative wireless four relay network over block quasi-static Rayleigh fading channels is proposed, which can achieve full cooperative diversity and improve the transmission rate.

3.3.2 The Offset Transmission Scheduling Model

In Figure 3.4, the relay model for the offset transmission scheduling method is illustrated. The four relay nodes are arranged as two groups of two relay nodes, both of which employ DSTC or DDSTC design, but with offset transmission scheduling, i.e., at the odd time slot, relay one and three receive the signal from the source, at the same time, relay two and four send the received signal which was received from the source at the previous time slot to the destination node. Therefore, the source can serially transmit data to the destination and the overall rate can be improved. However, the four-path relay scheme may suffer from inter-relay interference (IRI) which is caused by the simultaneous transmission of the source and another group of relays.

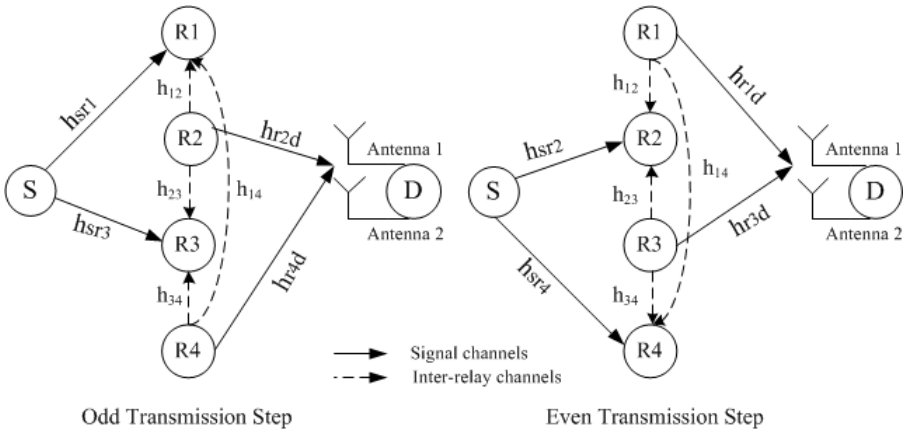

Figure 3.4. *A cooperative four relay network model with offset transmission scheme.*

An FIC approach is therefore used to remove the inter-relay interference at the destination node.

In Figure 3.4, h_{sri} $(i = 1, ..., 4)$ denote the channels from the transmitter to the four relays and h_{rid} $(i = 1, ..., 4)$ denote the channels from the four relays to the destination. There is no direct link between the source and the destination as path loss or shadowing is assumed to render it unusable. The inter-relay channels are assumed to be reciprocal, i.e. the gains from R1 and R3 to R2 and R4 are the same as those from R2 and R4 to R1 and R3, which are denoted h_{12}, h_{23}, h_{34} and h_{14}. The channels are assumed to be block quasi-static Rayleigh flat-fading: h_{sri} and h_{rid} are independent and identically distributed (i.i.d.) zero-mean and unit-variance complex Gaussian random variables. The usual requirement for space-time block coding is that the channel is constant for at least M time instants (channel uses). And all of the channel information is assumed known by the receiver. The FIC with DSTC scheme is next introduced to achieve asymptotically full rate and to completely remove IRI.

3.3.3 Interference Cancellation Scheme

Building on the approach followed in [64], it is assumed that the relay nodes R2 and R4 receive at time slots n-1 and n-3, and at the same times, the relay nodes R1 and R3 are transmitting to the destination nodes. It is assumed that the channel h_{rid} information is known by the receiver. Considering the received signal at the destination at time slot n-3:

$$\mathbf{y}_d(n-3) = \mathbf{t}_1(n-4)h_{r1d} + \mathbf{t}_3(n-4)h_{r3d} + \mathbf{w}_d(n-3), \tag{3.3.1}$$

where $\mathbf{w}_d$ is the Gaussian noise vector at the destination, and $\mathbf{t}_1(n-4)$ and $\mathbf{t}_3(n-4)$ are formed from the received signal vectors at R1 and R3 at time slot n-4, which are given by:

$$\mathbf{t}_1(n-4) = NA_1\mathbf{r}_1(n-4) \quad \text{and} \quad \mathbf{t}_3(n-4) = NB_2\overline{\mathbf{r}_3(n-4)}. \tag{3.3.2}$$

The received signal vectors $\mathbf{r}_1(n-4)$ and $\mathbf{r}_3(n-4)$ are given by:

$$\begin{aligned}\mathbf{r}_1(n-4) =& \sqrt{P_1 M}h_{sr1}U(n-4)\mathbf{ss}(n-6) + \mathbf{t}_2(n-5)h_{12} + \mathbf{t}_4(n-5)h_{14} \\ &+ \mathbf{v}_1(n-4),\end{aligned}$$

$$\begin{aligned}\mathbf{r}_3(n-4) =& \sqrt{P_1 M}h_{sr3}U(n-4)\mathbf{ss}(n-6) + \mathbf{t}_2(n-5)h_{23} + \mathbf{t}_4(n-5)h_{34} \\ &+ \mathbf{v}_3(n-4),\end{aligned} \tag{3.3.3}$$

where $U(n-4)$ can be obtained by the Alamouti code [47], as

$$U = \frac{1}{\sqrt{|s_1|^2 + |s_2|^2}} \begin{bmatrix} s_1 & -s_2^* \\ s_2 & s_1^* \end{bmatrix}, \tag{3.3.4}$$

where $|\cdot|$ denotes the modulus of a complex number, $\mathbf{v}_1$ and $\mathbf{v}_3$ are the Gaussian noise vectors at the relay nodes. The received signal vector can

also be obtained at the destination at time slot n-4 as:

$$\mathbf{y}_d(n-4) = \mathbf{t}_2(n-5)h_{r2d} + \mathbf{t}_4(n-5)h_{r4d} + \mathbf{w}_d(n-4). \tag{3.3.5}$$

ASSUMPTION 1: If multiple antennas were available at the destination node, and given that the relays are sufficiently spatially separated, the assumption that it is possible to separate out the individual relay components within $\mathbf{y}_d(n-4)$ is made

$$\mathbf{y}_d(n-4) = \mathbf{y}_{d1}(n-4) + \mathbf{y}_{d2}(n-4) + \mathbf{w}_d(n-4),$$

as given by

$$\mathbf{y}_{d1}(n-4) = \mathbf{t}_2(n-5)h_{r2d} \text{ and } \mathbf{y}_{d2}(n-4) = \mathbf{t}_4(n-5)h_{r4d}, \tag{3.3.6}$$

where the noise term is assumed to be insignificant in the current development, however this issue and the validity of this assumption is addressed further in the simulation studies. So

$$\mathbf{t}_2(n-5) = \frac{\mathbf{y}_{d1}(n-4)}{h_{r2d}} \quad \text{and} \quad \mathbf{t}_4(n-5) = \frac{\mathbf{y}_{d2}(n-4)}{h_{r4d}}. \tag{3.3.7}$$

Finally, substituting (3.3.2), (3.3.3) and (3.3.7) into (3.3.1) gives:

$$\begin{aligned}\mathbf{y}_d(n-3) = {} & N\sqrt{P_1 M}A_1 h_{r1d}h_{sr1}U(n-4)\mathbf{ss}(n-6)+ \\ & NA_1h_{r1d}\left(\frac{\mathbf{y}_{d1}(n-4)}{h_{r2d}}h_{12} + \frac{\mathbf{y}_{d2}(n-4)}{h_{r4d}}h_{14}\right) \\ & + N\sqrt{P_1 M}B_2 h_{r3d}\overline{h_{sr3}U(n-4)\mathbf{ss}(n-6)}+ \\ & NB_2h_{r3d}\left(\overline{\frac{\mathbf{y}_{d1}(n-4)}{h_{r2d}}h_{23} + \frac{\mathbf{y}_{d2}(n-4)}{h_{r4d}}h_{34}}\right) + \mathbf{w}_d^{'}(n-3),\end{aligned} \tag{3.3.8}$$

where $\mathbf{w}_d^{'}(n-3)$ is the noise vector which is given by:

$$\mathbf{w}_d^{'}(n-3) = NA_1\mathbf{v}_1 h_{r1d} + NB_2\bar{\mathbf{v}}_3 h_{r3d} + \mathbf{w}_d(n-4). \tag{3.3.9}$$

From (3.3.8), the inter-relay interference is found as a recursive term in the received signal vector at the destination nodes. For example, the IRI terms are

$$NA_1 h_{r1d}\left(\frac{\mathbf{y}_{d1}(n-4)}{h_{r2d}}h_{12} + \frac{\mathbf{y}_{d2}(n-4)}{h_{r4d}}h_{14}\right), \tag{3.3.10}$$

$$NB_2 h_{r3d}\left(\overline{\frac{\mathbf{y}_{d1}(n-4)}{h_{r2d}}h_{23} + \frac{\mathbf{y}_{d2}(n-4)}{h_{r4d}}h_{34}}\right), \tag{3.3.11}$$

which are functions only of the previous output values $\mathbf{y}_{d1}(n-4)$ and $\mathbf{y}_{d2}(n-4)$. Therefore, these terms can be completely removed from (3.3.8) in order to cancel the inter-relay interference at the receiver, which is given by:

$$\begin{aligned}\mathbf{y}_d^{'}(n-3) =& N\sqrt{P_1 M}A_1 h_{r1d}h_{sr1}U(n-4)\mathbf{ss}(n-6) + N\sqrt{P_1 M}B_2 h_{r3d}\\ & \overline{h_{sr3}U(n-4)\mathbf{ss}(n-6)}\mathbf{w}_d^{'}(n-3).\end{aligned} \tag{3.3.12}$$

As such, (3.3.12) has no inter-relay interference, and contains only the desired signal and the noise, and $\mathbf{ss} = U(n)\mathbf{ss}(n-2)$ and $\mathbf{ss}(n-4) = U(n-4)\mathbf{ss}(n-6)$, which is a reference signal for the next time slot. Next using the same method to obtain the received signal vector at time slot n-2 at the destination node and cancelling completely the IRI,

$$\begin{aligned}\mathbf{y}_d(n-2) =& N\sqrt{P_1 M}A_1 h_{r2d}h_{sr2}U(n-3)\mathbf{ss}(n-5)+\\ & NA_1 h_{r2d}\left(\frac{\mathbf{y}_{d1}(n-3)}{h_{r1d}}h_{12} + \frac{\mathbf{y}_{d2}(n-3)}{h_{r3d}}h_{23}\right)\\ & + N\sqrt{P_1 M}B_2 h_{r4d}\overline{h_{sr4}U(n-3)\mathbf{ss}(n-5)}+\\ & NB_2 h_{r4d}\left(\overline{\frac{\mathbf{y}_{d1}(n-3)}{h_{r1d}}h_{14} + \frac{\mathbf{y}_{d2}(n-3)}{h_{r3d}}h_{34}}\right) + \mathbf{w}_d^{'}(n-2),\end{aligned} \tag{3.3.13}$$

where $\mathbf{w}_d^{'}(n-2)$ is the noise vector which is given by:

$$\mathbf{w}_d^{'}(n-2) = NA_1\mathbf{v}_2h_{r2d} + NB_2\bar{\mathbf{v}}_4h_{r4d} + \mathbf{w}_d(n-3). \tag{3.3.14}$$

The second and fourth terms in the right hand side of (3.3.13) are IRI terms which can be removed as in (3.3.10) and (3.3.11). Therefore, (3.3.13) becomes

$$\begin{aligned}\mathbf{y}_d^{'}(n-2) =& N\sqrt{P_1M}A_1h_{r2d}h_{sr2}U(n-3)\mathbf{ss}(n-5) + N\sqrt{P_1M}B_2h_{r4d}\\ &\overline{h_{sr4}U(n-3)\mathbf{ss}(n-5)} + \mathbf{w}_d^{'}(n-2),\end{aligned} \tag{3.3.15}$$

and defining $\mathbf{ss}(n-3) = U(n-3)\mathbf{ss}(n-5)$, which is a reference signal for the next time slot. Compared with (3.3.12) and (3.3.15), the same structure is evident. However, according to the offset time slots, the alternate channels are switched regularly. And then the same method is used to obtain the received signal at time slots n-1 and n at the destination node and cancel completely the IRI

$$\begin{aligned}\mathbf{y}_d^{'}(n-1) =& N\sqrt{P_1M}A_1h_{r1d}h_{sr1}U(n-2)\mathbf{ss}(n-4) + N\sqrt{P_1M}B_2h_{r3d}\\ &\overline{h_{sr3}U(n-2)\mathbf{ss}(n-4)} + \mathbf{w}_d^{'}(n-1),\end{aligned} \tag{3.3.16}$$

$$\begin{aligned}\mathbf{y}_d^{'}(n) =& N\sqrt{P_1M}A_1h_{r2d}h_{sr2}U(n-1)\mathbf{ss}(n-3) + N\sqrt{P_1M}B_2h_{r4d}\\ &\overline{h_{sr4}U(n-1)\mathbf{ss}(n-3)} + \mathbf{w}_d^{'}(n).\end{aligned} \tag{3.3.17}$$

Therefore, the transmission symbols can be easily detected by the ML decoding, i.e.

$$\hat{U}(n) = \arg\max_{U(n)} \left\| \mathbf{y}_d^{'}(n) - U(n)\mathbf{y}_d^{'}(n-2) \right\|$$

and

$$\hat{U}(n-1) = \arg \max_{U(n-1)} \left\| \mathbf{y}_d^{'}(n-1) - U(n-1)\mathbf{y}_d^{'}(n-3) \right\|.$$

3.3.4 Simulation Studies

In this section, the simulated performance of the distributed differential space-time coding with the FIC approach is shown and compared with the performance of coherent distributed space-time coding. The performance is assessed by the BERs using BPSK symbols. The total power per symbol transmission is fixed as P. The reference signals $\mathbf{s}(1)$ and $\mathbf{s}(2)$ are chosen as $[1\ 0]^T$. And the length of the block over which the channels are assumed constant N is 8.

In Figure 3.5, firstly, the BER performance is shown without full inter-relay interference cancellation and with full inter-relay interference cancellation. The advantage of using the FIC scheme is clear, the BER performance is significantly better than without the FIC approach. In fact, without using FIC the scheme is unusable. The inter-relay interference considerably corrupts the transmission signal, thereby leading to the performance degradation. Secondly, the performance of differential Alamouti DSTCs with a two relay network, without inter-relay interference, and that of the FIC differential Alamouti DSTCs with a four relay network (Assumption 1) is compared. For the two hop cooperative four relay network, if the FIC scheme is used to completely remove the inter-relay interference, the performance closely matches Alamouti DSTCs, whilst essentially doubling the transmission rate. Finally, compared with the performance of coherent distributed space-time coding with FIC, the differential scheme has the expected 3db loss in coding [65].

In the next simulation study, the effect of relaxing Assumption 1 is considered. To model the effect that even with multiple antennas at the destination node there will be uncertainties in the values of $\mathbf{y}_{d1}(n-4)$ and $\mathbf{y}_{d2}(n-4)$

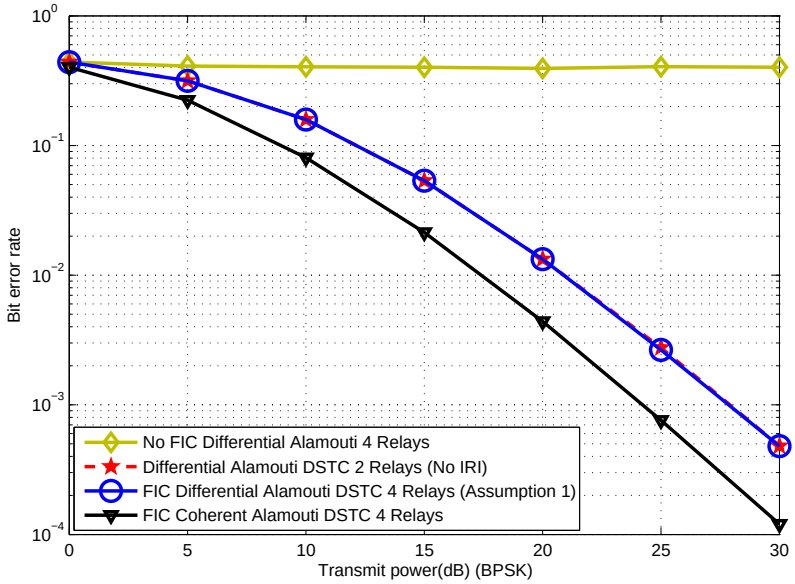

Figure 3.5. *End-to-end BER performance.*

in (3.3.6), due for example to estimation errors in beamforming, the noise vectors are added to yield $\mathbf{y}_{d1}(n-4) = \mathbf{t}_2(n-5)h_{r2d} + \mathbf{n}_1$ and $\mathbf{y}_{d2}(n-4) = \mathbf{t}_4(n-5)h_{r4d} + \mathbf{n}_2$, where all the elements of the $\mathbf{n}_1$ and $\mathbf{n}_2$ vectors are chosen to have noise powers of either -9 or -12dB, and these two cases are denoted **Assumption 2** and **Assumption 3**. The degradation in BER is shown in Figure 3.6, for example, at BER $= 10^{-3}$ the required transmit power increases from 27.5 to 33, and to 38 dB for the three cases. Through the use of Turbo Coding, with generating polynomials $g(D) = [1, 1 + D^2/1 + D + D^2]$ and four iterations, these powers can be reduced to 19, 21.5 and 22.5 dB. As such, additional outer coding is one method to mitigate the practical difficulties in achieving Assumption 1.

In Figure 3.7, the data rate performance of the two relay differential scheme and that of the four relay differential scheme is compared. When the

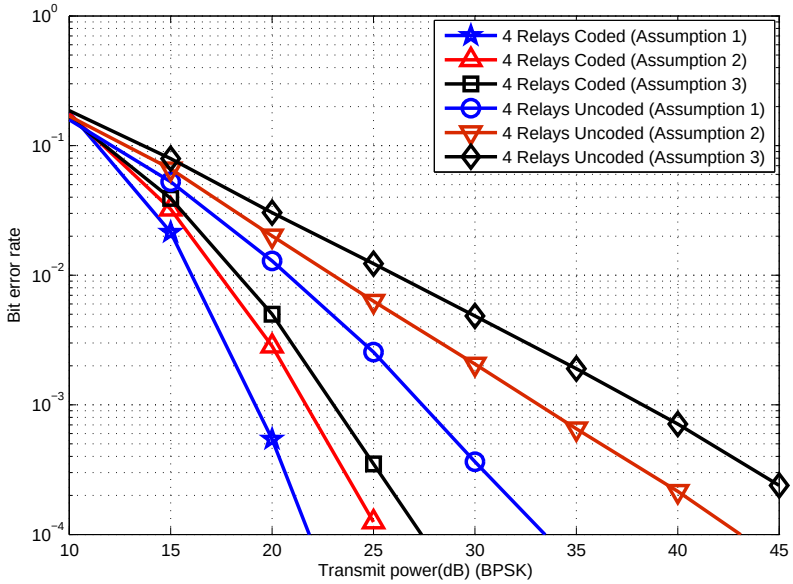

Figure 3.6. *End-to-end coded and uncoded BER performance of the differential STBC with FIC and varying uncertainty in Assumption 1.*

useful block size M is unity, the data rates of two and four relay schemes are the same which is 0.25. When the useful block size M is 10, the two relay scheme data rate is 0.46 whereas the four relay scheme data rate is 0.77. Obviously, when the useful block size M is large, the data rate of the four relay scheme is almost equal to unity, which is twice that of the two relay scheme, which is almost equal to 0.5.

3.4 Summary

In this chapter, full diversity and improved end-to-end transmission rate can be achieved because the offset transmission with FIC scheme was used. Using offset transmission, the source can serially transmit data to the destination. However, the four-path relay scheme may suffer from IRI which

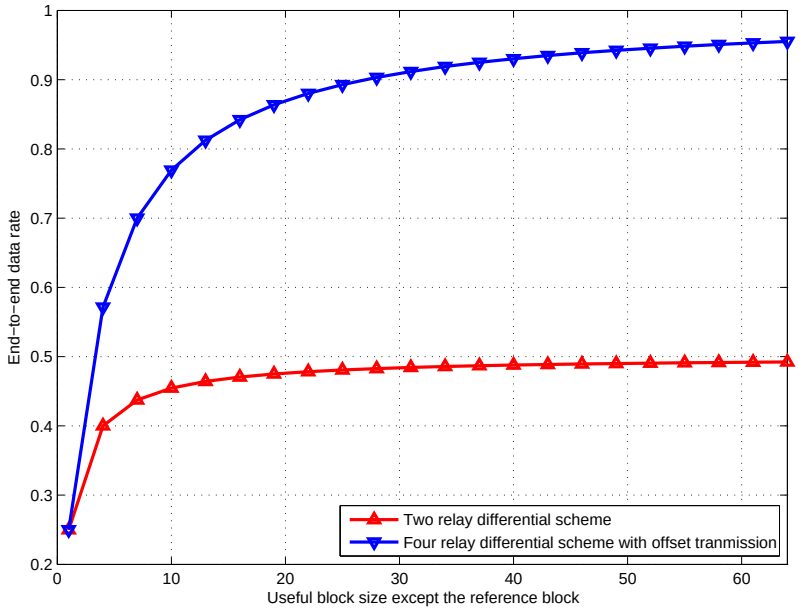

Figure 3.7. *The end-to-end data rate performance.*

is caused by the simultaneous transmission of the source and another group of relays. Therefore, the FIC scheme was used to remove fully these IRI terms. However, the FIC scheme is performed at the destination node, and so multiple antennas have to be used which maybe infeasible to achieve in practice. Assumption 1 is therefore likely to be only an approximation in a practical network environment and therefore the reason that uncertainly was introduced in the form of noise power in Assumption 2 and 3. Therefore, an FSIC scheme at the relay nodes within a four relay network was provided and the pairwise error probability approach has been used to analyze distributed diversity. The four single antenna relay nodes were arranged as two groups of spatially separated two relay groups with offset transmission scheduling. This approach can achieve the full available distributed diversity order 3.5 without precoding and its end-to-end transmission rate can asymptotically approach one when the number of samples is large. However, a synchronous system must be assumed in the above schemes, because the timing error can significantly degrade the end-to-end BER performance.

Chapter 4

PERFORMANCE ANALYSIS OF FOUR-RELAY SELECTION SCHEME FOR COOPERATIVE NETWORKS WITHOUT INTERFERENCE

In this chapter, the local measurements of the instantaneous channel conditions are used to select the best four relays from a set of N available relays, and then these best relays are used with the quasi-orthogonal distributed space-time block coding (QO-DSTBC) to improve the cooperative diversity gain and decrease the outage probability. This best four-relay selection scheme is shown to have robustness against feedback error in the relay selection and to outperform a scheme based on selecting only the best single-relay.

4.1 Introduction

In a cooperative relay network, many relays can help the source to transmit to the destination, however, sometimes some relays provide poor channel quality which can affect the transmission quality to a certain extent [66]. Therefore, the use of relay selection schemes is attracting considerable attention to overcome this problem and preserve the potential diversity gains, [67], [68] and [15]. In [67], the authors derived simple expressions for outage probabilities for several decode-and-forward (DF) (regenerative relaying protocol) cooperative diversity schemes in the context of selecting a single relay from a set of N available relays. This method, however, requires high complexity at the relays and destination. In [68], exact outage and diversity performance expressions for the best single-relay selection are provided for a wide range of signal-to-noise ratio (SNR) regimes in the context of an amplify-and-forward (AF) (transparent relaying protocol) cooperative transmission approach. The work in [15] relies on using instantaneous end-to-end wireless channel conditions to obtain the best single relay for cooperative diversity. This work was extended in [69] to obtain outage-optimal opportunistic relaying in the context of selecting a single relay from a set of N available relays. They show that cooperative diversity gain is achieved even when certain relays remain inactive. However, the optimal diversity performance is obtained when transmit maximal ratio combining (MRC) is performed across all the relays, assuming the channel state information (CSI) is known by each relay node. For the same total power consumption by relays, the transmit MRC based cooperative diversity scheme outperforms opportunistic relay selection. Also, using a best single-relay is not always sufficient to satisfy the required outage probability at a destination node. Moreover, these works have not considered feedback error within the relay selection process, which means sometimes the best relay cannot be

chosen because the wrong enable feedback information is received from the destination node. In [70], outage probability is calculated by using an approximate method to derive expressions for the moment generating function (MGF) of the generalized selection combining (GSC). However, a simple multi-dimensional integration approach can be used to obtain accurately the outage probability. Therefore, in this chapter, firstly, selecting the best four-relay from N available relays is considered. The outage probability of the best four-relay selection is compared with the conventional best single-relay selection. Secondly, the bit error rate (BER) performance of the best single-relay selection scheme and the best four-relay selection is examined with the closed-loop quasi-orthogonal STBCs scheme [71], in the presence of errors in the feedback of relay selecting information.

4.2 Conventional Relay Selection Scheme

In cooperation wireless networks, where each transmitted signal will pass through various paths causing different attenuation in the associated signals received at the destination, the overall system performance can be reduced when a high quality paths should be chosen by using relay selection techniques. Moreover, due to the random nature of the wireless environment the channel gains are different which results in some relays providing a poor channel quality. Therefore, to minimize this effect, high quality paths should be chosen by using one of the relay selection techniques. For a cooperative AF network, the $max-min$ policy can generally be used to choose the best relay node as below [15]

$$i_{best} = arg \max_{i \in N}(min(|h_{sr_i}|^2, |h_{r_i d}|^2)),$$

where h_{sr_i} and $h_{r_i d}$ are channel gains for the source-relay and the relay-destination links, respectively. N represents the set of indices of all available

relays. Then, a two- and four-relay selection scheme for cooperative AF type networks is used in order to overcome the degradation of end-to-end BER performance in single-relay selection networks when there are feedback errors in the destination to relay node links. The best four-relay selection scheme can be used in this chapter as

$$\mathbf{i}_{con} = arg \max_{i\in N} \max_{i'\in N-1} \max_{i''\in N-2} \max_{i'''\in N-3} (min(|h_{sr_i}|^2, |h_{r_id}|^2)),$$

where $\mathbf{i} = (i,\ i',\ i'',\ i''')$.

4.3 System Model

As is shown in Figure 4.1, cooperative communication over Rayleigh flat-fading channels is considered. There is one source node, one destination node and N available relay nodes, all equipped with single half-duplex antennas. Perfect channel state information is assumed to be known at the destination node.

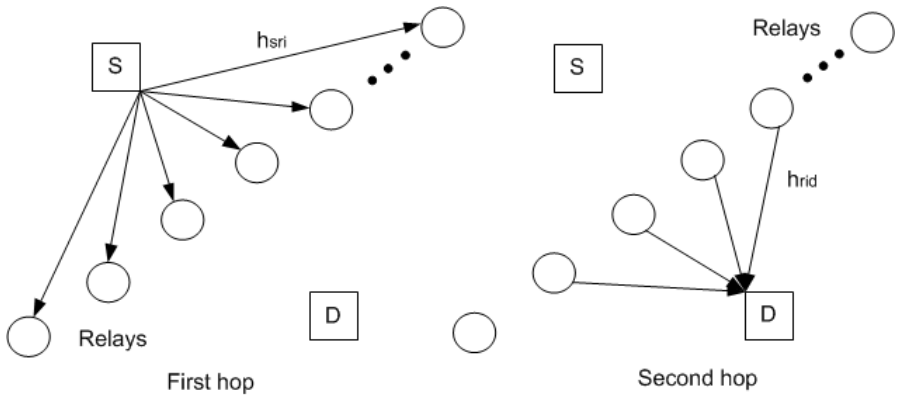

Figure 4.1. *A half-duplex dual-hop best four-relay selection system.*

Here the closed-loop quasi-orthogonal DSTBC with feedback scheme is used as in [71]. In the first hop, the source node transmits the signal vector $\mathbf{x} = [x_1\ \ -x_2^*\ \ -x_3^*\ \ x_4]^T$ to the relays. The received signal vector at the i^{th}

relay is given by

$$\mathbf{y}_{sr_i} = \sqrt{E_s} h_{sr_i} \mathbf{x} + \mathbf{n}_{r_i}, \tag{4.3.1}$$

where E_s is the average energy per symbol, h_{sr_i} is the channel gain between the source and the i^{th} relay node, and $\mathbf{n}_{r_i}$ is the complex additive white Gaussian noise vector at the i^{th} relay node. In the second hop of cooperation, the i^{th} selected relay amplifies and forwards its received signal, which is designed to be a linear function of its received signal and its conjugate in (4.3.2), to the destination through $h_{r_i d}$, which is the channel gain between the i^{th} relay node and the destination. The received signal at the destination node from the best four-relay selection is (4.3.3)

$$\mathbf{t}_{r_i d} = \sqrt{P_i}(A_i \mathbf{y}_{sr_i} + B_i \overline{\mathbf{y}}_{sr_i}), \tag{4.3.2}$$

$$\mathbf{y}_d = \sum_{i=1}^{N_s} h_{r_i d} \mathbf{t}_{r_i d} + \mathbf{n}_d, \tag{4.3.3}$$

where $\overline{\mathbf{y}}_{sr_i}$ is a conjugate of received signal vector at the i^{th} relay, N_s is the number of relays used, $N_s = 4$ in this chapter. According to [71], $A_1 = I_4$, $A_2 = A_3 = B_1 = B_4 = 0_4$,

$$A_4 = \begin{bmatrix} 0 & 0 & 0 & 1 \\ 0 & 0 & -1 & 0 \\ 0 & -1 & 0 & 0 \\ 1 & 0 & 0 & 0 \end{bmatrix}, B_2 = \begin{bmatrix} 0 & -1 & 0 & 0 \\ 1 & 0 & 0 & 0 \\ 0 & 0 & 0 & -1 \\ 0 & 0 & 1 & 0 \end{bmatrix}$$

$$B_3 = \begin{bmatrix} 0 & 0 & -1 & 0 \\ 0 & 0 & 0 & -1 \\ 1 & 0 & 0 & 0 \\ 0 & 1 & 0 & 0 \end{bmatrix},$$

and $\mathbf{n}_d$ is the complex additive white Gaussian noise vector at the destina-

tion. The i^{th} relay gain denoted by $\sqrt{P_i}$ is calculated from

$$P_i = \frac{E_s}{E_s|h_{sr_i}|^2 + N_0},$$

where N_0 is the noise variance [16]. Finally, the maximum likelihood (ML) decoding can be used at the destination node. Then, the instantaneous equivalent end-to-end signal-to-noise ratio (SNR) can be written as (4.3.4), because the MRC scheme is used at the destination.

$$\gamma_D = \sum_{i \in N_s} \frac{\gamma_{sr_i}\gamma_{r_i d}}{\gamma_{sr_i} + \gamma_{r_i d} + 1}, \tag{4.3.4}$$

where N_s denotes the set of relay indices for the relays chosen in the multi-relay selection scheme. The parameters $\gamma_{sr_i} = |h_{sr_i}|^2 E_s/N_0$ and $\gamma_{r_i d} = |h_{r_i d}|^2 E_s/N_0$ are the instantaneous SNR of the $S - R_i$ and $R_i - D$ links, respectively. Assuming that there is not any inter-relay interference between relays. The practical implementation of the MRC may, however, incur a capacity penalty due to the need to adopt a time multiplexing approach to transmission between the relays and the destination node; therefore, this section adopts an orthogonal transmission scheme, namely, the best four-relay selection with the closed-loop quasi-orthogonal DSTBC. For the Rayleigh flat fading channels, the probability density function (PDF) and the cumulative density function (CDF) of the SNR in the $u \in (sr_i, r_i d)$ links are given by

$$f_{\gamma_u}(\gamma) = \frac{1}{\check{\gamma}_u} e^{-\gamma/\check{\gamma}_u}, \tag{4.3.5}$$

$$F_{\gamma_u}(\gamma) = 1 - e^{-\gamma/\check{\gamma}_u}, \tag{4.3.6}$$

where $\check{\gamma}_u$ denotes the mean SNR for all links and $\gamma > 0$. According to [72],

$$\gamma_i = min(\gamma_{sr_i}, \gamma_{r_i d}) \geq \frac{\gamma_{sr_i}\gamma_{r_i d}}{\gamma_{sr_i} + \gamma_{r_i d} + 1}. \tag{4.3.7}$$

Therefore, the lower and upper bound for the equivalent end-to-end SNR can be given as

$$\frac{1}{2}\sum_{i=1}^{N_s}\gamma_i = \gamma_{low} \leq \gamma_D \leq \gamma_{up} = \sum_{i=1}^{N_s}\gamma_i, \tag{4.3.8}$$

where N_s denotes the set of relay indices for the relays chosen in the multi relay selection scheme. The upper bound SNR is more suitable for analysis in the medium and high SNR arrange. And then the CDF of $\gamma_i = min(\gamma_{sr_i}, \gamma_{r_id})$ can be expressed as [73]

$$\begin{aligned} F_{\gamma_i}(\gamma) &= 1 - Pr(\gamma_{sr_i} > \gamma)Pr(\gamma_{r_id} > \gamma) \\ &= 1 - [1 - Pr(\gamma_{sr_i} \leq \gamma)][1 - Pr(\gamma_{r_id} \leq \gamma)] \\ &= 1 - [1 - F_{\gamma_{sr_i}}(\gamma)][1 - F_{\gamma_{r_id}}(\gamma)]. \end{aligned} \tag{4.3.9}$$

Substituting (4.3.6) with the appropriate index into (4.3.9) yields

$$F_{\gamma_i}(\gamma) = 1 - e^{-\gamma/\check{\gamma}_{C_i}}, \tag{4.3.10}$$

where $\check{\gamma}_{C_i} = \frac{\check{\gamma}_{sr_i}\check{\gamma}_{r_id}}{\check{\gamma}_{sr_i}+\check{\gamma}_{r_id}}$. Since independent and identically distributed (i.i.d.) Rayleigh flat fading relay channels are assumed, then all relay links can be assumed to have the same average SNR, namely, $\check{\gamma}_{sr_i} = \check{\gamma}_{r_id} = \check{\gamma}_0 = E_s/N_0$, and $\check{\gamma}_{C_i} = \check{\gamma}_C = 0.5\check{\gamma}_0$. Therefore, the PDF of γ_i can be obtained by taking the derivative of the CDF (4.3.10) as

$$f_{\gamma_i}(\gamma) = \frac{1}{\check{\gamma}_{C_i}} e^{-\gamma/\check{\gamma}_{C_i}}. \tag{4.3.11}$$

In the next section, the outage probability analysis will be considered for the best four-relays selection scheme.

4.4 Outage Probability Analysis

Outage probability analysis for best four-relay selection is used in this section to show the advantage of multi-relay selection when no interference occurs at the relay nodes. In this approach the best four relay nodes are selected from N available relays, namely, the maximum γ_{max}, the second largest γ_{max-1}, the third largest γ_{max-2} and the fourth largest γ_{max-3} are selected from the N relays instantaneous SNR. Firstly, the selection of the L largest is not independent, therefore, according to [50], the joint distribution of the L most maximum values can be obtain as

$$f(x_1, x_2, ..., x_L) = L! \begin{pmatrix} N \\ L \end{pmatrix} [F(x_L)^{N-L}] \prod_{i=1}^{L} f(x_i), \tag{4.4.1}$$

where $x_1 \geq x_2 ... \geq x_L ... \geq x_N$ and $f(\cdot)$ and $F(\cdot)$ correspond to the PDF and CDF, respectively, and $\binom{N}{L} = \frac{N!}{L!(N-L)!}$ is the binomial coefficient. Therefore, the joint PDF of the four largest signal-to-noise ratios selection can be expressed as

$$\begin{aligned} f(w, x, y, z) =& N(N-1)(N-2)(N-3)[F(z)^{N-4}] \\ & f(w)f(x)f(y)f(z), \end{aligned} \tag{4.4.2}$$

where $w = \gamma_{max}$, $x = \gamma_{max-1}$, $y = \gamma_{max-2}$, $z = \gamma_{max-3}$, and $F(z) = 1 - e^{-z/\check{\gamma}_C}$ and $f(w) = 1/\check{\gamma}_C e^{-w/\check{\gamma}_C}$, $f(x) = 1/\check{\gamma}_C e^{-x/\check{\gamma}_C}$, $f(y) = 1/\check{\gamma}_C e^{-y/\check{\gamma}_C}$, $f(z) = 1/\check{\gamma}_C e^{-z/\check{\gamma}_C}$. Therefore,

$$\begin{aligned} f(w, x, y, z) =& \frac{N(N-1)(N-2)(N-3)}{\check{\gamma}_C^4} [1 - e^{-z/\check{\gamma}_C}]^{N-4} \\ & e^{-w/\check{\gamma}_C} e^{-x/\check{\gamma}_C} e^{-y/\check{\gamma}_C} e^{-z/\check{\gamma}_C}. \end{aligned} \tag{4.4.3}$$

Then the CDF $F_{\gamma_{up}}(\gamma)$ is calculated, where γ_{up} is the sum of w, x, y and z, which are identically distributed and formed as the ratios of exponential

random variables. Therefore, the CDF is obtained by

$$F_{\gamma_{up}}(\gamma) = Pr\{w + x + y + z \leq \gamma\}. \tag{4.4.4}$$

Given that w, x, y and z are non-negative, with $w \geq x \geq y \geq z$. Finally,

$$F_{\gamma_{up}}(\gamma) = \int_0^{\frac{\gamma}{4}} \int_z^{\frac{\gamma-z}{3}} \int_y^{\frac{\gamma-z-y}{2}} \int_x^{\gamma-x-z-y} f(w,x,y,z)\ dwdxdydz. \tag{4.4.5}$$

Using the PDF in (4.4.3) gives

$$\begin{aligned} F_{\gamma_{up}}(\gamma) = \int_0^{\frac{\gamma}{4}} \int_z^{\frac{\gamma-z}{3}} \int_y^{\frac{\gamma-z-y}{2}} \int_x^{\gamma-x-z-y} & \frac{N(N-1)(N-2)(N-3)}{\check{\gamma}_C^4} \\ & [1-e^{-z/\check{\gamma}_C}]^{N-4}\ e^{-w/\check{\gamma}_C}\ e^{-x/\check{\gamma}_C}\ e^{-y/\check{\gamma}_C}\ e^{-z/\check{\gamma}_C}\ dwdxdydz. \end{aligned} \tag{4.4.6}$$

The first integral for w is

$$I_1 = \int_x^{\gamma-x-z-y} e^{-w/\check{\gamma}_C}\ dw\ = \check{\gamma}_C\ e^{-\frac{x}{\check{\gamma}_C}} - \check{\gamma}_C\ e^{\frac{-\gamma+x+z+y}{\check{\gamma}_C}}. \tag{4.4.7}$$

And the second integral for x will be

$$\begin{aligned} I_2 = & \int_y^{\frac{\gamma-z-y}{2}} e^{-x/\check{\gamma}_C}\ [\check{\gamma}_C\ e^{-\frac{x}{\check{\gamma}_C}} - \check{\gamma}_C\ e^{\frac{-\gamma+x+z+y}{\check{\gamma}_C}}]\ dx \\ = & \ e^{\frac{-\gamma+z+y}{\check{\gamma}_C}}(\check{\gamma}_C y - \frac{{\check{\gamma}_C}^2}{2} - \check{\gamma}_C\frac{\gamma-z-y}{2}) + \frac{{\check{\gamma}_C}^2}{2}\ e^{\frac{-2y}{\check{\gamma}_C}}. \end{aligned} \tag{4.4.8}$$

Then, the next integral for y is

$$\begin{aligned} I_3 = & \int_z^{\frac{\gamma-z}{3}} e^{-y/\check{\gamma}_C}\ [e^{\frac{-\gamma+z+y}{\check{\gamma}_C}}(\check{\gamma}_C y - \frac{{\check{\gamma}_C}^2}{2} - \check{\gamma}_C\frac{\gamma-z-y}{2}) + \frac{{\check{\gamma}_C}^2}{2}\ e^{\frac{-2y}{\check{\gamma}_C}}]\ dy \\ = & \ e^{\frac{-\gamma+z}{\check{\gamma}_C}}(\frac{\gamma-z}{3}\frac{\check{\gamma}_C}{2}(\frac{\gamma-z}{3} - \frac{\check{\gamma}_C}{2} - (\gamma - z - \frac{2(\gamma-z)}{3})) + \frac{{\check{\gamma}_C}^3}{3} \\ & - z\frac{\check{\gamma}_C}{2}(z - \frac{\check{\gamma}_C}{2} - (\gamma - \frac{3z}{2}))) - \frac{{\check{\gamma}_C}^3}{3}e^{\frac{-3z}{\check{\gamma}_C}}. \end{aligned} \tag{4.4.9}$$

Finally, the last integral for z becomes

$$F_{\gamma_{up}}(\gamma) = \int_0^{\frac{\gamma}{4}} e^{-z/\check{\gamma_C}} \, [1 - e^{\frac{-z}{\check{\gamma_C}}}]^{N-4} \, I_3 \, dz \tag{4.4.10}$$

$$\begin{aligned} F_{\gamma_{up}}(\gamma) =& \frac{N(N-1)(N-2)(N-3)}{\check{\gamma}_C^3}\{\frac{\check{\gamma}_C^3}{24} - [\frac{\check{\gamma}_C^3}{24} + \frac{\gamma\check{\gamma}_C}{8}(\frac{\gamma+\check{\gamma}_C}{3}) - \frac{\gamma^2\check{\gamma}_C}{48} + \\ & \frac{\gamma^3}{144}]e^{-\frac{\gamma}{\check{\gamma}_C}} + \sum_{n=1}^{N-4}\binom{N-4}{n}(-1)^n\{\frac{\check{\gamma}_C^3}{6(n+4)} - [\frac{\check{\gamma}_C^3}{6(n+4)} - \frac{\check{\gamma}_C^3}{6n} + \\ & \frac{2\check{\gamma}_C^3}{3n^2} - \frac{8\check{\gamma}_C^3}{3n^3}]e^{-\frac{(n+4)\gamma}{4\check{\gamma}_C}} + [\frac{2\check{\gamma}_C^3}{3n^2} - \frac{\check{\gamma}_C^2(\check{\gamma}_C+\gamma)}{6n} - \frac{\gamma^2\check{\gamma}_C}{12n} + \frac{2\gamma\check{\gamma}_C^2}{3n^2} - \\ & \frac{8\check{\gamma}_C^3}{3n^3}]e^{-\frac{\gamma}{\check{\gamma}_C}}\}\} \end{aligned} \tag{4.4.11}$$

Therefore, the desired outage probability can be calculated. The outage probability is defined as when the average end-to-end SNR falls below a certain predefined threshold value, α. The outage probability can be expressed as

$$P_{out} = \int_0^{\alpha} f_{\gamma_b}(\gamma)d\gamma = F_{\gamma_{up}}(\alpha). \tag{4.4.12}$$

The outage probability of the best four-relays selection can be expressed by using the CDF expression (4.4.11) as

$$\begin{aligned} F_{\gamma_{up}}(\alpha) =& \frac{N(N-1)(N-2)(N-3)}{\check{\gamma}_C^3}\{\frac{\check{\gamma}_C^3}{24} - [\frac{\check{\gamma}_C^3}{24} + \frac{\alpha\check{\gamma}_C}{8}(\frac{\alpha+\check{\gamma}_C}{3}) - \frac{\alpha^2\check{\gamma}_C}{48} + \\ & \frac{\alpha^3}{144}]e^{-\frac{\alpha}{\check{\gamma}_C}} + \sum_{n=1}^{N-4}\binom{N-4}{n}(-1)^n\{\frac{\check{\gamma}_C^3}{6(n+4)} - [\frac{\check{\gamma}_C^3}{6(n+4)} - \frac{\check{\gamma}_C^3}{6n} + \\ & \frac{2\check{\gamma}_C^3}{3n^2} - \frac{8\check{\gamma}_C^3}{3n^3}]e^{-\frac{(n+4)\alpha}{4\check{\gamma}_C}} + [\frac{2\check{\gamma}_C^3}{3n^2} - \frac{\check{\gamma}_C^2(\check{\gamma}_C+\alpha)}{6n} - \frac{\alpha^2\check{\gamma}_C}{12n} + \frac{2\alpha\check{\gamma}_C^2}{3n^2} - \\ & \frac{8\check{\gamma}_C^3}{3n^3}]e^{-\frac{\alpha}{\check{\gamma}_C}}\}\} \end{aligned} \tag{4.4.13}$$

In the next section, the outage probability analysis verification will be considered.

4.5 Outage Probability Analysis Verification

In this section, in order to verify the results obtained from the above mathematical expressions, all relay links can be assumed to have the same average SNR, and there is no direct link between the source and the destination as path loss or shadowing renders it unusable. The SNR $\bar{\gamma}_0 = 10$ dB is assumed. Figure 4.2 shows the comparison of the outage probability of the best single-relay selection and the best four-relays selection schemes, using the formula given in (4.4.13). It can be seen that increasing the number of available relays, N, decreases the outage probability, and hence when the number of relays is large, the outage event (no transmission) becomes less likely, for example, with the total number of available relays increasing from 4 to 7, the outage probability of a best single-relay selection is decreased from almost 9% to 1.5%; at the same time, the outage probability of the best four-relay selection is decreased from almost 0.9% to 0.006%, when the threshold value α is 6 dB. This result confirms that the best four-relay selection provides more robust transmission than best single-relay selection, because for the best single-relay selection, it just uses a single relay to help the source to transmit the signal. Moreover, the curves show the analytical results and values found by simulations. A close match is observed between the analytical results and the simulations.

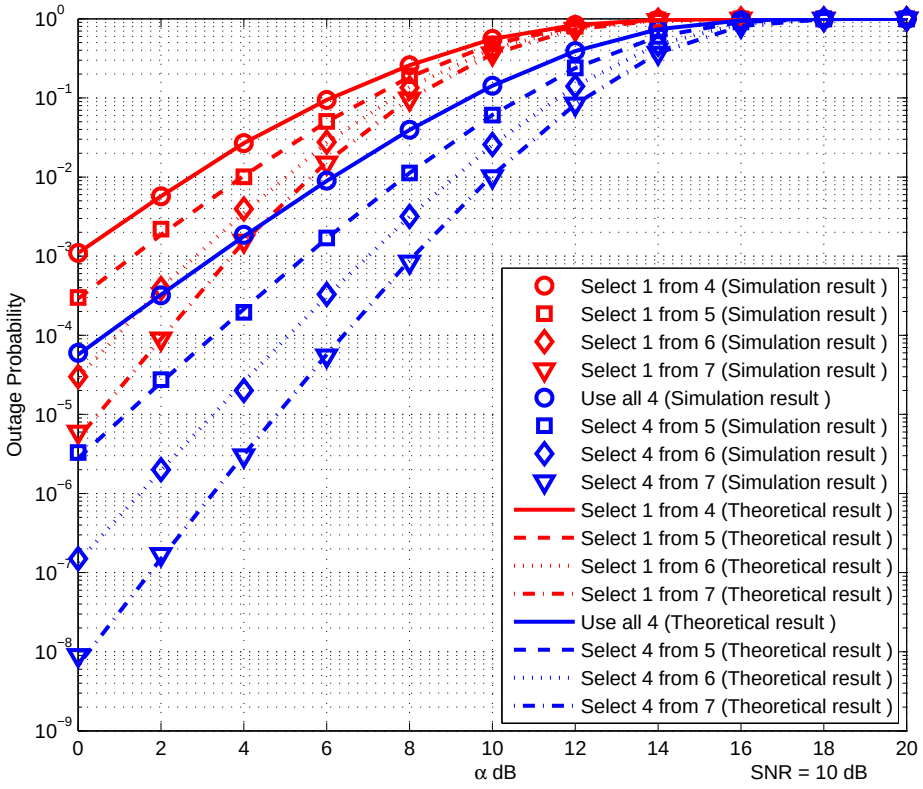

Figure 4.2. *Comparison of the outage probability of the best single-relay selection and the best four-relay selection schemes, the theoretical results are shown in line style and the simulation results as points.*

4.6 Analysis of The Impact of Feedback Errors

In this section, the BER performance of the best four-relay selection from a set of N available relays, i.e. $N = 6$, using DSTBC [71], is compared with the best single-relay selection in the presence of feedback errors, when QPSK symbols are used in transmission. In practise, such errors can be due to the delay in feeding back the information from the destination node. The channels may have changed and therefore the previous selection could need refining.

To simulate errors in the feedback of information from the destination, an error rate in the feedback is introduced. With an error rate of 0.5, for example, 50% of the selections are made in error, that is, rather than selecting the best relay, one of the other relays is chosen with equal probability of selection. As can be seen in Figure 4.3, when the destination node transmits perfect channel feedback to the relays, i.e. an error rate of 0, the BER performance of the best single-relay selection is worse than the best four-relays selection. Moreover, in the presence of errors in the channel feedback information, i.e. error rate over the range 0.5 to 1, the best four-relay selection outperforms the best single-relay selection. These results illustrate clearly the increased robustness of the best four-relay selection scheme over the single-relay selection scheme in the presence of moderate to severe feedback errors. For example, at the SNR = 12 dB, the BER for the best single-relay selection is reduced from almost 4×10^{-3} to 1.5×10^{-1} as the error rate changes from 0 to 1, whereas for the best four-relay selection the BER changes from almost 1.25×10^{-5} only to 5.75×10^{-4}, confirming the improved robustness.

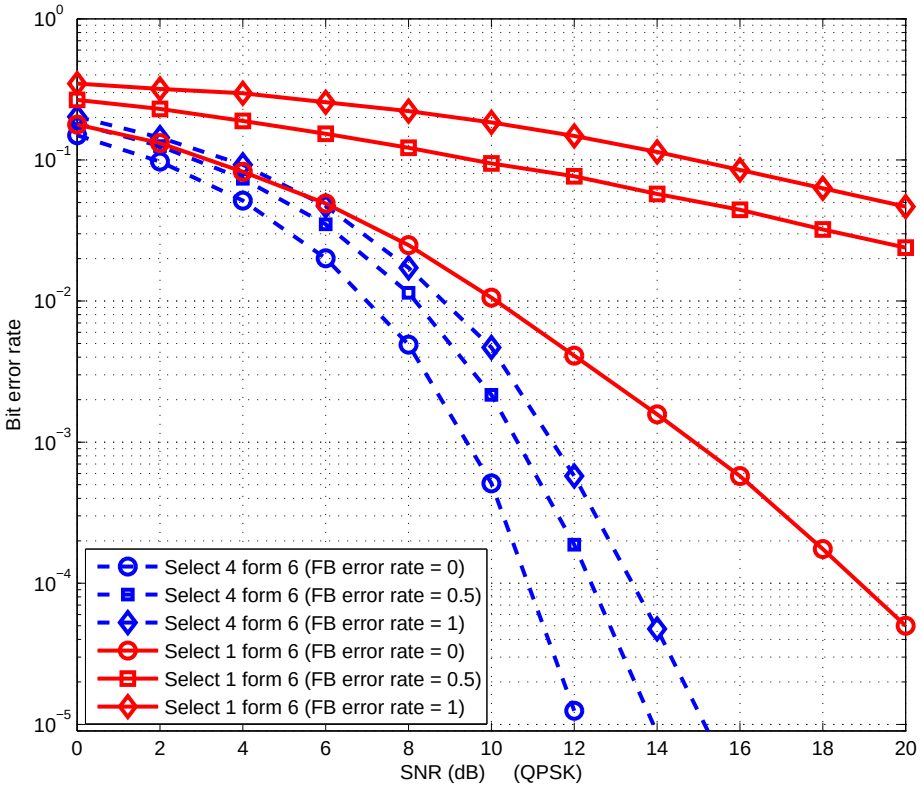

Figure 4.3. *BER performance comparison of the best four-relay selection (solid line) with the best single-relay selection (dashed line), with varying error in the feedback relay selection information from the destination.*

4.7 Summary

In this chapter, firstly, the local measurements of the instantaneous channel conditions were used to select the best four relays from a set of N available relays in the same cluster, and then these best relays were used with the Alamouti code to improve the diversity and decrease the outage probability. The best four-relay selection scheme was also shown to have robustness against feedback error and to outperform a scheme based on selecting only the best single-relay. Secondly, in order to further reduce the outage probability, the best four-relay were selected. Analytical expressions for the PDF and CDF of end-to-end SNR were derived together with closed form expressions for outage probability over Rayleigh flat fading channels. Numerical results were provided to show the advantage of the outage probability performance of the best four-relay selection in a cooperative communication system. The robustness of the best four-relay selection scheme is confirmed in the presence of moderate to severe feedback errors. In the next chapter, the outage probability analysis for different relay selection schemes will be introduced with inter-cluster interference only at the relay nodes.

Chapter 5

OUTAGE PROBABILITY ANALYSIS OF FULL RATE DISTRIBUTED TRANSMISSION SCHEME WITH INTER-RELAY INTERFERENCE

In this chapter, firstly, the local measurements of the instantaneous channel conditions are used to select the best two-relays from a set of N available relays and then these best two relays are used within amplify-and-forward two-path half duplex transmission with inter-relay self interference cancellation realised at one of the active relays. This best two relay selection scheme is shown to have robustness against feedback error in the relay selection schemes. Also, the effect of uncertainty in the inter-relay CSI at the relay is considered. Secondly, end-to-end BER evaluations confirm the advantage of using the interference-based relay selection scheme over the conventional $max - min$ approach.

5.1 Introduction

In cooperative communication systems [9], the amplify-and-forward (AF) half duplex relaying protocol has the advantage of being simpler to implement in practice as compared to the decode-and-forward (DF) protocol. A disadvantage of all relays operating in half duplex mode, is that the transmission of one data symbol from the source to destination via the relay occupies two channel uses which leads to a reduction in spectral efficiency [74]. For the two-relay topology proposed in [74] a two-path relaying protocol is used to recover a significant portion of the spectral efficiency loss in half duplex relaying. The DF version of this two-path relaying has been well studied in [75]. Achievable rates and capacity bounds for AF and DF two-path relaying are analysed in [75], [76] and [77].

Since the AF two-path relay scheme alternatively uses different relays to maximise spectral efficiency, an inter-relay interference term is additionally received at the destination [74]. Successive decoding at the destination with full or partial cancellation of this inter-relay interference term was proposed in [74]. However, this method only performs well for a weak to moderate inter-relay channel. The direct link from the source to the destination was not considered in [74]. In [78], it was assumed that the interference between the relays can be perfectly cancelled through successive interference cancellation (SIC) at the relay. This assumption of perfect SIC of the interference signal may not be applicable in practical scenarios because channel state information (CSI) is likely to contain error and any interference between relays will definitely degrade the end-to-end performance. In [61], AF two-path relaying with inter-relay self interference cancellation is proposed where the cancellation is performed at one of the relays. In [78] and [61] the direct link between source and destination is considered.

Currently, there is interest in relay selection schemes for multi-relay en-

vironments. In these approaches, selecting one relay based on instantaneous channel conditions offers the same diversity benefits with a lower complexity than distributed space-time codes (DSTC) [79] which require simultaneous relay transmissions [15] [22]. However, the proposed relay selection principle lacks the flexibility to deal with the presence or absence of interference effects and only remains optimal for ideal scenarios without interference [80]. Moreover, a best single-relay selection approach may not offer enough capacity. Therefore, a multi-relay selection scheme may be required.

The basic AF two-path half duplex relaying scheme is considered wherein inter-relay self interference affects the cooperation process. The effect of uncertainty in the inter-relay CSI on the end-to-end bit error rate (BER) performance is studied. A new relay selection scheme which accounts for the inter-relay interference level is introduced to provide improved end-to-end BER over a range of SNRs.

5.2 System Model

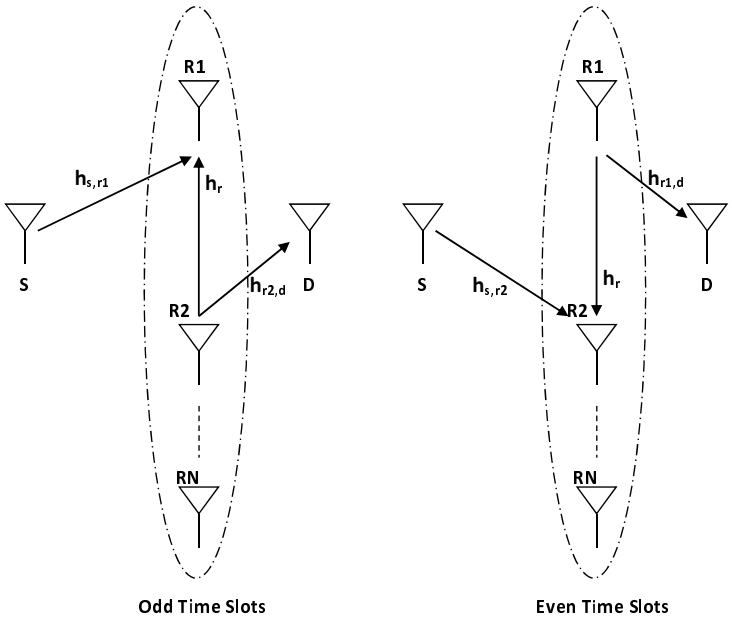

Figure 5.1. *Best pair AF two-path relaying scheme without direct link.*

Consider a cooperative network system in which one source node (S), one destination node (D) and a set of AF relays are available. Only the best pair of relays denoted ($R1$, $R2$) are used for communication between S and D. No precoding is assumed and all the nodes have a half-duplex single antenna. The source transmission is divided into frames, each containing L symbols. The k-th frame is denoted as $\mathbf{x}_k = [x_k(1)\ x_k(2)\ ...\ x_k(L)]^T$ with $E\{\mathbf{x}_k\mathbf{x}_k^H\}= \mathbf{I}_L$, where $\mathbf{I}_L$ is an identity matrix of size L. The destination will perform detection on a frame-by-frame basis. Without loss of generality, L is assumed to be even and the channel is presumed static within a frame. Also, perfect channel state information is presumed to be available at all receivers, except the inter-relay link. As in [61], the transmission protocol of the AF two-path relaying scheme within two repeated time slots is represented in Figure 5.1.

In this protocol, the source transmits the signal to the best selected relay $R1$, also the second best selected relay $R2$ broadcast the previous received signal to the destination node during the odd time slot. And during the even time slot, the source transmits the next signal to the second best selected relay $R2$; also the best selected relay $R1$ broadcasts the previous received signal to the destination node. In practice, the direct transmission link between S and D may or may not be available due to path loss or shadowing. Moreover, if is assumed that there is no or poor direct connection between the source and destination nodes as in Figure 5.1, therefore, the system model can be represented by the following equations. The received signals at the i-th relay and the destination node are given by

$$y_{Ri} = \sqrt{E_s}h_{s,Ri}x + \sqrt{E_s}h_r\acute{x} + n_{Ri}, \qquad i \in 1, 2, \tag{5.2.1}$$

$$y_d = \sqrt{P_i}h_{Ri,d}y_{Ri} + n_d, \tag{5.2.2}$$

where x and $\acute{x}$ are the signal from the source and the previous signal from

the other relay, respectively. E_s is the average energy per symbol (E_s=1), $h_{s,Ri}, h_r$ and $h_{Ri,d}$ are the channel gains between the source and i-th relay node, between the two best selected relays and between the i-th relay node and the destination node, respectively. And the complex additive white Gaussian noise n_{Ri} and n_d are modeled as zero-mean mutually independent, circularly-symmetric, complex Gaussian random variables with variance N_0 at the i-th relay and the destination node, respectively. The i-th relay gain denoted by $\sqrt{P_i}$ is calculated from

$$P_i = \frac{E_s}{E_s|h_{s,Ri}|^2 + E_s|h_r|^2 + N_0}. \tag{5.2.3}$$

Substituting (5.2.1) into (5.2.2) gives

$$y_d = \sqrt{P_i}\sqrt{E_s}h_{s,Ri}h_{Ri,d}x + \sqrt{P_i}\sqrt{E_s}h_r h_{Ri,d}\acute{x} + \sqrt{P_i}h_{Ri,d}n_{Ri} + n_d, \tag{5.2.4}$$

Let $y_{rj}(i)$ and $y_d(i)$ denote the received signal at the j-th relay, $j \in 1, 2$, and the received signal at D, at time slot i respectively. At time slot 1, $x(1)$ is sent from S. Therefore at $R1$ and D,

$$y_{r1}(1) = \sqrt{\rho}h_{s,r1}x(1) + n_{r1}(1), \tag{5.2.5}$$

$$y_d(1) = \sqrt{\rho}h_{s,d}x(1) + n_d(1), \tag{5.2.6}$$

where $\rho, h_{s,d} \sim \mathcal{CN}(0, \gamma^2_{s,d})$, and $h_{s,rj} \sim \mathcal{CN}(0, \gamma^2_{s,rj})$ are the average transmit power, the channel coefficients from S to D and S to j-th relay respectively; $n_{rj}(i) \sim \mathcal{CN}(0, \sigma^2)$ and $n_d(i) \sim \mathcal{CN}(0, \sigma^2)$ are the additive white Gaussian noise (AWGN) at the j-th relay and D respectively at the i-th time slot. Notice that $y_d(1)$ contains only $x(1)$ as $R2$ does not transmit in the first time slot. Then, at time slot 2, $x(2)$ is sent from S and $x_{r1}(2)$ is sent from

$R1$. Therefore at $R2$ and D,

$$y_{r2}(2) = \sqrt{\rho} h_{s,r2} x(2) + h_r x_{r1}(2) + n_{r2}(2), \tag{5.2.7}$$

$$y_d(2) = \sqrt{\rho} h_{s,d} x(2) + h_{r1,d} x_{r1}(2) + n_d(2), \tag{5.2.8}$$

where $x_{r1}(2) = g_{r1}(2) y_{r1}(1)$. Here $g_{rj}(i), h_{rj,d} \sim \mathcal{CN}(0, \gamma^2_{rj,d})$ and $h_r \sim \mathcal{CN}(0, \gamma^2_r)$ are the power scaling factor at the j-th relay in time slot i which will be defined later, the channel coefficients from the j-th relay to D and channel coefficient between the two relays respectively. It is assumed that h_r is reciprocal [61].

At time slot 3, $x(3)$ is sent from S, while $x_{r2}(3)$ is sent from R2. Therefore at $R1$ and D,

$$\begin{aligned} y_{r1}(3) &= \sqrt{\rho} h_{s,r1} x(3) + h_r x_{r2}(3) + n_{r1}(3) \\ &= \sqrt{\rho} h_{s,r1} x(3) + h_r g_{r2}(3) [\sqrt{\rho} h_{s,r2} x(2) \\ &\quad + h_r x_{r1}(2) + n_{r2}(2)] + n_{r1}(3), \end{aligned} \tag{5.2.9}$$

$$y_d(3) = \sqrt{\rho} h_{s,d} x(3) + h_{r2,d} x_{r2}(3) + n_d(3), \tag{5.2.10}$$

where $x_{r2}(3) = g_{r2}(3) y_{r2}(2)$ [61]. Notice that $y_{r1}(3)$ contains the inter-relay self interference term, $h_r g_{r2}(3) h_r x_{r1}(2)$, which is known at $R1$ and therefore it can be cancelled, but in practice the inter-relay self interference cancellation is unlikely to be completely perfect, so it is assumed that the inter-relay channel is only estimated. Thus, the transmit signal at time slot 4 from $R1$ will be

$$\begin{aligned} x_{r1}(4) &= g_{r1}(4) [y_{r1}(3) - g_{r2}(3) \hat{h}^2_r x_{r1}(2)] \\ &= g_{r1}(4) \{\sqrt{\rho} h_{s,r1} x(3) + h_r g_{r2}(3) [\sqrt{\rho} h_{s,r2} x(2) \\ &\quad + n_{r2}(2)] + e + n_{r1}(3)\} \end{aligned} \tag{5.2.11}$$

where $e = g_{r2}(3)x_{r1}(2)(h_r^2 - \hat{h}_r^2)$ which represents the uncancelled inter-relay interference. The study of e which is a focus of this chapter was not performed in [61].

At time slot 4, $x(4)$ is sent from S, while $x_{r1}(4)$ is sent from $R1$. Therefore at $R2$ and D,

$$y_{r2}(4) = \sqrt{\rho}h_{s,r2}x(4) + h_r x_{r1}(4) + n_{r2}(4), \tag{5.2.12}$$

$$y_d(4) = \sqrt{\rho}h_{s,d}x(4) + h_{r1,d}x_{r1}(4) + n_d(4), \tag{5.2.13}$$

The transmit signal at time slot 5 from $R2$ is $x_{r2}(5) = g_{r2}(5)y_{r2}(4)$. These transmission steps are then continuously repeated until L symbols have been transmitted from S. In practice, two additional time slots are required at the end as the terminating sequence. However, this slight loss in rate is asymptotically zero for large values of L. It is also required for D to wait for all $L+2$ transmissions to happen before performing decoding [80]. The power scaling factors in the i-th time slot $g_{r1}(i)$ and $g_{r2}(i)$ are expressed in [61] as

$$g_{r2}(i) = \sqrt{\frac{\rho}{\gamma_{s,r2}^2\rho + \gamma_r^2\rho + \sigma^2}} \quad , i = 3, 5, ..., L-1.$$

Here, ρ is the average transmitted power at the source and the two relays. Thus, $g_{r1}(i)$ which depends on $g_{r2}(i-1)$ is also constant for i = 4, 6, ..., L. Hence, both $g_{r1}(i)$ and $g_{r2}(i)$ are constants for $i \geq 3$. In the next section, the exploitation of the availability of multiple relays in the transmission scheme will be considered.

5.3 Outage Probability Analysis of Best Single-Relay Selection

This section focuses on the analysis of the effect of inter-relay interference on the relays which contains nodes linked by Rayleigh flat-fading quasi-static channels. For many application, it is not important what the exact value

of the BER is, as long as it stays below a certain threshold. For example, in transmission of coded speech sounds it is acceptable to a user as long as a certain threshold BER is not exceeded. It is meaningful to determine the percentage of time that acceptable speech quality will not be available. This percentage is known as outage probability [81]. Computation of outage probability becomes much simpler if rather than defining a maximum BER, a minimum SNR for the system to work properly is used. Then, the outage probability can be found as

$$P_{out} = P(\gamma < \gamma_o) = \int_0^{\gamma_o} f_\gamma(\gamma) d\gamma. \tag{5.3.1}$$

Outage probability can also be seen as another way of establishing a fading margin: the mean SNR that guarantees a certain outage is required [81].

5.3.1 Statistical Description

For clarity in development, it is supposed that the mean $\sigma^2_{s,Ri} = \sigma^2_{Ri,d}$ and the average signal-to-interference power ratio

$$L = \frac{\varepsilon(\gamma_{s,Ri})}{\varepsilon(\gamma_{INFi})} = \frac{\sigma^2_{s,Ri}}{\sigma^2_{R1,R2}}, \tag{5.3.2}$$

where $\gamma_{s,Ri}$ is the signal-to-noise ratio (SNR) of the link from the source to the relay and $\gamma_{INFi} = \gamma_{R_1,R_2}$ denotes the interference-to-noise ratio (INR) for the i-th relay. The symbol $\varepsilon(.)$ represents the statistical expectation operator. Note that the parameter L controls the level of interference at the relays. So the instantaneous equivalent end-to-end signal-to-interference-and-noise ratio (SINR) can be written as

$$\gamma_d = \frac{P_i |h_{s,Ri}|^2 |h_{Ri,d}|^2}{P_i |h_r|^2 |h_{Ri,d}|^2 + P_i |h_{Ri,d}|^2 N_0 + N_0}. \tag{5.3.3}$$

Substituting (5.2.3) into (5.3.3), the end-to-end SINR is

$$\gamma_d = \frac{\gamma_{s,Ri}\gamma_{Ri,d}}{\gamma_{INFi}(\gamma_{Ri,d}+1)+\gamma_{s,Ri}+\gamma_{Ri,d}+1}, \tag{5.3.4}$$

where $\gamma_{s,Ri} = |h_{s,Ri}|^2 E_s/N_0$ and $\gamma_{Ri,d} = |h_{Ri,d}|^2 E_s/N_0$ are the instantaneous SNR of the $S-R_i$ and R_i-D links, respectively. It is difficult to use (5.3.4) to find a closed form expression for the probability density function of γ_d, therefore, an asymptotic bound is provided in the following subsection.

5.3.2 Asymptotic Description

For high SNR, (5.3.4) as in [80] can be obtained as

$$\gamma_d \simeq \frac{\gamma_{s,Ri}}{\gamma_{INFi}}, \tag{5.3.5}$$

which is the ratio between the SNR of the first hop and the INR of the interference link, because when $SNR \to \infty$, then

$$\varepsilon[\gamma_{INFi}]\varepsilon[\gamma_{Ri,d}] \gg \varepsilon[\gamma_{INFi}] + \varepsilon[\gamma_{s,Ri}] + \varepsilon[\gamma_{Ri,d}] + 1. \tag{5.3.6}$$

In this case, the statistical description of the system is independent of the second hop. For this asymptotic case, the probability density function (PDF) and cumulative distribution function (CDF) of the ratio in (5.3.5), which is between two exponential random variables, are given in closed form as [82]

$$f(\gamma) = \frac{L}{(L+\gamma)^2} \qquad \text{and} \qquad F(\gamma) = \frac{\gamma}{L+\gamma}, \tag{5.3.7}$$

where $f(.)$ and $F(.)$ denote the PDF and the CDF, respectively. And L is the ratio between the average SNR of the source to relay channel link and the average INR of the interference link. These expressions assume a fixed number of available relays; in certain situations, however, additional relays will be available therefore relay selection is next considered.

5.3.3 Relay Selection with Outage Probability Analysis

In order to introduce the relay selection scheme, the conventional relay selection scheme is used to select the best relay $R1$ from the N available relays in the ideal distributed implementation without interference [15]. This requires the instantaneous signal SNR between the links from the source to the relay and the relay to the destination node to be known, and a particular relay is selected to maximize the minimum between them, the relay selection scheme can therefore be represented by

$$R_1 = arg \max_{i \in N_{relay}} min \left\{ \gamma_{s,R_i}, \gamma_{R_i,d} \right\}. \tag{5.3.8}$$

The conventional relay selection policy offers the relay with the best end-to-end path between source and destination and provides diversity gain on the order of the number of the relays [69]. However, this relay selection criterion is only considered for environments without interference, and the best single-relay selection is not always sufficient to satisfy the required outage probability at a destination node. Finally, when feedback error is present in the relay selection, the performance of the single-relay selection scheme is significantly degraded. Therefore, a second relay selection policy $R2$ is proposed for use in interference configurations for legacy networks which are restricted to adopt a $max(min(.,.))$ type policy. The proposed relay selection criterion is motivated by the simplified expression of the system at the high end-to-end SNR. As has been seen in (5.3.5) the asymptotic behavior of the system converges to the ratios between source to relay and interference links. Therefore, a second relay selection policy is to choose the best relay from the $N-1$ available relays which gives the maximum value of the ratio. The second relay selection $R2$ policy can be obtained as

$$R_2 = arg \max_{i \in N_{relay}-1} \left\{ \frac{\gamma_{s,R_i}}{\gamma_{INF_i}} \right\}, \tag{5.3.9}$$

where $R1$ in (5.3.8) denotes the best relay with the best link in N, and $R2$ in (5.3.9) is the best relay amongst the remaining $N-1$ with less interference. In this approach, the best two relay nodes $R1$ and $R2$ are selected to communicate between source and destination nodes from the N available relays in the environment. Assuming that $R1$ is a fixed selected relay node as a base station, and $R2$ is a mobile relay node selected by less interference as the previous asymptotic description. Then, calculate the CDF of the random variable $\gamma_d \simeq \frac{\gamma_{s,R}}{\gamma_{INF}}$ as

$$F(\gamma) = \left[\frac{\gamma}{L+\gamma}\right]^N. \tag{5.3.10}$$

Therefore, the outage probability is defined as when the average end-to-end SNR falls below a certain predefined threshold value, $\alpha = 2^{2I} - 1$, where I is the target rate. The outage probability can be expressed as

$$P_{out} = \int_0^{\alpha} f_{\gamma}(\gamma)\, d\gamma \;=\; F_{\gamma}(\alpha). \tag{5.3.11}$$

The outage probability of the best single-relay selection can be expressed by using the CDF expression as in (5.3.10). These theoretical expressions are next confirmed by numerical simulations.

5.3.4 Outage Probability Analysis Verification

In this section, in order to verify the results obtained from the above mathematical expressions, the source node and the relay nodes are assumed to use the same transmission power, also all relay links have the same average SNR as $\overline{\gamma}_0 = 10dB$, and there is no direct link between the source and the destination as path loss or shadowing render it unusable.

Figure 5.2 shows the outage probability of the best single-relay selection from N available relays, for different values of N and using the formula given in (5.3.10). It can be seen that increasing the number of relays, N, decreases the outage probability, and hence when the number of relays is large, the out-

age event becomes less likely, for example, with the total number of available relays increasing from 3 to 6, the outage probability is significant decreased from almost 0.38 to 0.14, when the threshold value α is 4 dB. Secondly, the curves show the analytical results and values found by simulations. A close match is observed between the analytical results and simulations.

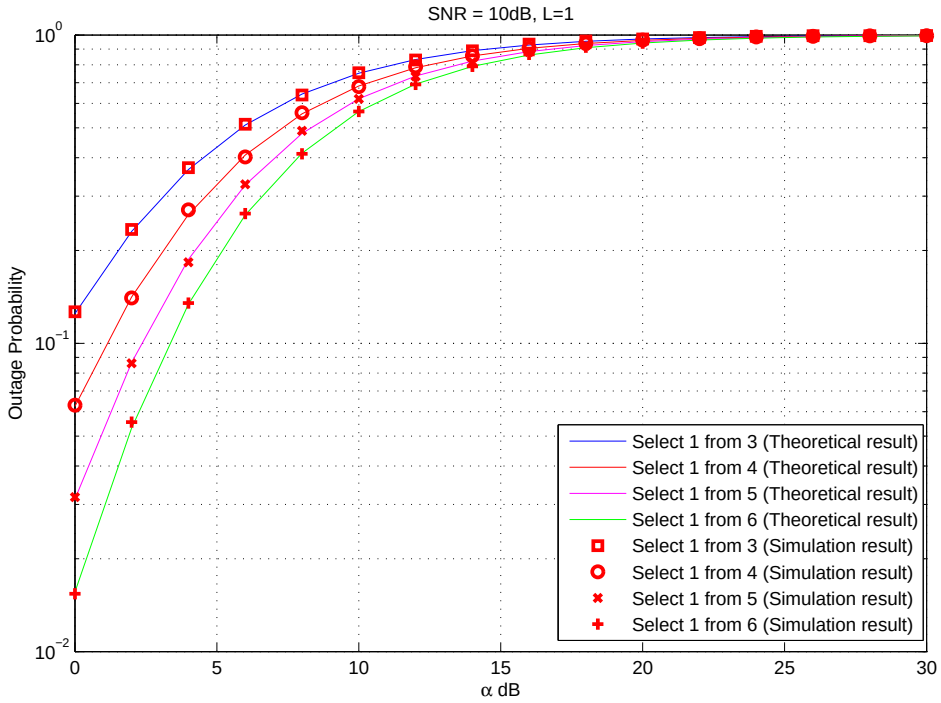

Figure 5.2. *Comparision of the outage probabilty of the best single-relay selection scheme, the theoretical results are shown in line style and the simulation results as points.*

Figure 5.3 shows the outage probability of the best single-relay selection from different numbers of N available relays with less interference at relay nodes, where the average INR of the interference link is equal 0.2, so the ratio between the average SNR of source to relay channel link and the average INR of the interference link is L=5. It can be seen that increasing the number of relays, N, decreases the outage probability, for example, the outage probability is significant decreased from almost 0.04 to 0.0015, when the total number of available relays increasing from 3 to 6, when the threshold value α is 4 dB. Then, the outage performance of the asymptotic case is better when the source-to-interference power ratio is increased. Moreover, it can be seen that the theoretical results match extremely well with the simulation results.

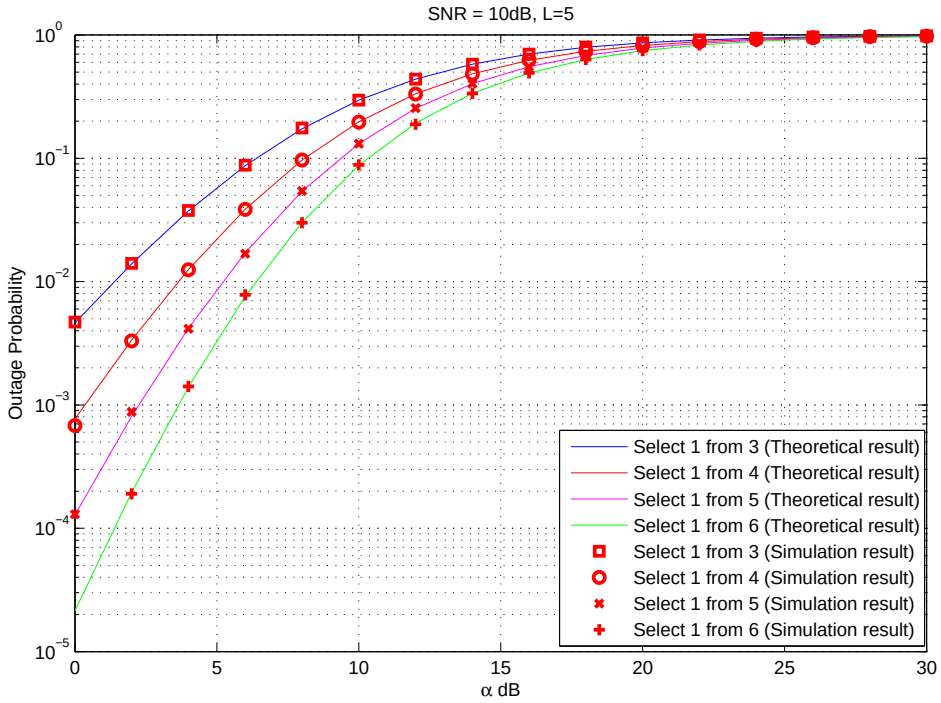

Figure 5.3. *Comparision of the outage probabilty of the best single-relay selection scheme with less interference, the theoretical results are shown in line style and the simulation results as points.*

Selecting a best single-relay scheme as explained in this chapter is not always sufficient to satisfy the required outage probability at a destination node. Therefore, in order to overcome this shortcoming, a multi-relay selection scheme will be employed. In order to derive these results it was necessary to make certain assumptions in the system model. Therefore the advantage of the proposed relay selection scheme is confirmed by evaluating the end-to-end BER. In the next figure, the end-to-end BER performance of the best single-relay selection from a group of N available relays, $N = 4, 6, 8$ is compared, when binary phase-shift keying (BPSK) symbols are used in transmission as described in Figure 5.1. The comparison between the best single-relay selection over a range of available relays and no relay selection scheme is shown.

As can be seen in Figure 5.4, the end-to-end BER performance of the no relay selection scheme is worse than the best single-relay selection schemes for the three different numbers of relays available. For example, to achieve an end-to-end BER of 10^{-2} with no relay selection requires approximately 20dB SNR whereas with relay selection only 15, 14, 13.5 dB SNRs are required with 4, 6 and 8 available relays. Note, however, that full spatial diversity is not achievable due to spatial interference. These results confirm the advantage of the proposed relay selection scheme and substantiate the value of the outage probability results.

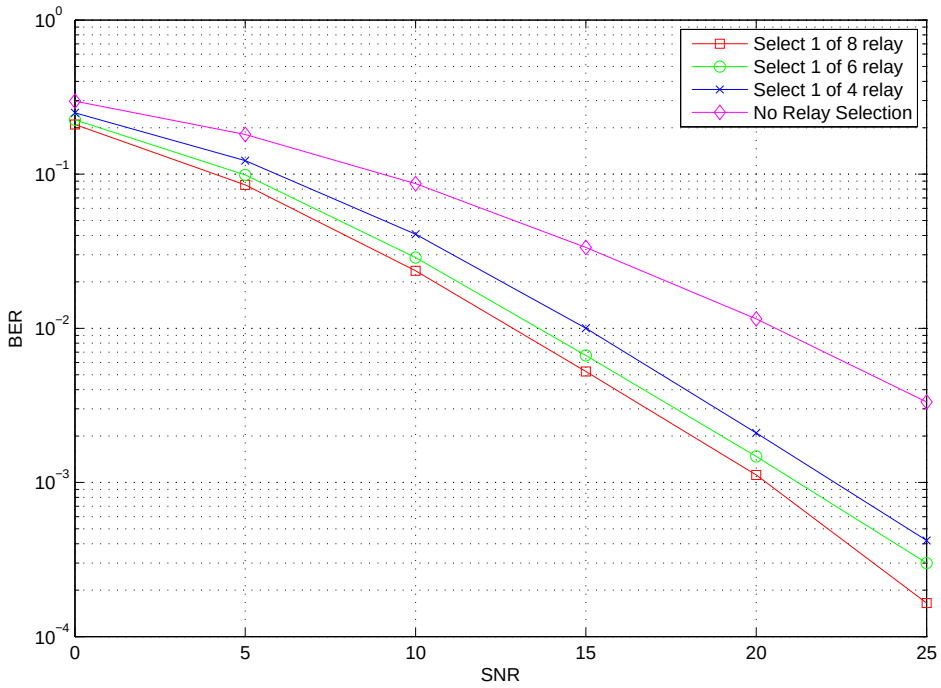

Figure 5.4. *BER performance of the best single-relay selection scheme with various numbers of relays.*

5.3.5 BER Analysis of Proposed Scheme with Error in Inter-Relay Interference Cancellation

In this section, the end-to-end BER performance of the best single-relay selection from four available relays with various levels of error in the inter-relay interference cancellation is compared, when binary phase-shift keying (BPSK) symbols are used in transmission as described in Figure 5.1.

In Figure 5.5 the end-to-end BER performance for various levels of CSI errors of inter-relay interference cancellation with interference-based relay selection scheme is shown. As can be seen in Figure 5.5, the end-to-end BER performance is worse when there is an error in inter-relay interference cancellation especially at higher SNR where an error floor is introduced. For example, to achieve an end-to-end BER of 10^{-2} with no relay selection requires approximately 15dB SNR whereas with 10% error with the inter-relay CSI, 20dB SNR is required with four available relays. As such, a significant increase in SNR maybe needed to compensate for errors in the interference cancellation.

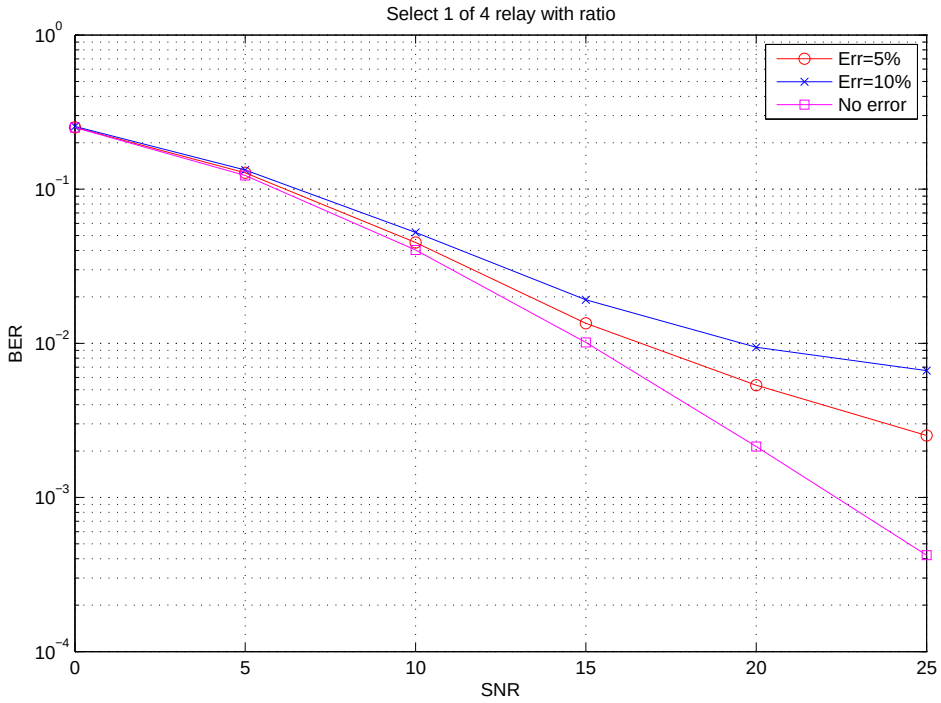

Figure 5.5. *BER performance of the best single-relay selection scheme with various number of relays with error in inter-relay interference cancellation.*

5.4 Outage Probability Analysis of Best Two-Relay Selection

5.4.1 Interference-based Relay Selection Scheme

The conventional relay selection scheme considered was proposed in [15] and is suitable for distributed implementation. It needs the instantaneous signal strength SNR between the links $S \rightarrow r$ and $r \rightarrow D$ ($r \in R_{relay}$) , where a set $R_{relay} = \{1, 2, ..., K\}$ of potential K relays, and the selected relay is chosen to maximize the minimum between them. The conventional relay selection scheme can be expressed as [80]

$$r_{Conv} = arg \max_{r \in R_{relay}} min \{\gamma_{s,r}, \gamma_{r,d}\} . \tag{5.4.1}$$

The conventional relay selection scheme ensures that the relay with the best end-to-end link between source and destination is used and provides diversity gain on the order of the number of relays [15]. In this work, the focus is the conventional $max - min$ selection scheme for AF systems. This selection scheme approximates the optimal AF selection for non-interference environments and optimizes the required computational overhead. The $max - min$ scheme is an efficient selection metric for the AF technique. It efficiently approximates the performance of the optimal AF selection scheme, which is based on instantaneous AF statistics.

In this section the best two relays (R1, R2) are first selected from the available relays to communicate between the source and the destination using the conventional relay selection scheme.

Moreover, a new two step approach is proposal to selection the best two relays. Firstly, the best relay R1 is first selected by considering the conventional relay selection scheme which is used in no-interference configurations as explained in the previous section. Secondly, the second best relay R2 is selected by using an extension of the conventional selection scheme [80]. It

is expressed as a simple ratio between the conventional *min* operation and the interference term and can be written as [80]

$$r_{inter} = arg \max_{r \in R_{relay}} \left\{ \frac{min\left\{\gamma_{s,r}, \gamma_{r,d}\right\}}{\gamma_{INF}} \right\}. \tag{5.4.2}$$

This interference-based selection scheme based on the conventional approach does not require complex structural modifications to the conventional mechanism. As the interference term is taken into account independently of the *min* operation, systems that already use this conventional relay selection can easily be updated to the proposed interference-based selection without modifying the *min* operation [80]. More specifically, all of the conventional relay selection schemes can be extended to the interference environment by simple division with the instantaneous interference term, as the interference term is considered outside of the *min* process.

5.4.2 Simulation Results

In this section, the performance of the simulations of the proposed schemes are provided, and the performance is shown by the end-to-end bit error rate (BER) using uncoded binary phase shift keying (BPSK) symbols versus SNR, also maximum likelihood (ML) decoding is used at D. In Figure 5.6, the performance of the AF two-path half-duplex relaying is compared with the inter-relay self interference cancellation scheme using different relay selection techniques, which select the best two relays to communicate between source and destination nodes.

From Figure 5.6 it can be seen that the BER performance for selecting the best two-relay of four relays by using the conventional relay selection scheme is the best technique compared with the interference-based relay selection scheme, when the inter-relay self interference cancellation is perfect. Also, the conventional relay selection scheme is better than the min-interference

relay selection scheme, which chooses the second best relay by focusing on the minimum interference between the best first selection relay and the other relays in the network. For example to attain a BER 10^{-4} approximately $21dB$ total power is required in the case without relay selection, however, in the case of select the best two-relay of four relays using the $max - min$ scheme approximately $16dB$ is required, approximately $5dB$ less than the fixed two relay design. The interference-based relay selection design also requires $4dB$ less than the fixed relay approach.

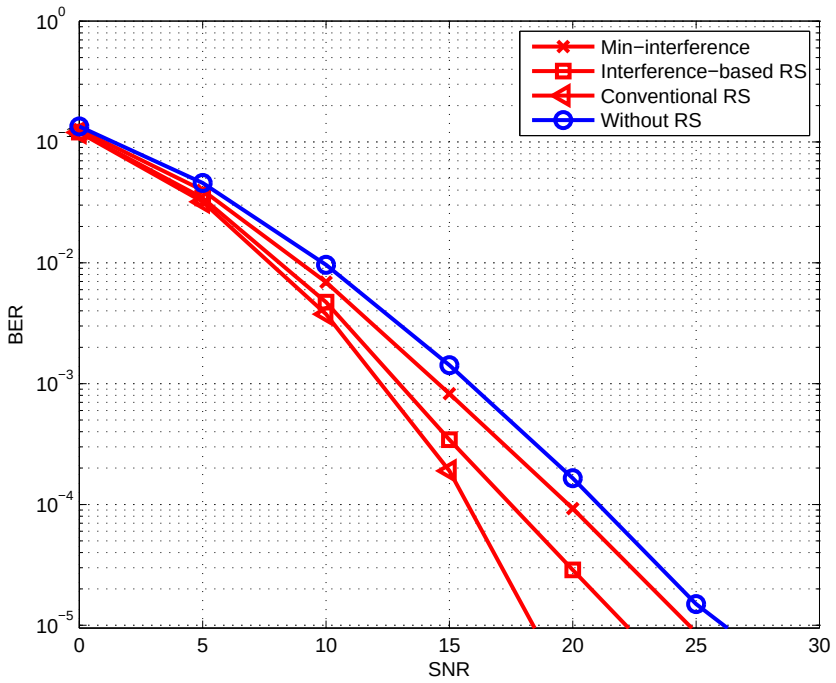

Figure 5.6. *BER performance for RS using different methods of best two- or four-relay assuming perfect inter-relay channel.*

In Figure 5.7 the BER performance for various levels of CSI errors of inter-relay interference cancellation with conventional and interference-based relay selection schemes is shown. The conventional scheme has better performance than the interference-based scheme when the inter-relay interference cancellation is perfect, but when there is an error in the inter-relay interference cancellation, the interference-based scheme, shown in red, has better performance especially at higher SNR. For example, above $15dB$ the interference-based scheme with 10% error of the inter-relay CSI has better performance than the conventional scheme and still remains better when the error is increased. So, the interference-based relay selection scheme is very useful in practice to mitigate the effect of CSI errors.

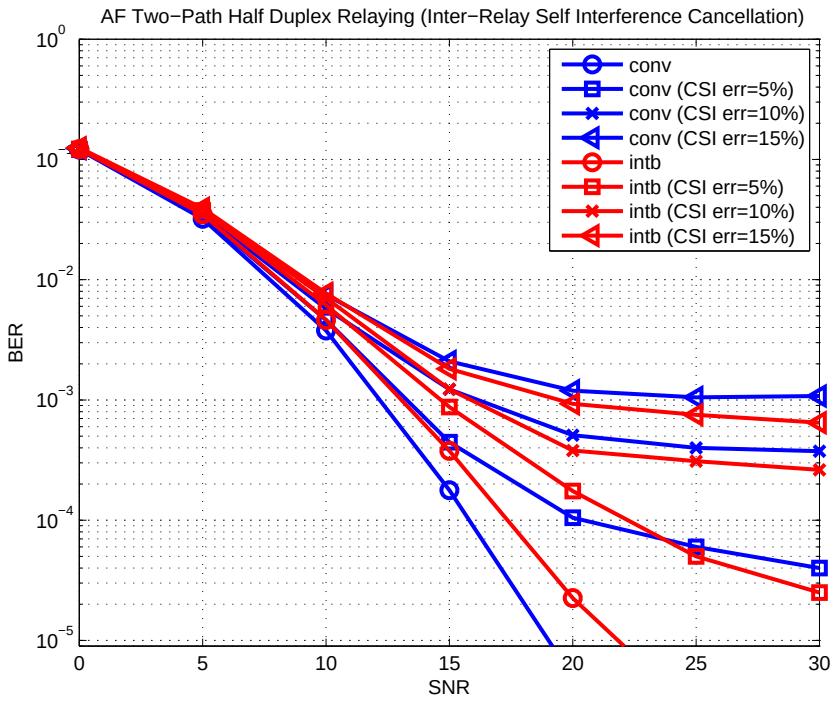

Figure 5.7. *BER performance with CSI errors in Inter-Relay Self Interference Cancellation, and relay selection: conventional (conv) and interference-based (intb).*

5.5 Summary

In this chapter, a system model has been proposed for a cooperative network based upon a best pair amplify-and-forward two-path half duplex transmission with inter-relay self interference cancellation scheme without direct link between source and destination nodes. Outage probability analysis was then considered. Finally, simulations were used to verify the analytical results. End-to-end bit error rate simulations were also used to confirm the advantage of relay selection. A critical weakness of the approach is shown by the sensitivity to errors in the CSI used within the interference cancellation. End-to-end bit error rate evaluations confirmed the advantage of using the interference-based relay selection scheme over the conventional $max - min$ approach. Therefore, in the next chapter, the outage probability in distributed transmission with inter-cluster interference based on multi-relay selection in legacy networks is considered.

Chapter 6

OUTAGE PROBABILITY IN DISTRIBUTED TRANSMISSION WITH INTER-CLUSTER INTERFERENCE BASED ON MULTI-RELAY SELECTION IN LEGACY NETWORKS

In this chapter, amplify and forward relaying in the presence of inter-cluster interference is considered. Multi-relay selection in such systems is addressed and asymptotic outage probability analysis is presented. Finally, the outage probability analysis is verified with simulations and the impact of relay selection feedback errors is assessed.

6.1 Introduction

The cooperative relaying method can be considered as an effective method to combat fading by exploiting spatial diversity [8], and as a way for two users with no or weak direct connection to attain a robust link. Single or multi nodes are generally used in such relaying to forward signals transmitted from the source node to the destination node. In a cooperative communication system, there are two major cooperative methods: amplify-and-forward (AF) (transparent relaying protocol) and decode-and-forward (DF) (regenerative relaying protocol) methods [13]. In the AF method, relay nodes only amplify the received signals then retransmit them, including noise, to the destination node. In the DF method, relay nodes decode the source information and then re-encode and retransmit the source information to the destination node. Therefore, AF type schemes, compared with DF, have the advantage of simple implementation and low complexity in practical scenarios. In addition to complexity benefits, the AF scheme has been shown in [38] to asymptotically, in terms of appropriate power control, to approach a DF one with respect to diversity.

Although, the AF scheme has been studied extensively in the literature [13] [38], little work has considered interference during the cooperation process. For example, a dedicated relay to forward the signal of one source to the destination is provided in [83], whereas many relays and hops are used to support the source to transmit their information to the destination node in [42]. Multi-relay interference is not however considered in either [83] or [42].

Moreover, in a cooperative relay network, when many relays can support the source to transmit information to the destination node, sometimes some relays provide a poor channel quality which can affect the end-to-end transmission quality [66]. Therefore, to overcome poor channel quality and preserve

the potential diversity gains, the use of a relay selection scheme is attracting considerable attention in [68], [15] and [69], whilst mitigating the problem in synchronizing a large number of cooperative nodes.

Exact outage and diversity performance expressions for a single-relay selection scheme are provided in [68] for a wide range of signal-to-noise ratio (SNR) regimes in the context of an AF transmission protocol. To obtain the best single-relay for cooperative diversity as in [15] relies on using instantaneous end-to-end wireless channel conditions. The work in [15] was extended in [69] to obtain outage-optimal opportunistic relaying in the context of selecting a single relay from a set of N available relays. They show that cooperative diversity gain even when certain relays remain inactive is achieved. However, these relay selection criteria lack the flexibility to deal with the interference effects. In [80] the effects of multi-user interference are considered for relay nodes and a single-relay selection scheme is used to overcome the effects of interference in the context of legacy networks. However, using best single-relay selection is not always sufficient to satisfy the required outage probability at a destination node. Moreover, these works have not considered feedback error for relay selection, which means sometimes the best relay cannot be chosen because the wrong feedback information is received from the destination node.

Therefore, in this chapter, in order to overcome these shortcomings, firstly, the basic AF protocol [16] is considered when unmanaged or external out-of-cell structural interference affects the cooperation process. However, to facilitate analysis, only the interference at the relays is considered and the effect of interference at the destination node is ignored, which matches the approach in [80]. Moreover, as in [80], this work is targeted at legacy systems where $max(min(\cdot,\cdot))$ method policies are used for relay selection. Secondly, this chapter focuses upon two selection schemes to select best two- and four-relay sets from a single group of relays. The outage probability expressions

for the two- and four-relay selection is considered and compared with the results for conventional best single-relay selection. Finally, the simulation of bit error rate (BER) performance of the best single-relay selection scheme and the best two- and four-relay selection scheme is examined, in the presence of errors in the feedback of relay selection information.

6.2 System Model

Two neighboring clusters of nodes denoted (C1, C2) as in [80] are shown in Figure 6.1.

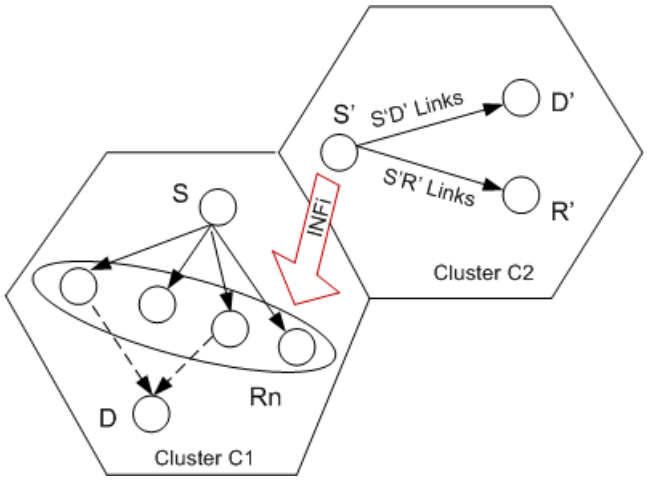

Figure 6.1. *The system model. C1: cluster of interest, which contains a cooperative network where best two-relay selection is used. S: source; D: Destination; Rn: potential relay group. C2: neighboring cluster, S': source; D': Destination. INFi: interference signal for the i^{th} relay (S'→ Rn).*

The analysis of the effect of inter-cluster interference on the relays in cluster C1 is the focus; this cluster contains nodes linked by independent Rayleigh flat-fading quasi-static channels. Moreover, cluster C1 has one source node and one destination node and many potential relay nodes grouped together, all equipped with single half-duplex antennas. Comparable relay configurations have been studied in [44] and [43].

For simplicity of exposition, there is no direct link between the source and the destination as path loss or shadowing is assumed to render it useless and the neighboring cluster uses direct transmission from the source to a relay or the destination. In this protocol, during the first time slot, the source broadcasts the signal to the relay nodes and during the second time slot, the i^{th} selected relay, from the available group transmits its received signal to the destination node. Moreover, the interference which is generated by the source of the neighboring cluster C2 is assumed only to affect the relay nodes and is ignored at the destination node. Therefore, the system model can be developed as follows: the received signal at the i^{th} relay node and the destination node are given by

$$y_{sr_i} = \sqrt{E_s} h_{sr_i} x + \sqrt{E_s} h_{s'r_i} x' + n_{r_i}, \tag{6.2.1}$$

$$y_{r_i d} = \sqrt{P_i} h_{r_i d} y_{sr_i} + n_d, \tag{6.2.2}$$

where x and x' are the source signals from the target C1 and neighboring C2 clusters, respectively, typically drawn from a prescribed finite constellation. E_s is the average energy per symbol; h_{sr_i}, $h_{s'r_i}$ and $h_{r_i d}$ are channel gains, which are the zero mean, independent, circularly-symmetric, complex Gaussian random variables with variances σ^2_{sri}, $\sigma^2_{s'ri}$ and σ^2_{rid}, between the source and the i^{th} relay node, between the neighboring source and the relay node and between the i^{th} relay node and the destination node; and the complex additive white Gaussian noise n_{r_i} and n_d are modelled as zero-mean mutually independent, circularly-symmetric, complex Gaussian random variables with variance N_0 at the i^{th} relay and the destination node, respectively. The i^{th} relay gain denoted by $\sqrt{P_i}$ is calculated from

$$P_i = \frac{E_s}{E_s |h_{sr_i}|^2 + E_s |h_{s'r_i}|^2 + N_0}. \tag{6.2.3}$$

In this model, the source powers at the target C1 and the neighboring C2 cluster are assumed to be the same. This model is representative of an ad-hoc network environment where there is no power control between neighboring clusters.

Next, because the two- or four-relay selection scheme is used, maximum ratio combining (MRC) is assumed to be used at the destination as in [72]. The practical implementation of the MRC may incur a capacity penalty due to the need to adopt a time multiplexing approach to transmission between the relays and the destination node; however, this can be mitigated by adopting an orthogonal transmission scheme, i.e. distributed space-time coding [42], which is available for two or four relays. Furthermore, increasing the number of selected relays will incur practical overheads such as increased complexity in synchronization. Thus, this chapter focuses on selection of two and four relays only. Therefore, the instantaneous equivalent end-to-end signal-to-interference plus noise ratio (SINR) can be formed as:

$$\gamma_D = \sum_{i \in N_s} \frac{P_i |h_{sr_i}|^2 |h_{r_i d}|^2}{P_i |h_{s'r_i}|^2 |h_{r_i d}|^2 + P_i |h_{r_i d}|^2 N_0 + N_0}, \tag{6.2.4}$$

where N_s denotes the set of two or four relay indices for the relays chosen in the two- or four-relay selection scheme. Substituting (6.2.3) into (6.2.4), the end-to-end SINR is

$$\gamma_D = \sum_{i \in N_s} \frac{\gamma_{sr_i} \gamma_{r_i d}}{\gamma_{INFi}(\gamma_{r_i d} + 1) + \gamma_{sr_i} + \gamma_{r_i d} + 1}, \tag{6.2.5}$$

where $\gamma_{sr_i} = |h_{sr_i}|^2 E_s/N_0$ and $\gamma_{r_i d} = |h_{r_i d}|^2 E_s/N_0$ are the instantaneous SNRs of the source to i^{th} relay and i^{th} relay to destination links, respectively. And $\gamma_{INFi} = \gamma_{s'ri} = |h_{s'r_i}|^2 E_s/N_0$ denotes the interference-to-noise ratio (INR) for the i^{th} relay as a result of the neighboring cluster C2 source. It is difficult to use (6.2.5) to find a closed form expression for the probability

density function (PDF) of γ_D, therefore, for high SNR, an asymptotic bound is provided as

$$\gamma_D \simeq \sum_{i \in N_s} \frac{\gamma_{sr_i}}{\gamma_{INFi}}, \tag{6.2.6}$$

which is the sum of the ratios between the SNR of the first hop and the INR of the interference, because when $SNR \to \infty$, then

$\varepsilon(\gamma_{INFi})\varepsilon(\gamma_{r_i d}) \gg \varepsilon(\gamma_{INFi}) + \varepsilon(\gamma_{sr_i}) + \varepsilon(\gamma_{r_i d}) + 1$.

In this case, the statistical description of the system is independent of the second hop between relays and destination. For this asymptotic case, the probability density function and cumulative distribution function (CDF) of each ratio in (6.2.6), which is between two exponential random variables [82], are given in closed form, as

$$f(\gamma) = \frac{L}{(L+\gamma)^2} \quad \text{and} \quad F(\gamma) = \frac{\gamma}{(L+\gamma)}, \tag{6.2.7}$$

where $f(\cdot)$ and $F(\cdot)$ denote the PDF and the CDF, respectively. The parameter $L = \frac{\varepsilon(\gamma_{sri})}{\varepsilon(\gamma_{INFi})} = \frac{\sigma^2_{sri}}{\sigma^2_{s'ri}}$. Note that the parameter L controls the level of interference in the target C1 and neighboring C2 clusters.

Furthermore, the two or four relay selection scheme assuming interference only at the relays will be considering and implemented as in the following sections.

6.3 Two or Four Relay Selection with Outage Probability Analysis

The conventional relay selection scheme will be firstly introduced, before introducing the two- or four-relay selection schemes.

6.3.1 Conventional Relay Selection

The conventional relay selection policy which is used in the ideal distributed implementation without interference is considered in [15]. The conventional

relay selection scheme requires the instantaneous SNR between the links from the source to i^{th} relay and the i^{th} relay to the destination node to be known, and then a particular relay is selected to maximize the minimum between them; the conventional relay selection scheme can be represented by

$$i_{conv} = arg \max_{i \in N} \min(\gamma_{sr_i}, \gamma_{r_i d}), \tag{6.3.1}$$

where N represents the set of indices of all available relays.

The conventional relay selection policy offers the relay with the "best" end-to-end path between source and destination nodes and provides diversity gain on the order of the number of the relays [69]. However, the best single-relay selection is not always sufficient to achieve the required outage probability at a destination node, as this relay selection criterion is only considered for environments without interference. Furthermore, when feedback error is present in the relay selection, the performance of the single-relay selection scheme is significantly degraded. Therefore, to overcome these problems two- and four-relay selection schemes are proposed for use in interference configurations for legacy networks which are restricted to pick a conventional relay selection $\max(min(\cdot,\cdot))$ type policy.

6.3.2 Asymptotic Two and Four Relay Selection

As has been seen in (6.2.6) the asymptotic behavior of the system converges to the sum of the ratios between source to relay and interference links. Therefore, a relay selection policy is to choose the best relay available which gives the maximum value of the ratio.

Best Two-Relay Selection

Start with the best two-relay selection for example, the asymptotic selection policy can be obtained as

$$\mathbf{i}_{Asy} = arg \max_{i \in N} \max_{i' \in N-1} (\frac{\gamma_{sr_i}}{\gamma_{INFi}}), \tag{6.3.2}$$

where $\mathbf{i} = (i, i^{'})$, i.e. a pair of relay indices, where i denotes the index of the relay with the best link in N, and i' is that of the best relay amongst the remaining N-1. In this approach the best two relay nodes are selected from the N available relays in the group in the cluster, namely, select the relays with the maximum γ_{max} and the second largest γ_{max-1} from the N relays instantaneous SNRs. Using the theory of order statistics [50], the selection of the maximum and the second largest is not independent, therefore the joint distribution of the two most maximum values is obtained as

$$f(x, y) = N(N-1)F(y)^{N-2} f(x) f(y), \tag{6.3.3}$$

where $\gamma_{max} = x$ and $\gamma_{max-1} = y$. Substituting (6.2.7) into (6.3.3), then

$$f(x, y) = \frac{N(N-1)L^2 y^{N-2}}{(L+y)^N (L+x)^2}. \tag{6.3.4}$$

Then the CDF of the random variable $F_{\gamma_{up}}^{Asy}(\gamma)$ is calculated, where γ_{up} is the sum of the random variables x and y, which are identically distributed exponential random variables. Therefore, the CDF is obtained as

$$F_{\gamma_{up}}^{Asy}(\gamma) = Pr\{x + y \leq \gamma\}. \tag{6.3.5}$$

Given that x and y are non-negative, with $x \geq y$, then,

$$F_{\gamma_{up}}^{Asy}(\gamma) = \int_0^{\frac{\gamma}{2}} \int_y^{\gamma - y} f(x, y) dx dy. \tag{6.3.6}$$

Using the PDF in (6.3.4), and after performing some manipulations, the CDF is obtained as

$$\begin{aligned} F_{\gamma_{up}}^{Asy}(\gamma) =& N(N-1)L^2\{\frac{(\frac{\gamma}{2})^{N-1}(LN+\frac{\gamma}{2})}{N(N-1)L^2(L+\frac{\gamma}{2})^N} - \frac{(\frac{\gamma}{2})^N}{(L+\frac{\gamma}{2})^N(L+\gamma)^2} \\ & [\frac{2(L+\gamma)(L+\frac{\gamma}{2})}{L(N-1)\gamma} + \frac{(\frac{L+\frac{\gamma}{2}}{L})^N F_{2,1}(N,N;N+1;-\frac{\gamma}{2L})}{N} \\ & + \frac{\frac{\gamma}{2}(\frac{L+\frac{\gamma}{2}}{L})^N F_1(N+1;N,1;N+2;-\frac{\gamma}{2L},\frac{\gamma}{2(L+\gamma)})}{LN+L+\gamma N+\gamma}]\}, \end{aligned} \tag{6.3.7}$$

where $F_{2,1}(a,b,c,z)$ is the first hypergeometric function, which can be calculated by using the Hypergeom Matlab function [84]. Furthermore, $F_1(a;b1,b2;c;x,y)$ is a formal extension of the Appell hypergeometric function of two variables, which can also be expressed by the simple integral in [85] as

$$\begin{aligned} F_1(a;b1,b2;c;x,y) =& \frac{\Gamma(c)}{\Gamma(a)\Gamma(c-a)} \int_0^1 t^{a-1}(1-t)^{c-a-1}(1-xt)^{-b_1} \\ & (1-yt)^{-b_2}dt \qquad \text{for } \mathbb{R}(c) > \mathbb{R}(a) > 0, \end{aligned}$$

where $\Gamma(n) = (n-1)!$ is the Gamma function.

Therefore, the outage probability is defined as when the average end-to-end SNR falls below a certain predefined threshold value, α. The outage probability can be expressed as

$$P_{out} = \int_0^{\alpha} f_{\gamma_b}(\gamma)d\gamma = F_{\gamma_{up}}(\alpha). \tag{6.3.8}$$

The outage probability of the best two-relay selection can be expressed by using the CDF expression as in equation (6.3.7).

Best Four-Relay Selection

A similar method of best two-relay selection can be used to obtain the outage probability for the best four-relay selection as follows. The asymptotic

selection policy can be obtained as

$$\mathbf{i}_{con} = arg \max_{i \in N} \max_{i' \in N-1} \max_{i'' \in N-2} \max_{i''' \in N-3} (\frac{\gamma_{sr_i}}{\gamma_{INFi}}), \tag{6.3.9}$$

where $\mathbf{i} = (i, i^{'}, i^{''}, i^{'''})$, i.e. four relay indices, in which i denotes the index of the relay with the best link in N; i' is the best relay amongst the remaining $N-1$, and i'' is the best relay amongst the remaining $N-2$, and i''' is the best relay amongst the remaining $N-3$. Then, the joint distribution of the four most maximum values is

$$f(w,x,y,z) = N(N-1)(N-2)(N-3)F(z)^{N-4}f(w)f(x)f(y)f(z), \tag{6.3.10}$$

where $\gamma_{max} = w$, $\gamma_{max-1} = x$, $\gamma_{max-2} = y$ and $\gamma_{max-3} = z$. Substituting (6.2.7) into (6.3.10),

$$f(w,x,y,z) = \frac{N(N-1)(N-2)(N-3)L^4 z^{N-4}}{(L+z)^{N-2}(L+w)^2(L+x)^2(L+y)^2}. \tag{6.3.11}$$

Then the CDF of γ_{up}, which is formed as the sum of w, x, y and z identically distributed random variables, $F^{Asy}_{\gamma_{up}}(\gamma)$ is calculated, Therefore, the CDF becomes

$$F^{Asy}_{\gamma_{up}}(\gamma) = Pr\{w+x+y+z \leq \gamma\}. \tag{6.3.12}$$

Given that w, x, y and z are non-negative, with $w \geq x \geq y \geq z$, then,

$$F^{Asy}_{\gamma_{up}}(\gamma) = \int_0^{\frac{\gamma}{4}} \int_z^{\frac{\gamma-z}{3}} \int_y^{\frac{\gamma-z-y}{2}} \int_x^{\gamma-z-y-x} f(w,x,y,z) dw dx dy dz. \tag{6.3.13}$$

Substituting (6.3.11) into (6.3.13),

$$\begin{aligned} F^{Asy}_{\gamma_{up}}(\gamma) = & \int_0^{\frac{\gamma}{4}} \int_z^{\frac{\gamma-z}{3}} \int_y^{\frac{\gamma-z-y}{2}} \int_x^{\gamma-z-y-x} \\ & \frac{N(N-1)(N-2)(N-3)L^4 z^{N-4}}{(L+z)^{N-2}(L+w)^2(L+x)^2(L+y)^2} dw dx dy dz, \end{aligned} \tag{6.3.14}$$

then, exploiting (6.3.14) as in (6.3.8), the outage probability can be evaluated, and the Mathematica software package [86] is employed to get the results shown in the simulation section.

In this section the two- or four-relay selection approaches are considered as they are immediately applicable within a cooperative network, which exploits distributed space time coding [43] to improve the end-to-end performance, such as an Alamouti or Quasi-Orthogonal code, according to the number of selected relays. Furthermore, for this relay selection policy, it requires only the SNR of the links from source to relay nodes and the INR of the interference links which can be obtained by the relay nodes during the early stage of transmission. Moreover, the information describing the links between the relay and destination is not required at the destination node, therefore, this policy has a lower complexity than that of [69] and may save feedback set-up time.

6.3.3 Semi-Conventional Two- and Four-Relay Selection

The semi-conventional two- and four-relay selection schemes are an extension of the conventional selection scheme and motivated by the expression of the general statistics (6.2.4). There are three advantages in the semi-conventional two- and four-relay selection scheme:

Firstly, because this scheme is based on the conventional approach, it does not involve complex computational operations, and can be easily obtained from the conventional case without modifying the $min(\cdot,\cdot)$ operation.

Secondly, it is suitable for ad-hoc systems with mobility that dynamically and continuously change between interference and non-interference environments.

Thirdly, the proposed scheme balances the gap between the conventional scheme and asymptotic case for the interference situation.

Therefore, in this section, a simple ratio between the conventional $min(\cdot,\cdot)$

operation and the interference term are considered, because it does not change the basic structural core of the system.

Best Two-Relay Selection

In the following, the best two-relay selection scheme becomes

$$\mathbf{i}_{Semi} = arg \max_{i \in N} \max_{i' \in N-1} \left(\frac{\min(\gamma_{sr_i}, \gamma_{r_i d})}{\gamma_{INFi}}\right). \tag{6.3.15}$$

where $\mathbf{i} = (i, i^{'})$, i.e. a pair of relay indices, where i denotes the index of the relay with the best link in N, and i' is that of the best relay amongst the remaining $N-1$. Here, the outage behavior of the ratio $\frac{\gamma_{sr_i}}{\gamma_{INFi}}$ according to the semi-conventional scheme needs to be considered. In order to simplify the approximation of the corresponding outage bound as in [80], two cases will be considered.

In the first case, the value $\min(\gamma_{sr_i}, \gamma_{r_i d}) = \gamma_{sr_i}$, which means the selected relay, the minimum between the two hops, is the link between source and relay. Therefore, the PDF and CDF are given in closed form and correspond to a ratio between the min operation and an exponential random variable, which are

$$f(\gamma) = \frac{2L}{(L+2\gamma)^2} \quad \text{and} \quad F(\gamma) = \frac{2\gamma}{L+2\gamma}, \tag{6.3.16}$$

where $f(\cdot)$ and $F(\cdot)$ denote the PDF and the CDF, respectively. Substituting (6.3.16) into (6.3.3),

$$f(x,y) = \frac{N(N-1)2^N L^2 y^{N-2}}{(L+2y)^N (L+2x)^2}. \tag{6.3.17}$$

Using the PDF in (6.3.17) and (6.3.6), and after performing some manipu-

lations,

$$\begin{aligned} F'_{\gamma_{up}}(\gamma) =& N(N-1)2^N L^2 \{ \frac{(\frac{\gamma}{2})^{N-1}(LN+\gamma)}{2N(N-1)L^2(L+\gamma)^N} - \frac{(\frac{\gamma}{2})^N}{2(L+\gamma)^N(L+2\gamma)^2} \\ & [\frac{2(L+2\gamma)(L+\gamma)}{L(N-1)\gamma} + \frac{2(\frac{L+\gamma}{L})^N F_{2,1}(N,N;N+1;-\frac{\gamma}{L})}{N} \\ & + \frac{2\gamma(\frac{L+\gamma}{L})^N F_1(N+1;N,1;N+2;-\frac{\gamma}{L},\frac{\gamma}{L+2\gamma})}{(N+1)(L+2\gamma)}] \}, \end{aligned} \tag{6.3.18}$$

the definitions for which have already been shown in the last subsection.

In the second case, the value $\min(\gamma_{sr_i}, \gamma_{r_i d}) = \gamma_{r_i d}$, which means the minimum between the two hops of the selected relay is the link from relay to destination which is not considered in the ratio of interest. According to the assumption of [80], the conventional asymptotic relay selection can be used as an outage bound in this case. Therefore, based on the above two equiprobable cases, the semi-conventional end-to-end CDF is given as

$$F^{Semi}_{\gamma_{up}}(\gamma) = \frac{1}{2} F^{Asy}_{\gamma_{up}}(\gamma) + \frac{1}{2} F'_{\gamma_{up}}(\gamma), \tag{6.3.19}$$

where $F^{Asy}_{\gamma_{up}}(\gamma)$ and $F'_{\gamma_{up}}(\gamma)$ are denoted by (6.3.7) and (6.3.18), respectively. And the outage probability can be obtained by using (6.3.19).

Best Four-Relay Selection

A similar method is used to obtain the best four relays in the following processing. The semi-conventional selection policy can be obtained as

$$\mathbf{i}_{Semi} = arg \max_{i \in N} \max_{i' \in N-1} \max_{i'' \in N-2} \max_{i''' \in N-3} (\frac{\min(\gamma_{sr_i}, \gamma_{r_i d})}{\gamma_{INFi}}), \tag{6.3.20}$$

where $\mathbf{i} = (i, i', i'', i''')$, i.e. four relay indices, wherein i denotes the index of the relay with the best link in N; i' is that of the best relay amongst the remaining $N-1$, and i'' is that of the best relay amongst the remaining

$N-2$, and i''' is that of the best relay amongst the remaining $N-3$. In the first case, the joint distribution of the four most maximum values can be obtained by substituting (6.3.16) into (6.3.10), yielding

$$f(w,x,y,z) = \frac{N(N-1)(N-2)(N-3)2^N L^4 z^{N-4}}{(L+2z)^{N-2}(L+2w)^2(L+2x)^2(L+2y)^2}. \tag{6.3.21}$$

By substituting (6.3.21) into (6.3.13), then

$$\begin{aligned} F'_{\gamma_{up}}(\gamma) = \int_0^{\frac{\gamma}{4}} \int_z^{\frac{\gamma-z}{3}} \int_y^{\frac{\gamma-z-y}{2}} \int_x^{\gamma-z-y-x} \\ \frac{N(N-1)(N-2)(N-3)2^N L^4 z^{N-4}}{(L+2z)^{N-2}(L+2w)^2(L+2x)^2(L+2y)^2} dwdxdydz. \end{aligned} \tag{6.3.22}$$

Therefore, the final end-to-end CDF can be obtained as

$$F^{Semi}_{\gamma_{up}}(\gamma) = \frac{1}{2}F^{Asy}_{\gamma_{up}}(\gamma) + \frac{1}{2}F'_{\gamma_{up}}(\gamma), \tag{6.3.23}$$

where $F^{Asy}_{\gamma_{up}}(\gamma)$ and $F'_{\gamma_{up}}(\gamma)$ are given by (6.3.14) and (6.3.22), respectively. And the outage probability can be evaluated by using (6.3.8) and (6.3.23), for example with the Mathematica software package [86].

6.4 Simulation Results for Outage Probability Analysis

In this section, in order to verify the results obtained from the above mathematical expressions, the target source node and the neighboring source node use the same unity transmission power is assumed. Also, there is no direct link between the source and the destination as path loss or shadowing render it unusable. Figure 6.2 shows the comparison of the outage probability of the best two-relay selection schemes, where $L = 5$ and 20. It can be seen that increasing the number of relays, N, decreases the outage probability, and hence when the number of relays is large, the outage event (no transmission) becomes less likely, for example, with the total number of available

relays increasing from 4 to 6, the outage probability of the best two-relay selection is decreased from almost 0.308 to 0.162 for the semi-conventional case; and from 0.192 to 0.073 for the asymptotic case when the target rate is 2 and $L = 5$. The outage performance of the asymptotic case closely matches the simulation results, when SNR = 40 dB. Moreover, with increased source-to-interference power ratio, the performance in terms of outage probability is improved.

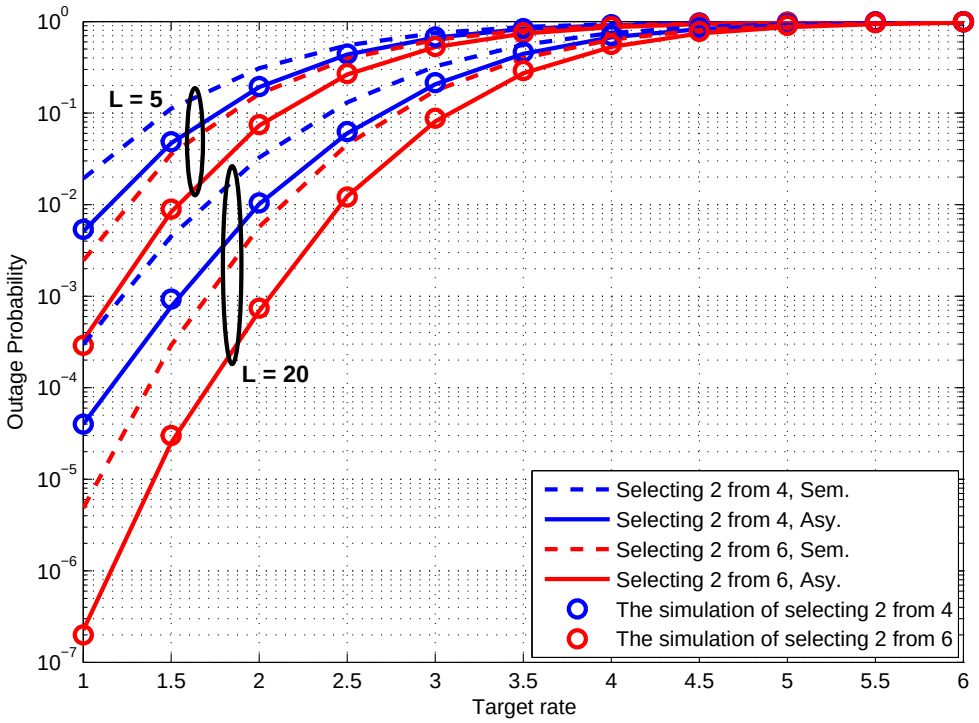

Figure 6.2. *Comparison of the outage probability of the best two-relay selection schemes, the theoretical results are shown in line style and the simulation results as points.*

Figure 6.3 shows the outage probability of the best four-relay selection schemes, where $L = 5$ and 20. It can be seen that increasing the number of relays, decreases the outage probability, for example, with the total number of available relays increasing from 6 to 8, the outage probability of the best four-relays selection is decreased from almost 0.013 to 0.0025 for the semi-conventional case; and from 0.0022 to 1.6×10^{-4} for the asymptotic case when the target rate is 1.5 and $L = 5$. With increased source-to-interference power ratio, the performance of outage probability again improves. Moreover, the asymptotic results match very well with the simulation results, when SNR = 40 dB.

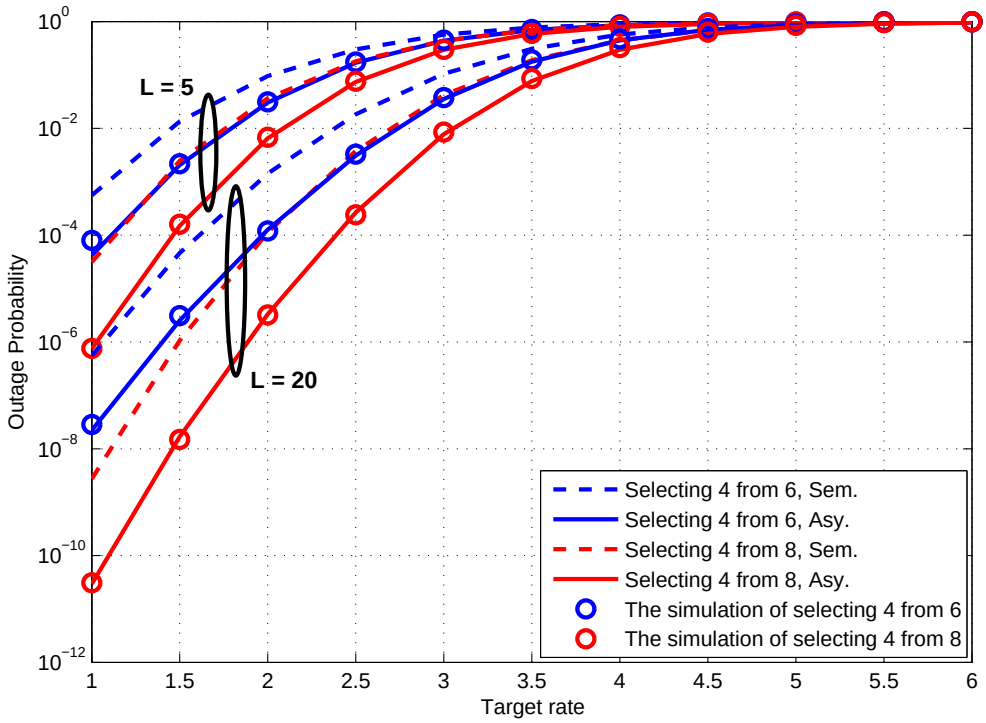

Figure 6.3. *Comparison of the outage probability of the best four-relay selection schemes, the theoretical results are shown in line style and the simulation results as points.*

Figure 6.4 shows the comparison of the outage probability of the best single-relay selection and the best two- and four-relay selection schemes, SNR = 40 dB and $L = 5$ or 10. Obviously, with increasing the number of selected relays, the outage probability decreases. For example, for the semi-conventional case, when the total number of available relays is 6, $L = 5$ and the target rate is 1.5, the outage probability of a single-, two- and four-relay selections are almost 0.1, 0.036 and 0.013, respectively. Furthermore, for the asymptotic case, when $N = 6$, $L = 10$ and the target rate is 1.5, the outage probability of the best signle-, two- and four-relay selections are almost 0.0045, 5.59×10^{-4} and 9.01×10^{-5}, respectively. These results confirm that two- and four-relay selection schemes provide more robust transmission than single-relay selection, because for the single-relay selection, it just uses a single relay to help the source to transmit the signal. Therefore, a different number of relays can be selected to communicate with the source and destination node, according to the target outage probability. In the next section how the end-to-end BER performance of the relay selection schemes degrade is considered when there is error in selecting the particular relay(s) to use in transmission.

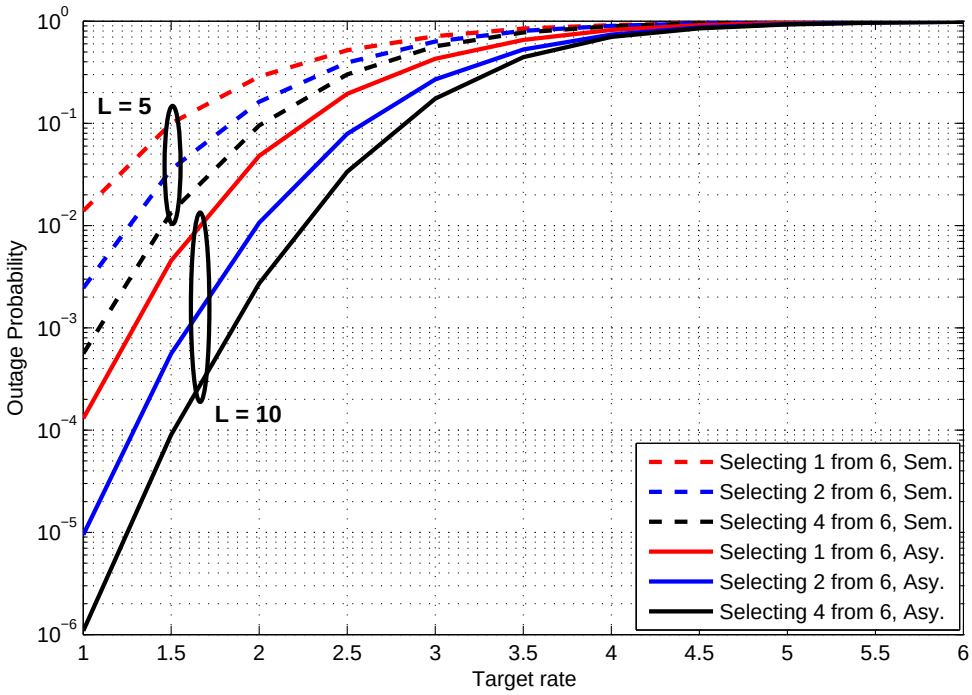

Figure 6.4. *Comparison of the outage probability of the best single-, two- and four-relay selection schemes.*

6.5 Analysis of the BER Performance and Impact of Relay Selection Feedback Errors

In this section, the BER performance of the best two-relay selection from a group of N available relays, $N = 4$, is compared with distributed Alamouti code with the best single-relay selection in the presence of relay selection feedback errors, when QPSK symbols are used in transmission. Figure 6.5 shows the comparison between the best two-relay selection and the single-relay selection in a representative relay selection feedback error environment, and the signal-to-interference power ratio $L = 50$ is assumed. To simulate errors in the feedback of relay selection information from the destination, an error rate in the feedback is introduced. An error rate of 0.5 corresponds to 50% of the selections being made in error; that is, rather than selecting the best relay, one of the other relays is chosen with equal probability of selection. When an error rate of 0 is selected, the BER performance of the best single-relay selection is worse than the best two-relay selection for the three different relay selection schemes, which are denoted by circular, square and diamond dotted lines for the conventional, asymptotic and semi-conventional schemes, respectively. Moreover, in the presence of errors in the relay selection, i.e. error rate over the range 0 to 1, all of the different best two-relays selection schemes outperform that of the best single-relay selection. These results illustrate clearly the increased robustness of the best two-relay selection scheme over the single-relay selection scheme in the presence of moderate to severe relay selection feedback errors. For example, for the conventional best two-relay selection scheme, when the SNR is 20 dB, the BER for the conventional best two-relay selection changes from almost 1×10^{-4} only to 4.9×10^{-3} as the error rate changes from 0 to 1, whereas the BER for the single-relay selection is increased from almost 2.15×10^{-4} to 5.1×10^{-2}, confirming the improved robustness.

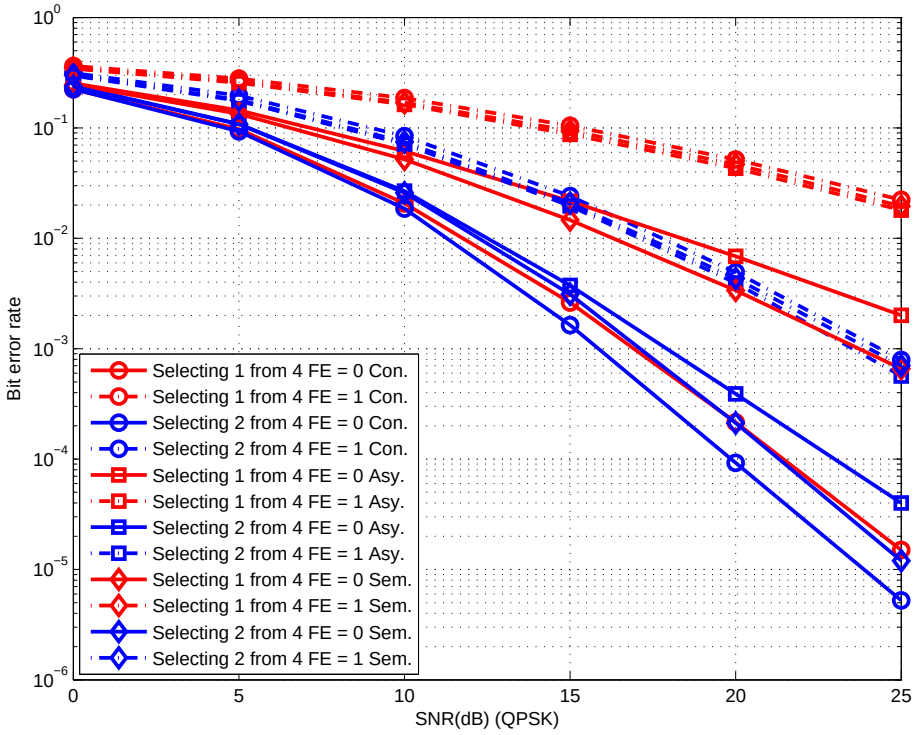

Figure 6.5. *BER performance comparison of different best two-relay selection schemes (blue line) with the different best single-relay selection schemes (red line), with varying error in the feedback relay selection information from the destination.*

6.6 Summary

This chapter has firstly examined two different selection schemes which are asymptotical and semi-conventional policies to select the best two- and four-relay from a group of available relays in the same cluster by using local measurements of the instantaneous channel conditions in the context of legacy systems which adopt $\max(min(\cdot,\cdot))$ type policies. New analytical expressions for the PDF, and CDF of end-to-end SINR were derived together with closed form expressions for outage probability over Rayleigh fading channels. Secondly, the best single-relay selection from a group of available relays by using local measurements of the instantaneous channel conditions in the context of cooperative systems which adopt a selection policy to maximize end-to-end SINR was provided, when inter-cluster interference was considered at the relay nodes. Moreover, numerical results were provided to show the advantage of the outage probability performance of the best two- and four-relay selection in a cooperative communication system. Also, through simulation study, the robustness of the best single- and two-relay selection schemes is confirmed in the presence of moderate to severe relay selection feedback errors. In the next chapter, outage probability analysis for a cognitive amplify and forward relay network with single-, two- and four-relay selection will be introduced.

Chapter 7

OUTAGE PROBABILITY ANALYSIS FOR A COGNITIVE AF RELAY NETWORK WITH SINGLE AND MULTI-RELAY SELECTION

This chapter evaluates the outage probability of a cognitive amplify and forward relay network with cooperation between certain secondary users, based on the underlay approach, which requires adherence to an interference constraint on the primary user. The relay selection is performed either on the basis of a $max-min$ strategy or based on maximizing exactly the end-to-end SNR. To achieve the relay selection schemes within the secondary networks, a predetermined threshold for the power of the received signal in the primary receiver is assumed. To assess the performance advantage of adding additional secondary relays, analytical expressions for the PDF, and CDF of the received SNR are derived. Closed form and near closed form expressions for

outage probability over Rayleigh frequency flat fading channels are obtained. In particular, lower and upper bound expressions for outage probability are presented and then the exact expression for outage probability is provided. Finally, these analytical results are verified by numerical simulation.

7.1 Introduction

Cognitive radio (CR) is an effective method to improve spectrum utilization by spectrum sharing between primary users and cognitive radio users (secondary users); that is the secondary user (SU) can be permitted to take advantage of the licensed band provided the data transmission of the primary users can be protected by using spectrum underlay, overlay and interweave approaches [28]. In the underlay approach, the secondary user is allowed to use the spectrum of the primary user (PU) as long as the interference from the secondary user is less than the interference level which the primary user can tolerate. Therefore, the transmission power of the secondary user is constrained not to exceed the interference threshold. In the overlay approach, the secondary user employs the same spectrum concurrently with the primary user while maintaining or improving the transmission of the primary user by applying sophisticated techniques [28]. In the interweave approach, the secondary user utilizes the spectrum not currently being used by the primary user, known as a spectrum hole, identified by some form of spectrum sensing, however this is sensitive to issues such as the hidden terminal problem. As such, the underlay approach is more practical than others, and is the focus in this chapter.

A relay network can moreover be investigated as an effective method to combat fading by exploiting spatial diversity [8], and as a way for two users with no or weak direct connection to attain a robust link. Single or multi-relay nodes can be used to forward signals transmitted from the source node

to the destination node. Inspired by cognitive radio and relay networks, cognitive relay networks have been considered as a potential way to improve secondary user throughput using one of two schemes: cooperation between primary and secondary users [87], and cooperation between secondary users [88–91].

For cooperation between secondary users, [88] explained the approximate outage performance in cognitive DF relay networks. Exact outage probability in cognitive relay networks was investigated in [89], and [90] proposed a distributed transmit power allocation scheme for multihop cognitive radio networks. Additionally, [91] studied outage probability and diversity for cognitive DF relay networks with single-relay selection. However, these works have only studied the DF relay scheme, and little previous work has considered multi-relay selection in cognitive AF relay networks.

Therefore, this chapter examines the performance of a cognitive AF relay network using best single-, two- and four-relay selection to allow cooperation between secondary users just as the underlay approach and limit this study to four-relay selection as practical distributed space-time block coding schemes are typically designed for no more than four relays [42]. Moreover, three outage probability analysis methods are addressed, namely, ones based on well known lower and upper bounds and a new one using an exact outage probability analysis. The contributions of this chapter are to show that:
1) The outage probability for the secondary user is affected by two factors: the first factor is in the form of ratios of channel gains, i.e., in the secondary transmission, the ratio between the gain of the secondary source to chosen secondary relay channel, to the gain of the secondary source to the primary receiver channel, together with the ratio between the gain of the chosen secondary relay to secondary destination channel to the gain of the chosen secondary relay to the primary receiver channel; and the second factor is the interference threshold for the primary user.

2) Two- and four-relay selection according to these approaches can achieve low outage probability in the secondary user even when the power of the secondary source and relays is constrained.
3) A new exact outage probability analysis is much more useful for end-to-end performance analysis than those based on the previous bounds.

7.2 System Model

The cognitive AF relay network model shows in Figure 7.1. In this figure, SS, SR_i ($i \in (1, ..., N)$), SD and PD represent a secondary source, N secondary relays, a secondary destination, and a primary destination, respectively. The operation of the secondary relays is assumed to be performed in a half duplex AF mode. SS broadcasts its signal to all SR_i in the first time slot, and the selected SR_i(s) relay(s) forward their received signal(s) to SD in the second time slot.

For simplicity of exposition, there is no direct link between the secondary source and the secondary destination node as path loss or shadowing is assumed to render it unusable [92]. The coefficients h_{sp}, h_{sr_i}, h_{r_id} and h_{r_ip} are the instantaneous channels of the links between SS and PD, SS and SR_i, SR_i and SD, and SR_i and PD, respectively. Statistically, the channel gains $g_j = |h_j|^2$ ($j = sp, sr_i, r_id, r_ip$) are independent exponentially distributed random variables with mean values λ_j ($j = sp, sr_i, r_id, r_ip$), and perfect channel information is assumed to be available at the secondary relays and secondary destination.

In the underlay technique SS and SR_i can share the primary user's spectrum if the power of the received interference signal in PD from SS and SR_i satisfies a predetermined threshold defined by I_{th}. And because the two- and four-relay selection scheme is used in this chapter, the limits

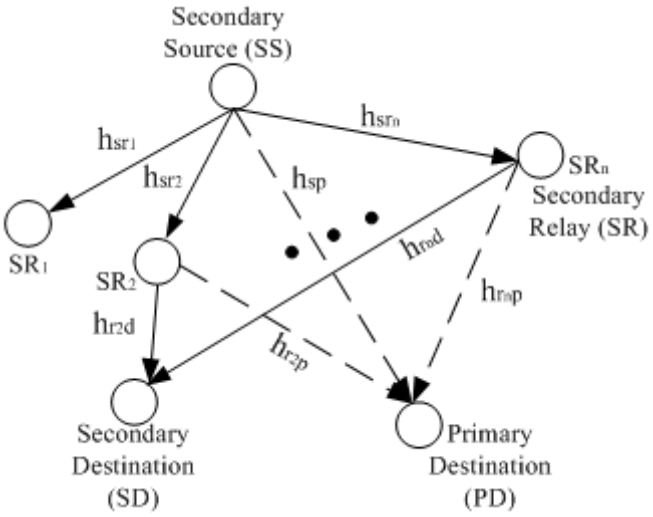

Figure 7.1. *The cognitive AF relay network model wherein the dashed lines denote the interference links and the solid lines denote the selected transmission links, i.e., only SR_2 and SR_n are used for relaying to the secondary destination.*

on power for SS and SR_i are given by

$$g_{sp}P_{SS} \leq I_{th} \qquad \text{and} \qquad g_{r_ip}P_{SR_i} \leq \frac{I_{th}}{|N_s|}, \tag{7.2.1}$$

where $|N_s|$ denotes the cardinality of the set of relay indices for the selected relays; P_{SS} and P_{SR_i} are the transmission power of SS and SR_i, respectively. Therefore, this design is for the worst case when the interference terms at the primary destination combine coherently, the maximum transmission powers of SS and SR_i are equal to $\frac{I_{th}}{g_{sp}}$ and $\frac{I_{th}}{g_{r_ip}|N_s|}$, respectively. Using these powers, the received signal vector at SR_i is

$$\mathbf{y}_{sr_i} = h_{sr_i}\sqrt{\frac{I_{th}}{g_{sp}}}\mathbf{s} + \mathbf{n}_r, \tag{7.2.2}$$

where $\mathbf{s}$ is a transmitted signal vector from SS, and $\mathbf{n}_r$ is an AWGN vector

with zero mean and σ_r^2 variance elements received in the SR_i node. The received signal vector at SD from the selected SR_i can be obtained as

$$\begin{aligned}\mathbf{y}_{r_i d} &= h_{r_i d}\sqrt{\frac{I_{th}}{g_{r_i p}|N_s|}}P_{R_i}\mathbf{y}_{sr_i} + \mathbf{n}_d \\ &= h_{r_i d}h_{sr_i}\sqrt{\frac{I_{th}^2}{g_{sp}g_{r_i p}|N_s|}}P_{R_i}\mathbf{s} + h_{r_i d}\sqrt{\frac{I_{th}}{g_{r_i p}|N_s|}}P_{R_i}\mathbf{n}_r + \mathbf{n}_d,\end{aligned} \tag{7.2.3}$$

where $\mathbf{n}_d$ is an AWGN vector with zero mean and σ_d^2 variance elements received in the SD node, and P_{R_i} is the limited output amplify gain of SR_i which is defined in [93] as

$$P_{R_i}^2 = \frac{g_{sp}}{g_{sr_i}I_{th} + \sigma_r^2 g_{sp}}. \tag{7.2.4}$$

Next, because the two- and four-relay selection scheme is used, the MRC is assumed to be used at the destination node [72]. The practical implementation of the MRC will, however, incur a capacity penalty due to the need to adopt a time multiplexing approach to transmission between the relays and the destination node; however, this can be mitigated by adopting an orthogonal transmission scheme, i.e. distributed space-time coding, which is available for two or four relays. Furthermore, increasing the number of selected relays will incur practical overheads such as increased complexity in synchronization. Therefore, this chapter focuses on selection of best single-, two- and four-relay. Then from (7.2.3) the overall instantaneous equivalent end-to-end SNR can be written as:

$$\gamma_{eq}^E = \sum_{i\in N_s}\frac{\gamma_i^0\gamma_i^1}{\gamma_i^0 + \gamma_i^1 + 1}, \tag{7.2.5}$$

where N_s denotes the set of relay indices for the relays chosen in the single-, two- and four-relay selection schemes. The terms $\gamma_i^0 = \frac{g_{sr_i}I_{th}}{g_{sp}\sigma_r^2}$ and $\gamma_i^1 = \frac{g_{r_i d}I_{th}}{g_{r_i p}\sigma_d^2|N_s|}$ are the SNRs of the first time slot and the second time slot, re-

spectively. In this chapter, three schemes to calculate the statistics (i.e., the PDF and CDF) of (7.2.5) will be provided. First two bounds on (7.2.5) by using the well known $\frac{1}{2}min(\gamma_i^0, \gamma_i^1)$ (lower bounded) and $min(\gamma_i^0, \gamma_i^1)$ (upper bounded) [72] are given, and note, as will be shown in the simulation section, that

$$\gamma_{eq}^{UB} = \sum_{i \in N_s} min(\gamma_i^0, \gamma_i^1) \geq \gamma_{eq}^{E} \geq \sum_{i \in N_s} \frac{1}{2} min(\gamma_i^0, \gamma_i^1) = \gamma_{eq}^{LB}. \tag{7.2.6}$$

And then a new and more accurate analysis for the statistics of (7.2.5) is provided. Therefore, in the next section, the PDF and CDF of (7.2.5) will be formed by using the two bounds in (7.2.6) and a direct exact calculation, respectively; and the outage probability of the cognitive AF relay network will be analyzed.

7.3 Relay Selection Scheme with Outage Probability Analysis

In this section, three types of outage probability analysis approaches will be presented for the best single-, two- and four-relay selection. Firstly, the PDF and CDF of the per time slot SNR, wherein γ_i^0 is an exponential random variable, are calculated based on g_{sr_i}. To facilitate analysis g_{sp} is assumed to be replaced by its constant mean value, so that each γ_i^0 can be assumed independent, and γ_i^1 is the ratio between two exponential random variables $g_{r_i d}$ and $g_{r_i p}$, where $0 \leq \gamma_i^j \leq \infty$, $j \in (0, 1)$, and according to [82], can be written as

$$\begin{aligned} f_{\gamma_i^0}(\gamma) &= \frac{1}{L_0} e^{-\frac{\gamma}{L_0}} \quad \text{and} \quad F_{\gamma_i^0}(\gamma) = 1 - e^{\frac{-\gamma}{L_0}}, \\ f_{\gamma_i^1}(\gamma) &= \frac{L_1}{(L_1+\gamma)^2} \quad \text{and} \quad F_{\gamma_i^1}(\gamma) = \frac{\gamma}{(L_1+\gamma)}, \end{aligned} \tag{7.3.1}$$

where $f(\cdot)$ and $F(\cdot)$ denote the PDF and the CDF of the end-to-end SNR, respectively. The terms $L_0 = \phi_0 \frac{I_{th}}{\sigma_r^2}$ and $L_1 = \phi_1 \frac{I_{th}}{\sigma_d^2 |N_s|}$, where $\phi_0 = \frac{\lambda_{sr_i}}{\lambda_{sp}}$

and $\phi_1 = \frac{\lambda_{r_i d}}{\lambda_{r_i p}}$ are the mean channel gain ratios. Basically, the mean value of the channel gain incorporates the path-loss and the shadowing effect. Using these mean values does not necessarily imply that the relays are all at the same distance from the source and destination node, as one path could experience more shadowing but be closer to the source or destination node than another relay which has a better link.

7.3.1 The CDF and PDF of Lower Bound SNR

For the lower bound analysis, the CDF of $\gamma_{eq_i}^{LB} = \frac{1}{2} min(\gamma_i^0, \gamma_i^1)$ can be expressed as [73]

$$F_{\gamma_{eq_i}^{LB}}(\gamma) = 1 - Pr(\gamma_i^0 > 2\gamma) Pr(\gamma_i^1 > 2\gamma) = 1 - [1 - F_{\gamma_i^0}(2\gamma)][1 - F_{\gamma_i^1}(2\gamma)]. \tag{7.3.2}$$

Therefore, substituting (7.3.1) into (7.3.2), the CDF of the $\gamma_{eq_i}^{LB}$ can be obtain as

$$F_{\gamma_{eq_i}^{LB}}(\gamma) = 1 - \frac{L_1 e^{-\frac{2\gamma}{L_0}}}{L_1 + 2\gamma}, \tag{7.3.3}$$

and the PDF of $\gamma_{eq_i}^{LB}$ can be obtained by taking the derivative of the CDF (7.3.3) as

$$f_{\gamma_{eq_i}^{LB}}(\gamma) = \frac{2L_1 e^{-\frac{2\gamma}{L_0}}(L_0 + L_1 + 2\gamma)}{L_0(L_1 + 2\gamma)^2}. \tag{7.3.4}$$

7.3.2 The CDF and PDF of Upper Bound SNR

For the upper bound analysis, the CDF of $\gamma_{eq_i}^{UB} = min(\gamma_i^0, \gamma_i^1)$ can be expressed as [73]

$$F_{\gamma_{eq_i}^{UB}}(\gamma) = 1 - Pr(\gamma_i^0 > \gamma) Pr(\gamma_i^1 > \gamma) = 1 - [1 - F_{\gamma_i^0}(\gamma)][1 - F_{\gamma_i^1}(\gamma)]. \tag{7.3.5}$$

Therefore, substituting (7.3.1) into (7.3.5), the CDF of the $\gamma_{eq_i}^{UB}$ can be obtain as

$$F_{\gamma_{eq_i}^{UB}}(\gamma) = 1 - \frac{L_1 e^{-\frac{\gamma}{L_0}}}{L_1 + \gamma}, \tag{7.3.6}$$

and the PDF of $\gamma_{eq_i}^{UB}$ can be obtained by taking the derivative of the CDF (7.3.6) as

$$f_{\gamma_{eq_i}^{UB}}(\gamma) = \frac{L_1 e^{-\frac{\gamma}{L_0}}(L_0 + L_1 + \gamma)}{L_0(L_1 + \gamma)^2}. \tag{7.3.7}$$

7.3.3 The CDF and PDF of Exact SNR

Then, for the new exact outage probability analysis for relay selection the CDF and PDF of the end-to-end per time slot SNR need to be obtained. Firstly, let $x = \gamma_i^0$ and $y = \gamma_i^1$ so that $f_{\gamma_i^0}(\gamma) = f_x(x) = \frac{1}{L_0} e^{-\frac{x}{L_0}}$ and $f_{\gamma_i^1}(\gamma) = f_y(y) = \frac{L_1}{(L_1+y)^2}$, where $x > 0$ and $y > 0$, and exploiting independence, obtain

$$f_{xy}(x, y) = f_x(x) f_y(y) = \frac{L_1}{L_0} \frac{e^{-\frac{x}{L_0}}}{(L_1 + y)^2}. \tag{7.3.8}$$

Then, the CDF of $Z = \frac{xy}{x+y+1}$, where $Z = \gamma_{eq_i}^{E}$, becomes

$$\begin{aligned} F_Z(z) &= P\left(\frac{xy}{x+y+1} \leq z\right) = P\left(x \leq \frac{yz+z}{y-z}\right) \\ &= \int_0^z \int_0^\infty f_{xy}(x, y) dx dy + \int_z^\infty \int_0^{\frac{yz+z}{y-z}} f_{xy}(x, y) dx dy, \end{aligned} \tag{7.3.9}$$

where $P(.)$ denotes probability value. Therefore,

$$\begin{aligned} F_{\gamma_{eq_i}^{E}}(\gamma) &= \int_0^\gamma \int_0^\infty f_{xy}(x, y) dx dy + \int_\gamma^\infty \int_0^{\frac{y\gamma+\gamma}{y-\gamma}} f_{xy}(x, y) dx dy \\ &= \frac{L_1}{L_0} \left(\int_0^\gamma \int_0^\infty \frac{e^{-\frac{x}{L_0}}}{(L_1 + y)^2} dx dy + \int_\gamma^\infty \int_0^{\frac{y\gamma+\gamma}{y-\gamma}} \frac{e^{-\frac{x}{L_0}}}{(L_1 + y)^2} dx dy \right) \\ &= 1 - \frac{L_1 e^{-\frac{\gamma}{L_0}}}{L_1 + \gamma} + \frac{L_1 \gamma(\gamma + 1) e^{\frac{(1-L_1)\gamma}{(L_1+\gamma)L_0}} \mathrm{Ei}(1, \frac{\gamma(1+\gamma)}{L_0(L_1+\gamma)})}{L_0(L_1 + \gamma)^2}, \end{aligned} \tag{7.3.10}$$

where Ei(a,b) represents the exponential integral, namely $\mathrm{Ei}(a,b) = \int_1^\infty e^{-xb} x^{-a} dx$. And the PDF of $\gamma_{eq_i}^E$ can be obtained by taking the derivative of the CDF (7.3.10) as

$$\begin{aligned} f_{\gamma_{eq_i}^E}(\gamma) = & \frac{L_1(L_1^2 - L_1 + L_1L_0 + L_0\gamma)e^{-\frac{\gamma}{L_0}}}{L_0(L_1+\gamma)^3} \\ & + \frac{[L_1^2(2\gamma+1) - L_1\gamma]e^{\frac{(1-L_1)\gamma}{(L_1+\gamma)L_0}}\mathrm{Ei}(1, \frac{\gamma(1+\gamma)}{L_0(L_1+\gamma)})}{L_0(L_1+\gamma)^3} \\ & + \frac{L_1^2\gamma(\gamma+1)(1-L_1)e^{\frac{(1-L_1)\gamma}{(L_1+\gamma)L_0}}\mathrm{Ei}(1, \frac{\gamma(1+\gamma)}{L_0(L_1+\gamma)})}{L_0^2(L_1+\gamma)^4}. \end{aligned} \tag{7.3.11}$$

7.3.4 Outage Probability Analysis of the Best Single-Relay Selection

The best relay node is selected as the one providing the highest end-to-end SNR from the N available secondary relays. By using the theory of order statistics [50], the CDF of γ_{eq}^{LB}, γ_{eq}^{UB} and γ_{eq}^E correspond to the selection of the largest $\gamma_{eq_i}^{LB}$, $\gamma_{eq_i}^{UB}$ and $\gamma_{eq_i}^E$ from the N independent relays instantaneous SNRs in the right and left side of (7.2.6) and (7.2.5), respectively, with a statistic which is given by (7.3.3), (7.3.6) and (7.3.10). Therefore, the outage probability is defined as when the average end-to-end SNR falls below a certain predefined threshold value, α. The outage probability can be expressed as

$$P_{out}^{LB} = \int_0^\alpha f_{\gamma_{eq}^{LB}}(\gamma)d\gamma = F_{\gamma_{eq}^{LB}}(\alpha) = \left[F_{\gamma_{eq_i}^{LB}}(\gamma)\right]^N = \left[1 - \frac{L_1 e^{-\frac{2\alpha}{L_0}}}{L_1+2\alpha}\right]^N, \tag{7.3.12}$$

$$P_{out}^{UB} = \int_0^\alpha f_{\gamma_{eq}^{UB}}(\gamma)d\gamma = F_{\gamma_{eq}^{UB}}(\alpha) = \left[F_{\gamma_{eq_i}^{UB}}(\gamma)\right]^N = \left[1 - \frac{L_1 e^{-\frac{\alpha}{L_0}}}{L_1+\alpha}\right]^N, \tag{7.3.13}$$

$$\begin{aligned} P_{out}^E = & \int_0^\alpha f_{\gamma_{eq}^E}(\gamma)d\gamma = F_{\gamma_{eq}^E}(\alpha) = \left[F_{\gamma_{eq_i}^E}(\gamma)\right]^N \\ = & \left[1 - \frac{L_1 e^{-\frac{\alpha}{L_0}}}{L_1+\alpha} + \frac{L_1\alpha(\alpha+1)e^{\frac{(1-L_1)\alpha}{(L_1+\alpha)L_0}}\mathrm{Ei}(1, \frac{\alpha(1+\alpha)}{L_0(L_1+\alpha)})}{L_0(L_1+\alpha)^2}\right]^N. \end{aligned} \tag{7.3.14}$$

7.3.5 Outage Probability Analysis of the Best Two-Relay Selection

Then the best two-relay nodes selection, namely, select the maximum and the second $\gamma_{eq_i}^{LB}$, $\gamma_{eq_i}^{UB}$ and $\gamma_{eq_i}^{E}$ from the N available secondary relays instantaneous SNRs in the right and left side of (7.2.6) and (7.2.5) are provided, respectively. According to [50], the selection of the maximum and the second largest is not independent, therefore the joint distribution of the two most maximum values can be obtained as

$$f^{K}(x_1, x_2) = N(N-1)\left[F_{\gamma_{eq_{x2}}^{K}}(x_2)\right]^{N-2} f_{\gamma_{eq_{x1}}^{K}}(x_1) f_{\gamma_{eq_{x2}}^{K}}(x_2), \tag{7.3.15}$$

where $x_1 \geq x_2 \geq x_N \geq 0$, and $K \in (LB, UB \text{ and } E)$. Substituting (7.3.3) and (7.3.4), (7.3.6) and (7.3.7) and (7.3.10) and (7.3.11) into (7.3.15), respectively, the three types of joint distribution can be obtained as

$$\begin{aligned} f^{LB}(x_1, x_2) = N(N-1)&\left[1 - \frac{L_1 e^{-\frac{2x_2}{L_0}}}{L_1 + 2x_2}\right]^{N-2} \\ &\frac{L_1 e^{-\frac{2x_1}{L_0}}(L_0 + L_1 + 2x_1)}{L_0(L_1 + 2x_1)^2} \frac{L_1 e^{-\frac{2x_2}{L_0}}(L_0 + L_1 + 2x_2)}{L_0(L_1 + 2x_2)^2}, \end{aligned} \tag{7.3.16}$$

$$\begin{aligned} f^{UB}(x_1, x_2) = N(N-1)&\left[1 - \frac{L_1 e^{-\frac{x_2}{L_0}}}{L_1 + x_2}\right]^{N-2} \\ &\frac{L_1 e^{-\frac{x_1}{L_0}}(L_0 + L_1 + x_1)}{L_0(L_1 + x_1)^2} \frac{L_1 e^{-\frac{x_2}{L_0}}(L_0 + L_1 + x_2)}{L_0(L_1 + x_2)^2}, \end{aligned} \tag{7.3.17}$$

$$
\begin{aligned}
f^E(x_1,x_2) =& N(N-1)[\frac{L_1(L_1^2-L_1+L_1L_0+L_0x_2)e^{-\frac{x_2}{L_0}}}{L_0(L_1+x_2)^3} \\
&+\frac{[L_1^2(2x_2+1)-L_1x_2]e^{\frac{(1-L_1)x_2}{(L_1+x_2)L_0}}\mathrm{Ei}(1,\frac{x_2(1+x_2)}{L_0(L_1+x_2)})}{L_0(L_1+x_2)^3} \\
&+\frac{L_1^2x_2(x_2+1)(1-L_1)e^{\frac{(1-L_1)x_2}{(L_1+x_2)L_0}}\mathrm{Ei}(1,\frac{x_2(1+x_2)}{L_0(L_1+x_2)})}{L_0^2(L_1+x_2)^4}] \\
&[\frac{L_1(L_1^2-L_1+L_1L_0+L_0x_1)e^{-\frac{x_1}{L_0}}}{L_0(L_1+x_1)^3} \\
&+\frac{[L_1^2(2x_1+1)-L_1x_1]e^{\frac{(1-L_1)x_1}{(L_1+x_1)L_0}}\mathrm{Ei}(1,\frac{x_1(1+x_1)}{L_0(L_1+x_1)})}{L_0(L_1+x_1)^3} \\
&+\frac{L_1^2x_1(x_1+1)(1-L_1)e^{\frac{(1-L_1)x_1}{(L_1+x_1)L_0}}\mathrm{Ei}(1,\frac{x_1(1+x_1)}{L_0(L_1+x_1)})}{L_0^2(L_1+x_1)^4}] \\
&\left[1-\frac{L_1e^{-\frac{x_2}{L_0}}}{L_1+x_2}+\frac{L_1x_2(x_2+1)e^{\frac{(1-L_1)x_2}{(L_1+x_2)L_0}}\mathrm{Ei}(1,\frac{x_2(1+x_2)}{L_0(L_1+x_2)})}{L_0(L_1+x_2)^2}\right]^{N-2}.
\end{aligned}
\tag{7.3.18}
$$

Then the CDF of the random variable γ_{eq}^K is calculated, formed as the sum of the x_1 and x_2 random variables. Therefore, the three types of CDF can be obtained from

$$
F_{\gamma_{eq}^K}(\gamma) = Pr\{x_1+x_2 \le \gamma\}. \tag{7.3.19}
$$

Given that x_1 and x_2 are non-negative, with $x_1 \ge x_2$, then,

$$
F_{\gamma_{eq}^K}(\gamma) = \int_0^{\frac{\gamma}{2}} \int_{x_2}^{\gamma-x_2} f^K(x_1,x_2)dx_1dx_2. \tag{7.3.20}
$$

Substituting (7.3.16), (7.3.17) and (7.3.18) into (7.3.20), respectively, and

after performing some manipulations,

$$F_{\gamma_{eq}^{LB}}(\gamma) = N(N-1)\frac{2L_1^2}{L_0}\int_0^{\frac{\gamma}{2}}\left(1-\frac{L_1 e^{-\frac{2x_2}{L_0}}}{L_1+2x_2}\right)^{N-2} \left[\frac{e^{-\frac{4x_2}{L_0}}(L_0+L_1+2x_2)}{(L_1+2x_2)^3} - \frac{e^{-\frac{2\gamma}{L_0}}(L_0+L_1+2x_2)}{(L_1+2x_2)^2(L_1+\gamma-2x_2)}\right] dx_2, \tag{7.3.21}$$

$$F_{\gamma_{eq}^{UL}}(\gamma) = N(N-1)\frac{L_1^2}{L_0^2}\int_0^{\frac{\gamma}{2}}\left(1-\frac{L_1 e^{-\frac{x_2}{L_0}}}{L_1+x_2}\right)^{N-2} \left[\frac{e^{-\frac{2x_2}{L_0}}(L_0+L_1+x_2)}{(L_1+x_2)^3} - \frac{e^{-\frac{\gamma}{L_0}}(L_0+L_1+x_2)}{(L_1+x_2)^2(L_1+\gamma-x_2)}\right] dx_2, \tag{7.3.22}$$

$$\begin{aligned} F_{\gamma_{eq}^{E}}(\gamma) = N(N-1)\int_0^{\frac{\gamma}{2}} & \Big[\frac{L_1(L_1^2-L_1+L_1L_0+L_0x_2)e^{-\frac{x_2}{L_0}}}{L_0(L_1+x_2)^3} \\ & + \frac{[L_1^2(2x_2+1)-L_1x_2]e^{\frac{(1-L_1)x_2}{(L_1+x_2)L_0}}\,\mathrm{Ei}(1,\frac{x_2(1+x_2)}{L_0(L_1+x_2)})}{L_0(L_1+x_2)^3} \\ & + \frac{L_1^2x_2(x_2+1)(1-L_1)e^{\frac{(1-L_1)x_2}{(L_1+x_2)L_0}}\,\mathrm{Ei}(1,\frac{x_2(1+x_2)}{L_0(L_1+x_2)})}{L_0^2(L_1+x_2)^4}\Big] \\ & \Big[\frac{L_1e^{-\frac{x_2}{L_0}}}{L_1+x_2} - \frac{L_1x_2(x_2+1)e^{\frac{(1-L_1)x_2}{(L_1+x_2)L_0}}\,\mathrm{Ei}(1,\frac{x_2(1+x_2)}{L_0(L_1+x_2)})}{L_0(L_1+x_2)^2} - \frac{L_1e^{-\frac{\gamma-x_2}{L_0}}}{L_1+\gamma-x_2} \\ & + \frac{L_1(\gamma-x_2)(\gamma-x_2+1)e^{\frac{(1-L_1)(\gamma-x_2)}{(L_1+\gamma-x_2)L_0}}\,\mathrm{Ei}(1,\frac{(\gamma-x_2)(1+\gamma-x_2)}{L_0(L_1+\gamma-x_2)})}{L_0(L_1+\gamma-x_2)^2}\Big] \\ & \left[1-\frac{L_1e^{-\frac{x_2}{L_0}}}{L_1+x_2}+\frac{L_1x_2(x_2+1)e^{\frac{(1-L_1)x_2}{(L_1+x_2)L_0}}\,\mathrm{Ei}(1,\frac{x_2(1+x_2)}{L_0(L_1+x_2)})}{L_0(L_1+x_2)^2}\right]^{N-2} dx_2. \end{aligned} \tag{7.3.23}$$

The outage probability can then be defined as the probability that the average end-to-end SNR falls below a certain predefined threshold value, α. The three types of outage probability can therefore be expressed as

$$P_{out}^{K} = \int_0^{\alpha} f_{\gamma_{eq}^{K}}(\gamma)d\gamma = F_{\gamma_{eq}^{K}}(\alpha). \tag{7.3.24}$$

7.3.6 Outage Probability Analysis of the Best Four-Relay Selection

The selection of the four largest SNRs is again not independent, therefore, according to [50], the joint distribution of the four most maximum values can be obtained as

$$f^K(x_1,x_2,x_3,x_4) = N(N-1)(N-2)(N-3)\left[F_{\gamma^K_{eq_{x4}}}(x_4)\right]^{N-4}\prod_{i=1}^{4} f_{\gamma^K_{eq_{xi}}}(x_i), \tag{7.3.25}$$

where $x_1 \geq x_2 \geq x_3 \geq x_4 \geq 0$, $f(\cdot)$ and $F(\cdot)$ correspond to the PDF and CDF. Then the CDF of the random variable γ^K_{eq} is calculated, formed as the sum of the random variables from x_1 to x_4, which are identically distributed exponential random variables. Therefore, the three types of CDF are obtained from

$$F_{\gamma^K_{eq}}(\gamma) = Pr\{x_1 + x_2 + x_3 + x_4 \leq \gamma\}. \tag{7.3.26}$$

and finally,

$$F_{\gamma^K_{eq}}(\gamma) = \int_0^{\frac{\gamma}{4}} \int_{x_4}^{\frac{\gamma-x_4}{3}} \int_{x_3}^{\frac{\gamma-x_4-x_3}{2}} \int_{x_2}^{\gamma-x_4-x_3-x_2} f^K(x_1,x_2,x_3,x_4)dx_1dx_2dx_3dx_4. \tag{7.3.27}$$

Finally, (7.3.24) and (7.3.27) can be used to calculate the outage probability of the best four-relay selection, based on the different CDF and PDF of the approximate overall end-to-end SNR, such as (7.3.3) and (7.3.4) for the lower bound, (7.3.6) and (7.3.7) for the upper bound and (7.3.10) and (7.3.11) for the exact outage probability analysis. This result has been provided in Figure 7.3 by using the Mathematica software package [86]. In the next section, these analytical results are verified by numerical simulations.

7.4 Outage Probability Analysis Verification

In this section, in order to verify the results obtained from the above mathematical expressions, the noise variances σ_r^2 and σ_d^2 are set to unity and $\lambda_{SR_i} = \lambda_{R_iD} = 40$ dB.

Figure 7.2 shows comparison of the theoretical and simulated three types of outage probability analysis schemes for the best two-relay selection. That is, in this simulation, the predetermined threshold I_{th} in the primary receiver is assumed to be 2, and $\phi_0 = 5$ and $\phi_1 = 10$. From Figure 7.2, the upper bound and lower bound can be confirmed, because the real simulation results are in between the lower and upper bound. Secondly, it can be seen that increasing the number of relays, N, decreases the outage probability, and hence when the number of relays is large, the outage event (no transmission) becomes less likely, for example, with the total number of available secondary relays increasing from 4 to 8, the exact theoretical outage probability of the best relay selection is decreased from almost 0.2 to 0.027, when the target rate is 1.5.

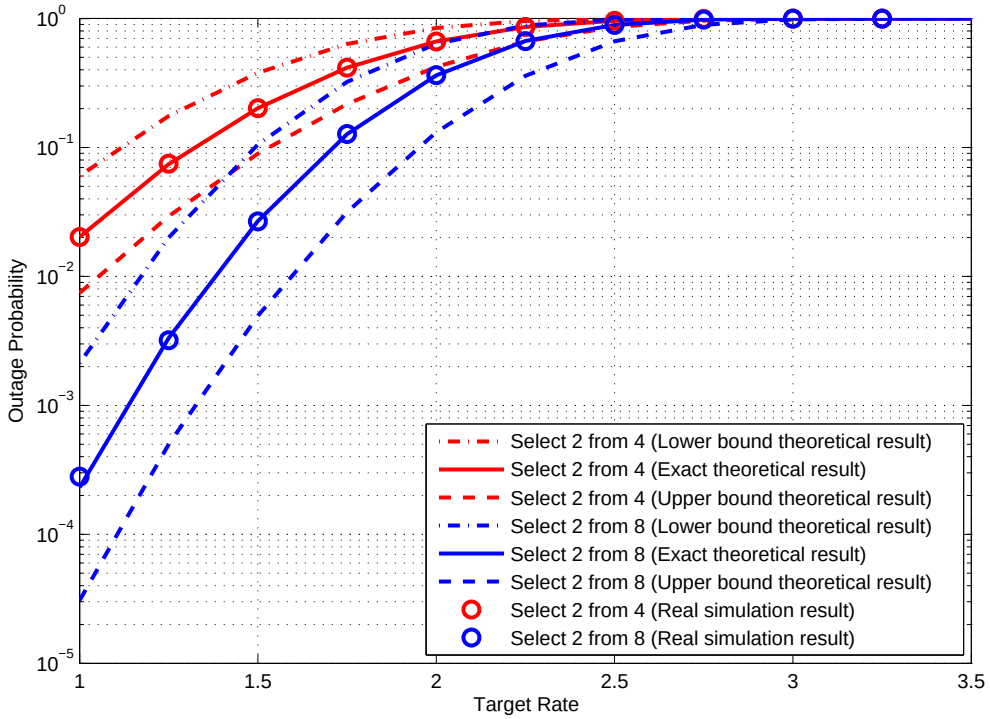

Figure 7.2. *Comparison of the theoretical and simulated three types of outage probability analysis schemes for the best two-relays selection* ($\phi_0 = 5,\ \phi_1 = 10$ *and* $I_{th} = 2$).

Figure 7.3 shows the comparison of the exact outage probability analysis for single-, two- and four-relay selection schemes. To facilitate analysis, the predetermined threshold I_{th} in the primary receiver is assumed to be 2, $N = 8$ and $\phi_0 = 5$ and $\phi_1 = 10$. It is clearly seen that the exact outage probability is decreased when the number of selected relay is increased, for example, when the target rate is 1.5, the number of selected relays is raised from 1 to 2 and then 4, the exact outage probability is reduced from approximately 0.1 to 0.028 to 0.019, respectively. Therefore, when the predetermined threshold I_{th} in the primary receiver and the total number of available selected relay N are restricted, more relays can be selected to communicate in order to provide sufficiently low outage probability for the secondary users.

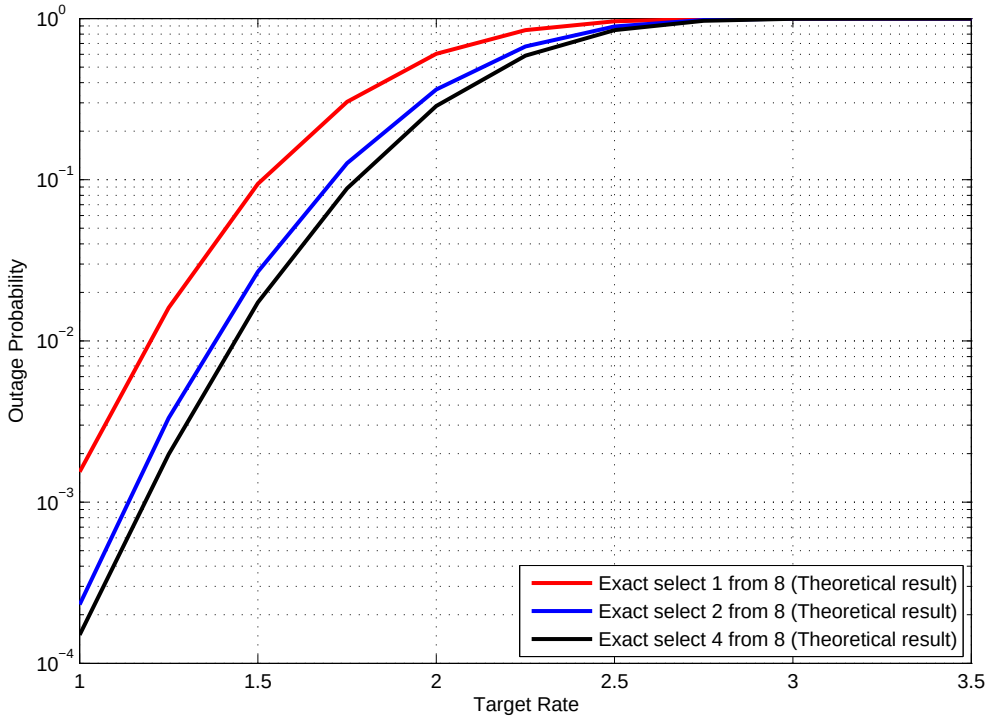

Figure 7.3. *Comparison of the exact theoretical outage probability for the best single-, two- and four-relay selection* ($\phi_0 = 5,\ \phi_1 = 10$ *and* $I_{th} = 2$).

Figure 7.4 shows comparison of the exact theoretical outage probability of the single-relay selection and the best two-relay selection for the different thresholds I_{th} and mean channel gain ratios, ϕ_0 and ϕ_1 as in the figure legend. Firstly, there are the same trends for the outage probability for best single- and two-relay selections. Therefore, taking the best two-relay selection as an example. When $N = 8$, the target rate is 1.5, with increasing the mean channel gain ratios, the outage probability decreases, when the predetermined threshold is fixed, i.e., when the mean channel gain ratio ϕ_1 is increased from 5 to 10 and $\phi_0 = 5$ and $I_{th} = 1$, the outage probability of the best two-relay selection is decreased from almost 0.55 to 0.31. Moreover, with increasing the predetermined threshold, the outage probability is decreased, when the mean channel gain ratio is fixed. For example, when I_{th} is increased from 1 to 2 and $\phi_0 = 5$ and $\phi_1 = 10$, the outage probability of the best two-relay selection is decreased from almost 0.31 to 0.026. These best relays could then be exploited for transmitting an orthogonal coding scheme such as [42] and thereby induce robustness to possible feedback errors in single-relay selection schemes, which is confirmed in [94].

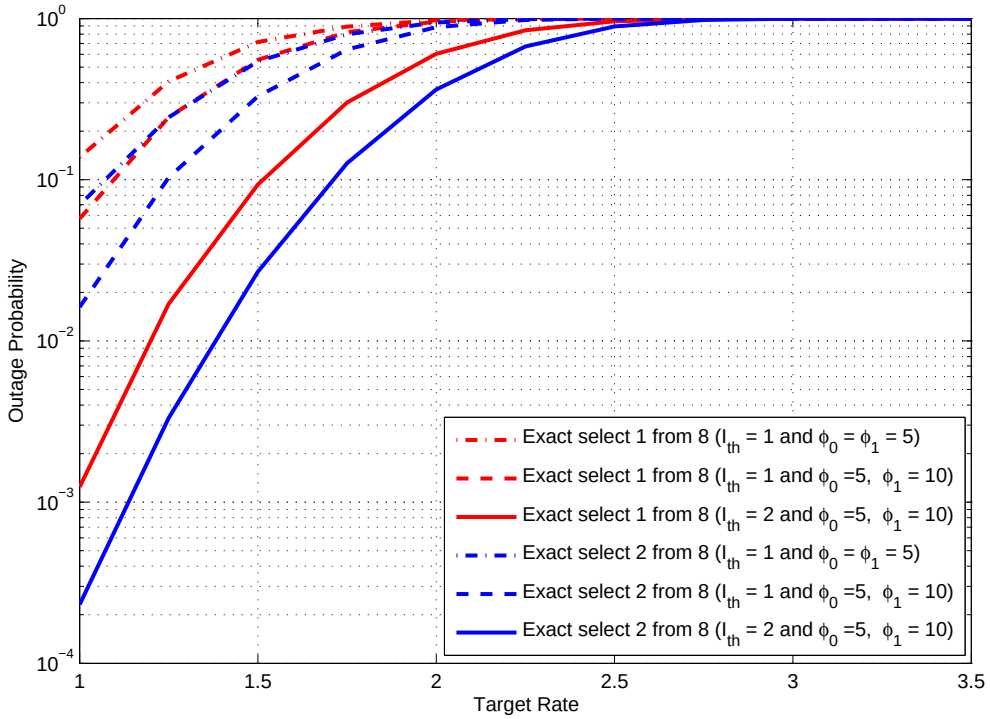

Figure 7.4. *Comparison of the exact outage probability for a best single- and two-relay selection for different thresholds I_{th} and mean channel gain ratios, ϕ_0 and ϕ_1, $N = 8$.*

7.5 Summary

This chapter has examined three types of outage probability analysis strategies for a cognitive AF network with single-, two- or four-relay selection from the potential cooperative secondary relays based on the underlay approach, while adhering to an interference constraint on the primary user. New analytical expressions for the PDF, and CDF of end-to-end SNR were derived together with near closed form expressions for outage probability over Rayleigh frequency fading channels. Numerical results were provided to show the advantage of the outage probability performance of the best two- and four-relay selection in a cooperative communication system, i.e., more suitable relays can be selected to provide enough capacity for the secondary users when the predetermined threshold and the total number of available selected relays cannot be increased. Moreover, the theoretical values for the new exact outage probability match the simulated results can be confirmed. In the next chapter, the summary and conclusion to the thesis and possible future work will be provided.

Chapter 8

CONCLUSIONS AND FUTURE WORK

The conclusions that can be drawn from the contributions of this thesis are summarized in this chapter. Furthermore, a discussion on possible research directions for the future work is also included.

8.1 Conclusions

In this thesis, the research has focused on two aspects of improving the performance of wireless cooperative networks. An offset transmission scheme with full interference cancellation, and full inter-relay self interference cancellation schemes, to enhance the transmission rate and remove interference from other relays has been presented. Two- and four-relay selection for cooperative AF networks with and without inter-cluster interference has then been studied, in conventional and cognitive networks. Outage probability analysis was applied for performance assessment. Considering the chapters in detail:

In Chapter 1, the basic concept and characteristic advantages of MIMO systems were provided. Moreover, a general introduction to cooperative networks was presented. Then, relay selection was presented for application in cooperative networks. In addition, a brief introduction to the main functions of cognitive radio systems and the features of cooperative cognitive networks

was provided. Finally, the thesis outline was briefly discussed.

In Chapter 2, an overview of the various methodologies in cooperative networks that are used in the thesis was presented. A brief introduction to distributed space-time coding schemes with orthogonal and quasi-orthogonal codes was given. A practically important method for distributed space-time coding, which does not need CSI at the receiver for decoding, which is differential space-time coding, was then described. This was followed by performance analysis of wireless cooperative networks. Two approaches were applied for performance analysis, one was pairwise error probability analysis, and the other was outage probability analysis. Finally, some methods to achieve coding gain in transmission were considered. A simulation result was included to confirm the performance advantage of distributed transmission with and without outer coding.

In Chapter 3, unity end-to-end transmission rate was achieved through offset transmission with a full interference cancellation scheme. Using offset transmission, the source can continually transmit data to the destination. However, the four-path relay scheme suffered from inter-relay interference which was caused by the simultaneous transmission of the source and another group of relays. Therefore, the FIC scheme was used to remove these IRI terms. However, a full inter-relay self interference scheme was employed at the relay nodes within a four relay network and the pairwise error probability approach was used to analyze the cooperative diversity. This scheme was shown to achieve the full available distributed diversity order, 3.5, without precoding and the end-to-end transmission rate to asymptotically approach unity when the number of samples is large.

In Chapter 4, outage probability analysis of the best single-relay and four-relay selection schemes in a cooperation amplify-and-forward network without any interference was provided. Also the best four-relay selection scheme was shown to have robustness to feedback error and to outperform

a scheme based on selecting only the best single-relay.

In Chapter 5, the local measurements of the instantaneous channel conditions were used to select the best relay pair from the number of available relays in a cooperative amplify-and-forward network with inter-relay interference, and then these best relays were used to decrease the outage probability, i.e. when the target SNR = 4 dB, the outage probability was decreased from almost 10^{-2} for the best single-relay selection to 10^{-3} for the best two-relay selection. Also, BER analysis of the proposed scheme with error in inter-relay interference cancellation was compared.

In Chapter 6, firstly, two different schemes namely asymptotical and semi-conventional policies to select the best two- and four-relay from a group of available relays in the same cluster were presented. These policies used local measurements of the instantaneous channel conditions in the context of legacy systems which adopt $\max(min(\cdot,\cdot))$ type selection when inter-cluster interference is present only in the relay nodes. New analytical expressions for the PDF, and CDF of end-to-end SINR were obtained together with near closed form expressions for outage probability over Rayleigh flat fading channels. Secondly, the best single-relay selection from a group of available relays by using local measurements of the instantaneous channel conditions in the context of cooperative systems which adopt a selection policy to maximize end-to-end SINR was studied. Inter-cluster interference was considered at the relay nodes only. Finally, a new exact closed form expression for outage probability in the high SNR region was provided.

In Chapter 7, three types of outage probability analysis strategies for a cognitive AF network with single-, two- or four-relay selection from the potential cooperative secondary relays based on the underlay approach, while adhering to an interference constraint on the primary user, were examined. New analytical expressions for the PDF, and CDF of end-to-end SNR were derived together with near closed form expressions for outage probability

over Rayleigh flat fading channels. Numerical results were provided to show the advantage of the outage probability performance of the best two- and four-relay selection in a cooperative communication system, i.e., more suitable relays can be selected to provide enough capacity for the secondary users when the predetermined threshold cannot be increased. For example, when the threshold α value is 7 dB and $\phi_0 = 5$, $\phi_1 = 10$, $I_{th} = 2$, and the number of selected relays was increased from 1 to 4, the exact outage probability was decreased from almost 0.1 to 0.019. Moreover, the simulation of the theoretical values for the new exact outage probability were confirmed.

In conclusion, the original goal for the thesis of increasing transmission and overcoming fading channels have been achieved by exploiting distributed transmission, interference cancellation and relay selection.

8.2 Future Work

There are several ways in which the research presented in this thesis could be extended. The solutions presented in this thesis were for channels which are assumed Rayleigh flat fading; but a wider class of fading channel conditions, modeled by for example the Nakagami-m distribution [95] and [96], could be considered. The Nakagami-m fading distribution has gained much attention lately since this fading distribution often gives the best fit to land-mobile and indoor mobile multipath propagation environments as well as scintillating ionospheric radio links [97].

Secondly, in Chapter 3, the robustness of the best two- and four-relay selection schemes in the presence of moderate to severe feedback errors is only confirmed by simulation results. In suggesting future work, a theoretical analysis should be considered. Furthermore, as only outage probability analysis of two- and four-relay selection schemes was provided in this thesis, there is opportunity for further diversity multiplexing tradeoff analyses to

be performed.

Finally, the security of wireless communication is becoming a topical area of research as shown in [98] and [99]. In particular, physical layer security is becoming an important issue for future research. The possibility of achieving perfect secrecy data wireless transmission among the intended network nodes could be considered [100].

A similar security issue also occurs in cognitive relay networks (CRNs), where the primary user enhances its performance through cooperation with secondary users. In return, the cooperating SUs can gain opportunities for their own transmission. However, almost all the related works assume that SUs are trustworthy, which may not always be true in reality. There could be some dishonest users, even malicious ones in the system, corrupting or disrupting the normal operation of the CRN. Consequently, the performance can therefore be compromised. Finally, this security issue also needs to be considered for emerging cognitive relay networks.

References

[1] H. Bertoni, "Radio propagation for modern wireless systems," *Prentice Hall, Upper Saddle River, NJ*, 1999.

[2] H. Jafarkhani, "Space-time coding theory and practice," *Cambridge University Press*, 2005.

[3] F. Khan, "LTE for 4G mobile broadband: air interface technologies and performance," *Cambridge University Press*, 2009.

[4] A. Paulraj, R. Nabar, and D. Gore, "Introduction to space-time wireless communications," *Cambridge University Press*, 2003.

[5] C. B. Chae, A. Forenza, R. W. Heath, M. R. Mckay, and L. B. Collings, "Adaptive MIMO transmission techniques for broadband wireless communication systems," *IEEE Commun. Mag.*, vol. 48, no. 5, pp. 112–118, May 2010.

[6] I. E. Telatar, "Capacity of multi-antenna Gaussian channels," *European Trans. Tel.*, vol. 10, no. 6, pp. 585–595, Nov. 1999.

[7] D. Tse and P. Viswanath, "Fundamentals of wireless communication," *Cambridge University Press*, 2005.

[8] J. N. Laneman and G. W. Wornell, "Distributed space-time-coded protocols for exploiting cooperative diversity in wireless networks," *IEEE Trans. Inf. Theory*, vol. 49, no. 10, pp. 2415–2425, Oct. 2003.

[9] A. Nosratinia, T. E. Hunter, and A. Hedayat, "Cooperative communication in wireless networks," *IEEE Commun. Mag.*, vol. 42, no. 10, pp. 74–80, Oct. 2004.

[10] R. Pabst, B. H. Walke, D. C. Schultz, P. Herhold, H. Yanikomeroglu, S. Mukherjee, H. Viswanathan, M. Lott, W. Zirwas, M. Dohler, H. Aghvami, D. D. Falconer, and G. P. Fettweis, "Relay-based deployment concepts for wireless and mobile broadband radio," *IEEE Commun. Mag.*, vol. 42, pp. 80–89, Sep. 2004.

[11] Y. Yang, H. Hu, J. Xu, and G. Mao, "Relay technologies for WiMAX and LTE-advanced mobile systems," *IEEE Commun. Mag.*, vol. 47, pp. 100–105, Oct. 2009.

[12] K. Letaief and W. Zhang, "Cooperative communications for cognitive radio networks," *IEEE Commun. Mag.*, vol. 97, pp. 878–893, May 2009.

[13] M. Dohler and Y. H. Li, "Cooperative communications: hardware, channel & PHY," *John Wiley Sons Ltd*, 2010.

[14] J. N. Laneman, "Cooperative diversity in wireless networks: Algorithms and architectures," *Massachusetts Institute of Technology, Cambridge, MA, USA: PhD dissertation*, Aug. 2002.

[15] A. Bletsas, A. Knisti, D. P. Reed, and A. Lippman, "A simple cooperative diversity method based on network path selection," *IEEE J. Sel. Areas Commun.*, vol. 24, no. 3, pp. 659–672, Mar. 2006.

[16] J. N. Laneman, D. N. C. Tes, and G. W. Wornell, "Cooperative diversity in wireless networks: effifient protocols and outage behavior," *IEEE Trans. Inf. Theory*, vol. 50, no. 12, pp. 3062–3080, Dec. 2004.

[17] S. Ikki and M. H. Ahmed, "Performance analysis of dual-hop relaying

communications over generalized Gamma fading channels," *in Proc. of the IEEE Global Communications Conference, Washington, DC*, Nov. 2007.

[18] Z. Yi and I. M. Kim, "Diversity order analysis of the decode-and-forward cooperative networks with relay selection," *IEEE Trans. Wireless Commun.*, vol. 7, no. 5, pp. 1792–1799, May 2008.

[19] T. Q. Duong and V. N. Q. Bao, "Performance analysis of selection decode-and-forward relay networks," *IET Electronic Lett.*, vol. 44, no. 20, pp. 1206–1207, Sep. 2008.

[20] M. O. Hasna and M. S. Alouini, "Harmonic mean and end-to-end performance of transmission system with relays," *IEEE Trans. Commun.*, vol. 52, no. 1, pp. 130–135, Jan. 2004.

[21] L. Sun and M. R. McKay, "Opportunistic relaying for MIMO wireless communication: Relay selection and capacity scaling laws," *IEEE Trans. Wireless Commun.*, vol. 10, no. 6, pp. 1786–1797, June 2011.

[22] I. Krikidis, J. S. Thompson, and S. McLaughlin, "Amplify-and-forward with partial relay selection," *IEEE Commun. Lett.*, vol. 12, no. 4, pp. 235–237, Apr. 2008.

[23] F. C. Commission, "Facilitating opportunities for flexible, efficient, and reliable spectrum use employing cognitive radio technologies," *ET Docket*, no. 03-108, Mar. 2005.

[24] B. Fette, "Cognitive radio technology," *Elsevier, Oxford, UK*, 2nd ed., 2009.

[25] S. Haykin, "Cognitive radio: Brain-empowered wireless communications," *IEEE J. Sel. Areas Commun.*, vol. 23, no. 2, pp. 201–220, Feb. 2005.

[26] C. Cordeiro, K. Challapali, and D. Birru, "IEEE 802.22: An introduction

to the first wireless standard based on cognitive radios," *J. Commun.*, vol. 1, pp. 38–47, Apr. 2006.

[27] C. R. Sevension, "In reply to comments of IEEE 802.18. 2004," [Online] Available: http://ieee802.org/18.

[28] A. Goldsmith, S. A. Jafar, I. Maric, and S. Srinivasa, "Breaking spectrum gridlock with cognitive radios: an information theoretic perspective," *Proc. IEEE*, vol. 97, no. 5, pp. 894–914, May 2009.

[29] W. Su, J. D. Matyjas, and S. N. Batalama, "Active cooperation between primary users and cognitive users in cognitive ad hoc networks," *in Proc IEEE ICASSP, Dallas, USA*, 2010.

[30] X. F. Tao, X. D. Xu, and Q. M. Cui, "An overview of cooperative communication," *IEEE Commun. Mag.*, vol. 50, no. 6, pp. 65–71, June 2012.

[31] C. E. Shannon, "Two-way communication channels," *in Proc. 4th Berkeley Symp. Math. Stat. Prob*, pp. 611-644, 1961.

[32] T. Cui, F. Gao, and C. Tellambura, "High-rate codes that are linear in space and time," *IEEE Trans. Commun.*, vol. 57, no. 10, pp. 2977–2987, Oct. 2009.

[33] R. Vaze, K. T. Truong, S. Weber, and R. W. Heath, "Two-way transmission capacity of wireless ad-hoc networks," *IEEE Trans. Wireless Commun.*, vol. 11, no. 6, pp. 1966–1975, June 2011.

[34] V. Tarokh, N. Seshadri, and A. R. Calderbank, "Space-time codes for high data rate wireless communication: Performance criterion and code construction," *IEEE Trans. Inf. Theory*, vol. 44, no. 2, pp. 744–765, Mar. 1998.

[35] V. Tarokh, H. Jafarkhani, and A. R. Calderbank, "Space-time block codes from orthogonal designs," *IEEE Trans. Inf. Theory*, vol. 44, no. 2, pp. 1456–1467, July 1999.

[36] A. Sendonaris, E. Erkip, and B. Aazhang, "User cooperation diversity-Part I: System description," *IEEE Trans. Wireless Commun.*, vol. 51, no. 11, pp. 1927–1938, Nov. 2003.

[37] K. Azarian, H. E. Gamal, and P. Schniter, "On the achievable diversity-multiplexing tradeoff in half-duplex cooperative channels," *IEEE Trans. Inf. Theory*, vol. 51, no. 12, pp. 4152–4172, Dec. 2005.

[38] R. U. Nabar, H. Bolcskei, and F. W. Kneubhler, "Fading relay channels: performance limits and space-time signal design," *IEEE J. Sel. Areas commun.*, vol. 22, no. 6, pp. 1099–1109, Aug. 2004.

[39] H. Muhaidat, M. Uysal, and R. Adve, "Pilot-symbol-assisted detection scheme for distributed orthogonal space-time coding," *IEEE Trans. Wireless Commun.*, vol. 8, no. 3, pp. 1057–1061, Mar. 2009.

[40] G. S. Rajan and B. S. Rajan, "Leveraging coherent distributed space-time codes for noncoherent communication in relay networks via training," *IEEE Trans. Wireless Commun.*, vol. 8, no. 2, pp. 683–688, Feb. 2009.

[41] B. Hassibi and B. M. Hochwald, "High-rate codes that are linear in space and time," *IEEE Trans. Inf. Theory*, vol. 48, no. 7, pp. 1804–1824, July 2002.

[42] Y. Jing and B. Hassibi, "Distributed space-time coding in wireless relay networks," *IEEE Trans. Wireless Commun.*, vol. 5, no. 12, pp. 3524–3536, Dec. 2006.

[43] Y. Jing and H. Jafarkhani, "Using orthogonal and quasi-orthogonal designs in wireless relay networks," *IEEE Trans. Inf. Theory*, vol. 53, no. 11, pp. 4106–4118, Nov. 2007.

[44] S. M. Alamouti, "A simple transmit diversity technique for wireless communications," *IEEE J. Sel. Areas Commun.*, vol. 16, no. 8, pp. 1451–1458, Oct. 1998.

[45] H. Jafarkhani, "A quasi-orthogonal space-time block codes," *IEEE Trans. Commun.*, vol. 49, no. 1, pp. 1–4, Jan. 2001.

[46] H. Jafarkhani, "Space-time coding: theory and practice," *Cambridge U.K.: Academic*, 2005.

[47] Y. Jing and H. Jafarkhani, "Distributed differential space-time coding for wireless relay networks," *IEEE Trans. Wireless Commun.*, vol. 56, no. 7, pp. 1092–1100, July 2008.

[48] V. Tarokh and H. Jafarkhani, "A differential detection scheme for transmit diversity," *IEEE J. Sel. Areas Commun.*, vol. 18, no. 7, pp. 1169–1174, July 2000.

[49] J. G. Proakis, "Digital communication," *4th ed. New York: McGrawhill, Inc.*, 2001.

[50] N. Balakrishnan and A. C. Cohen, "Order statistics and inference: estimation methods," *London : Academic Press*, 1991.

[51] M. O. Damen, K. Abed-Meraim, and M. S. Lemdani, "Further results on the sphere decoder algorithm," *in proc. IEEE ISIT, Washington, DC*, June 2001.

[52] L. Ge, G. J. Chen, and J. A. Chambers, "Relay selection in distributed transmission based on the Golden code using ML and sphere decoding in wireless networks," *International Journal of Inf. Technology and Web Engineering in IGI Global Disseminator of Knowledge*, vol. 6, no. 4, 2011.

[53] M. Evans, N. Hastings, and B. Peacock, "Statistical Distributions," *Wiley, 2nd ed.*, 1993.

[54] A. J. Viterbi, "Error bounds for convolutional codes and an asymptotically optimum decoding algorithm," *IEEE Trans. Inf. Theory*, vol. 13, pp. 260–269, Apr. 1967.

[55] B. Sklar, "Digital Communications-Fundamentals and Applications," *Prentice Hall*, 1988.

[56] W. Song, M. H. Lee, G. Zeng, and Y. Guo, "Orthogonal space-time block codes design using jacket transform for MIMO transmission system," *IEEE Inter. Conf. on Commun.*, pp. 766–769, May. 2008.

[57] W. Song and M. Lee, "Fast distributed space-time block code in wireless relay networks," *IEEE Inter. Conf. on Commun.*, pp. 145–148, Oct. 2009.

[58] F. Fazel and H. Jafarkhani, "Quasi-orthogonal space-frequency and spact-time-frequency block codes for MIMO OFDM channels," *IEEE Trans. on Wireless Commun.*, vol. 7, pp. 184–192, Jan. 2008.

[59] A. Y. Al-Nahari, F. A. Abd El-Samie, and M. I. Dessouky, "Distributed space-time code for amplify-and-forward cooperative networks," *in Proc. 5th Future Infomation Technology, Busan, Korea*, June 2010.

[60] G. Chen and J. A. Chambers, "Full interference cancellation for an asymptotically full rate cooperative four relay network," *IEEE International Coference on Inf. Theory and Inf. Security, Being, China*, Dec. 2010.

[61] H. Wicaksana, S. H. Ting, C. K. Ho, W. H. Chin, and Y. L. Guan, "AF two-path half duplex relaying with inter-relay self interference cancellation: Diversity analysis and its improvement," *IEEE Trans. Wireless Commun.*, vol. 8, no. 9, pp. 4720–4729, Sep. 2009.

[62] P. Herhold, E. Zimmermann, and G. Fettweis, "On performance of cooperative amplify-and-forward relay networks," *in Proc. International ITG Conf. Source Channel Coding (SCC'04), Erlangen, Germany*, 2004.

[63] B. M. Hochwald and T. L. Marzetta, "Unitary space-time modulation for multiple-antenna communication in Rayleigh flat fading," *IEEE Trans. Inf. Theory*, vol. 46, pp. 543–564, Mar. 2000.

[64] C. Luo, Y. Gong, and F. Zheng, "Full interference cancellation for two-path cooperative communications," *Proc. IEEE WCNC., Budapest, Hungary*, 2009.

[65] B. Hughes, "Differential space-time modulation," *IEEE Trans. Inf. Theory*, vol. 46, no. 7, pp. 2567–2578, Nov. 2000.

[66] Z. Bali, W. Ajib, and H. Boujemaa, "Distributed relay selection strategy based on source-relay channel," *in Proc. IEEE ICT, Doha, Qatar*, pp. 138–142, April 2010.

[67] K. Woradit, W. Suwansantisuk, H. Wymeersch, L. Wuttisittikulkij, and M. Z. Win, "Outage behavior of cooperative diversity with relay selection," *in Proc. IEEE Globecom, New Orleans, LA, USA*, 2008.

[68] A. Adinoyi, Y. J. Fan, H. Yanikomeroglu, H. V. Poor, and F. Al-Shaalan, "Performance of selection relaying and cooperative diversity," *IEEE Trans. Wireless Commun.*, vol. 12, no. 8, pp. 5790–5795, Dec. 2009.

[69] A. Bletsas, H. Shin, and M. Z. Win, "Cooperative communications with outage-optimal opportunistic relaying," *IEEE Trans. Wireless Commun.*, vol. 6, no. 9, pp. 3450–3460, Sep. 2007.

[70] A. Annamalai, G. Deora, and C. Tellambura, "Analysis of generalized selection diversity systems in wireless channel," *IEEE Trans. Veh. Tech.*, vol. 55, no. 6, pp. 1765–1775, Nov. 2006.

[71] C. Toker, S. Lambotharan, and J. A. Chambers, "Closed-loop quasi-orthogonal STBCs and their performance in multipath fading environments and when combined with Turbo codes," *IEEE Trans. Wireless Commun.*, vol. 3, no. 6, pp. 1890–1896, Nov. 2004.

[72] P. A. Anghel and M. Kaveh, "Exact symbol error probability of a coop-

erative network in a Rayleigh-fading environment," *IEEE Trans. Wireless Commun.*, vol. 3, no. 5, pp. 1416–1421, Sep. 2004.

[73] A. Papoulis, "Probability, random variables, and stochastic processes," *McGraw-Hill*, 1991.

[74] B. Rankov and A.Wittneben, "Spectral efficient protocols for half-duplex fading relay channels," *IEEE J. Sel. Areas Commun.*, vol. 25, no. 2, pp. 379–389, Feb. 2007.

[75] F. Xue and S. Sandhu, "Cooperation in a half-duplex gaussian diamond relay channel," *IEEE Trans. Inf. Theory*, vol. 53, no. 10, pp. 3806–3814, Oct. 2007.

[76] W. Chang, S. Chung, and Y. H. Lee, "Capacity bounds for alternating two-path relay channels," *in Proc. Allerton Conf. Commun., Control Computing, Monticello, IL*, Oct. 2007.

[77] R. Zhang, "Characterizing achievable rates for two-path digital relaying," *in Proc. IEEE International Conf. on Commun. (ICC), Beijing, China*, pp. 1113–1117, May 2008.

[78] Y. Fan, C. Wang, J. Thompson, and H. V. Poor, "Recovering multiplexing loss through successive relaying using repetition coding," *IEEE Trans. Wireless Commum.*, vol. 6, no. 12, pp. 4484–4493, Dec. 2007.

[79] G. Scutari and S. Barbarossa, "Distributed space-time coding for regenerative relay networks," *IEEE Trans. Wireless Commum.*, vol. 4, pp. 2387–2399, Sept. 2005.

[80] I. Krikidis, J. S. Thompson, S. McLaughlin, and N. Goertz, "Max-min relay selection for legacy amplify-and-forward systems with interference," *IEEE Trans. Wireless Commun.*, vol. 8, no. 6, pp. 3016–3027, June 2009.

[81] A. F. Molisch, "Wireless communications," *IEEE Press., IEEE Communications Society, John Wiley and Sons LTD*, 2005.

[82] S. Nadarajah and S. Kotz, "On the product and ratio of Gamma and Weibull random variables," *Econometric Theory, Cambridge University Press*, vol. 22, pp. 338–344, Feb. 2006.

[83] L. Lai, K. Liu, and H. E. Gamal, "The three-node wireless network: achievable rates and cooperation strategies," *IEEE Trans. Inf. Theory*, vol. 52, no. 10, pp. 805–828, Mar. 2006.

[84] A. Gilat and V. Subramaniam, "Numerical methods for engineers and scientists: An introduction with applications using Matlab," *John Wiley Sons Ltd*, 2011.

[85] W. N. Bailey, "On the reducibility of Appell's function," *Quart. J. Math. Oxford*, pp. 291–292, 1934.

[86] S. Wolfram, "The Mathematica Book," *Wolfrom Media Press*, 5th ed., 2003.

[87] O. Simeone, U. Spagnolini, and Y. Bar-Ness, "Stable throughput of cognitive radios with and without relaying capacity," *IEEE Trans. Commun.*, vol. 55, no. 12, pp. 2351–2360, Dec 2007.

[88] K. Lee and A. Yener, "Outage performance of cognitive wireless relay networks," *in Proc. IEEE Globecom, New Orleans, LA, USA, San Francisco, USA*, Nov. 2006.

[89] H. A. Suraweera, P. J. Smith, and N. A. Surobhi, "Exact outage probability of cooperative diversity with opportunistic spectrum access," *in Proc. IEEE ICC, Beijing, China*, pp. 79–84, May 2008.

[90] J. Mietzner, L. Lampe, and R. Schober, "Distributed transmit power al-

location for multihop cognitive radio systems," *IEEE Trans. Wireless Commun.*, vol. 8, no. 10, pp. 5187–5201, Oct. 2009.

[91] J. Lee, H. Wang, J. Andrews, and D. Hong, "Outage probability of cognitive relay networks with interference constraints," *IEEE Trans. Wireless Commun.*, vol. 10, no. 2, pp. 390–395, Feb. 2011.

[92] D. S. Michalopoulos and G. K. Karagianidis, "Performance analysis of single relay selection in Rayleigh fading," *IEEE Trans. Wireless Commun.*, vol. 7, no. 11, pp. 3718–3724, Oct. 2008.

[93] J. N. Laneman and G. W. Wornell, "Energy efficient antenna sharing and relaying for wireless networks," *IEEE Wireless. Commun. and Networking conf. (WCNC), Chicago, USA*, vol. 49, no. 1, pp. 7–12, Oct. 2000.

[94] G. J. Chen and J. A. Chambers, "Outage probability in distributed transmission based on best relay pair selection," *IET Commun.*, vol. 6, no. 12, pp. 1829–1836, Aug. 2012.

[95] M. Nakagami, "The m-distribution - a general formula of intensity distribution of rapid fading," *In W. C. Hoffman: Statistical Methods of Radio Wave Propagation*, Oxford, England, 1960.

[96] P. L. Yeoh, M. Elkashlan, T. Duong, N. Yang, and D. B. da Costa, "Transmit antenna selection in cognitive relay networks with nakagami-m fading," *in Proc. IEEE International Conf. on Commun. (ICC), Budapest, Hungary*, pp. 2775–2779, Jun 2013.

[97] M. K. Simon, J. K. Omura, R. A. Scholtz, and B. K. Levitt, "Spread spectrum communication handbook," *McGraw-Hill Inc, New York, revised edition*, 1994.

[98] S. K. Miller, "Facing the challenge of wireless security," *Computer*, vol. 34, no. 7, pp. 16–18, July 2001.

[99] W. A. Arbaugh, "Wirless security is different," *Computer*, vol. 36, no. 8, pp. 99–101, Aug. 2003.

[100] M. Sarkar and T. Ratnarajah, "Enhancing security in the cognitive relay assisted co-existing radio systems with interferences," *in Proc. IEEE International Conf. on Commun. (ICC), Budapest, Hungary*, pp. 4729–4733, 2013.